Manufacture and Characterization of Fiber Reinforced Epoxy for Application in Cowling Panels of Recreational Aircraft

A Thesis Submitted to the College of
Graduate Studies and Research
In Partial Fulfillment of the Requirements
For the Degree of Master of Science
In the Department of Mechanical Engineering
University of Saskatchewan
Saskatoon

By

OLALEKAN SUNDAY SABA

PERMISSION TO USE

In presenting this thesis in partial fulfillment of the requirements for a Postgraduate degree from the University of Saskatchewan, I agree that the Libraries of this University may make it freely available for inspection. I further agree that permission for copying of this thesis in any manner, in whole or in part, for scholarly purposes may be granted by the professor who supervised my thesis work, Prof. Akindele Odeshi, or, in his absence, by the Head of the Department or the Dean of the College in which my thesis work is done. It is understood that any copying or publication or use of this thesis or parts thereof for financial gain shall not be allowed without my written permission. It is also understood that due recognition shall be given to me and to the University of Saskatchewan in any scholarly use which may be made of any material in my thesis.

Request for permission to copy or to make other uses of materials in this thesis in whole or part should be addressed to:

Head of Department of Mechanical Engineering
University of Saskatchewan,
57 Campus Drive, Saskatoon
Saskatchewan S7N 5A9
Canada.

ABSTRACT

In this study, glass and Kevlar® fibers reinforced epoxy composites were manufactured and characterized using different techniques. The effect of thermal exposure on the flexural properties of the composites was investigated to ascertain its suitability for the intended application in cowling panels of light engine aircraft. Thermogravimetric analysis (TGA) was carried out on both reinforced and unreinforced epoxy resin to evaluate their thermal stability at elevated temperatures. Dynamic mechanical thermal analysis was carried out to evaluate the effects of thermal exposure, applied strain and frequency on the dynamic mechanical response of the composites. The effects of the applied resin hardener and thermal exposure on the flexural strength, flexural modulus and dynamic impact response of the composites were also investigated. The flexural properties were determined using 3-point bending test, while the impact test was carried out using Split Hopkinson Pressure Bar (SHPB). TGA analysis of the reinforced and unreinforced epoxy showed no significant weight loss until the test samples were heated above 250°C in an inert atmosphere. Dynamic Mechanical Thermal Analysis (DMTA) on the composites indicated the glass transition temperature to lie between 80 and 100°C.

The results of the flexural and impact tests showed that the mechanical integrity of both glass and Kevlar® fiber reinforced epoxy composites remained unimpaired by radiative or convective heat exposure for up to 3 h until the exposure temperature exceeded 200°C. This is much higher than the service temperature of cowling panels of light engine recreational aircrafts. When the manufactured fiber reinforced epoxy composites were exposed to temperature above 200°C matrix degradation occurred, which became very significant when the exposure temperature was higher than 250°C. Extensive delamination and matrix cracking occurred when the composites were exposed to the temperature range 250°C - 300°C for 1 h. Fiber-matrix debonding was not observed in the composite except after failure under impact loading. This is evidence of the fact that the epoxy matrix was adequately wetted by both the glass and Kevlar® fibers resulting in the strong fiber/matrix interfacial bonding. While the Kevlar® reinforced epoxy displayed a better damage tolerance under flexural and impact loading, glass fiber reinforced epoxy showed higher strength but lower damage tolerance. Glass fiber reinforced epoxy also showed more resistance to damage under exposure to thermal flux than Kevlar® reinforced epoxy. Under impact loading, the Kevlar® reinforced composite failed by delamination with no fiber rupture, whereas the glass fiber reinforced epoxy failed by matrix cracking, debonding, fiber rupture and fiber pullout.

The results from this research have established the effect of radiative and convective thermal exposure on the mechanical behavior of the fabricated Kevlar® fiber and glass reinforced epoxy composites. The maximum temperature reached on the inner surface of the cowling panels of a typical light engine recreational aircraft due to

heat radiations from the engine block has been estimated to be about 65°C. This is lower than the glass transition temperature of the epoxy matrix as obtained from DMTA. The low temperature rise is due to inflow cooling air into the cowling chamber in flight. The results of the current investigations suggest the suitability of composite materials for the intended application. The intensity of thermal exposure, to which the materials will be exposed in such application, may not cause any significant damage to the mechanical integrity of the composite. However, since the difference between the possible exposure temperature and the glass transition temperature is only a little over 20°C, a layer of thermal insulator on the inner surface of the cowling made of fiber reinforced epoxy will be desirable to further sustain the mechanical integrity of the composites when selected for use as choice materials for cowling panels of light engine aircraft.

ACKNOWLEDGEMENTS

A research on suitability of fiber reinforced epoxy as choice material for cowling panels of small recreational aircrafts is considered a worthy cause that can contribute to energy conservation and environmental preservation. This is due to the low density of fiber reinforced plastics, which can translate to increased efficiency.

Special thanks to Mr. Dave Deutscher, Mr. Rob Peace and Mr. Hans Steinmetz for all laboratory support offered. Thanks to Alex Tacik, a final year undergraduate student in Mechanical Engineering, for his assistance in sample preparations for microscopy and microscopic analysis of the samples. I sincerely appreciate my advisory committee members; Prof David Torvi, for his valuable input in the cause of my research, providing support and granting permission to use his cone calorimeter and to Prof Ike Oguocha for all his scholastic advice and contributions drawn from his wealth of experience. I thank Mrs. Kelley Neale for her great support. I express my profound appreciation to my mentor and supervisor, Prof. Akindele Odeshi for all the guidance, support and help patiently provided, to ensure this program came out successful.

Thanks to the management of Champion Airpark Canada, a recreation Aircraft operating company in Estevan, for insightful discussion on generation and distribution of heat flux inside the cowling of light engine aircrafts. To the management of Nexans Inc. Canada, I thank you for every support given on this research endeavor. I appreciate my parents, Mr. Abiodun Samuel Shaba and Mrs. Leah Adesoye Shaba for their parental training and guidance over the years. Also to my siblings; Bosede Shaba, Tunde Shaba, Bayo Shaba, Wale Shaba and Elizabeth Shaba, I say thank you all for your great support. God has brought us this far. To my dear friends, Folake Ademorijinmi, Douglas Akhimienmhonan, Ehimai Ohiozebau, Ifedi Odinakaeze, Unyime Umoh and Ayodele Olagunju, I appreciate you all for staying closely with me all through this work. Your support and encouragement were so lifting. To my precious jewel and dearest wife, Olatoyosi, and to my wonderful sons – Richard, Ritchie and Raymond, thanks for your unflinching love. We won again by the power of the LORD! Thanks for your understanding all through the stressful moment when my attention was completely taken away from home. To all members of Redeemed Christian Church of God, Peculiar Peoples Parish in Regina, thank you for your unflinching support. Love you all!

DEDICATION

This work is dedicated to my **Lord Jesus Christ**, the Lover of my soul.
To God be the glory.

And to my loving wife,
Olatoyosi Mercy.
You are blessings to my world.

To my wonderful sons,
Richard, Ritchie and Raymond
…. The joy you gave each day has strengthened me all through.

And to my lovely parents,
Mr. Abiodun Samuel Shaba and Mrs. Leah Adesoye Shaba
God is fulfilling your dreams in us…. your prayers of years past till today are greatly rewarding.

TABLE OF CONTENTS

LIST OF TABLES

LISTS OF FIGURES

NOMENCLACTURES

Acronymes

AMC	Aluminum Matrix Composite
ASTM	American Society for Testing and Materials
CFRC	Ceramic Fiber Reinforced Ceramics
CMC	Ceramic Matrix Composite
CTE	Coefficient of Thermal Expansion
CVD	Chemical Vapor Deposition
DMTA	Dynamic Mechanical Thermal Analysis
FRP	Fiber Reinforced Plastic
MMC	Metal Matrix Composite
MOL	Material Operational Limit
OM	Optical Microscopy
PMC	Polymer Matrix Composite
RIM	Resin Infusion Molding
RTM	Resin Transfer Molding
SEM	Scanning Electron microscopy
TGA	Thermo-Gravimetric Analysis
Tg	Glass Transition temperature

Symbols

ε	The emissivity of the exposed surface,
E	The emissive power, W/m^2
E_f	Flexural Modulus of elasticity, (MPa)
ϵ_f	Strain in the outer surface, (mm/mm)
G	The irradiation, W/m^2
h	Conventional heat transfer coefficient, W/m^2K
q''_{conv}	Convective heat flux
q''_{rad}	Radiative heat flux, kW/m^2
T_{eng}	Exposed surface temperature, K (Engine block temperature).
T_∞	Surrounding chamber gas temperature, K.
T_{cowl}	Temperature of the cowling, K

τ_d	Interfacial debond strength
τ_f	interfacial shear strength
σ	The Stefan-Boltzmann constant =5.67 x 10^{-8} W/m^2 K^4
σ_a	Applied stress
σ_d	Debond stress
σ_f	Fiber stress, (Stress in outer fibers at midpoint), MPa
σ_m	Matrix stress, MPa
V_f	Volume fraction of fiber
V_m	Volume fraction of matrix

1. INTRODUCTION

1.1 Overview

Engineering design has experienced significant advancement through the development of engineered materials with well-tailored properties not found in traditional engineering materials. Typical examples include synthetic composite materials, which consist of two or more distinct materials with different properties to form a single material having combination of properties not possessed by either of the constituent components. Their application has gained very wide popularity in the field of engineering. Lightweight fiber reinforced polymer matrix composites materials, also called fiber reinforced plastics (FRP), are finding widespread application in advanced technology due to their unique combination of properties such as high specific strength and modulus and low thermal expansion coefficient [1]. The use of composite materials is evident in various aspects of human endeavor. This ranges from recreation equipment such as golf clubs, recreational boats and tennis racquets [2] and commercial building construction to structural applications in automobiles, trains and aircraft.

Weight reduction is a very important design criterion in engineered products and structures such as aircraft, automobiles, boats and ships. Weight reduction in these structures may cause increased speed and payloads, which enhance fuel efficiency and reduction in green house gas emission. The introduction of FRP in the design of load bearing structures of transportation vehicles offers viable solution to the challenges of weight reduction in the engineering structures. The superior strength, chemical and physical properties of FRP make them choice materials for structural application not only in the transportation industry but also in modern building designs [3]. Fatigue is one of the major causes of failures and air crashes in the aviation sector. In addition to their higher specific strength fiber reinforced composites show excellent fatigue behaviour. Successful application of polymers, especially FRP in structural applications in engineering is therefore seen as a major achievement, but not without some inherent challenges. For example, because of their chemical structure, prolonged exposure of fiber reinforced polymer to elevated temperatures can lead to polymer degradation, delamination, debonding and matrix cracking which can result in loss of mechanical integrity [3, 4]. One of the major structural applications of FRP is in the field of military and commercial aircraft, for which weight reduction is very critical for high speed and increased payloads [5, 6]. The development of excellent material with an improved deformation and fracture resistance under dynamic shock loading is very important, especially for applications such as in automobile body panel or aircraft fuselage

where exposure to high velocity impact cannot be ruled out. Hence it is very important to understand the effects of service condition and processing variables on the resistance of FRP to fracture under dynamic impact loading.

1.2 Motivation

A Large amount of drag force was experienced at the frontal section of the Cessna 177 Cardinal recreational aircraft due to oversized cooling inlets as well as poorly positioned air intake when operated in Saskatchewan. Redesigning of the cowling geometry was considered necessary to correct this problem, reduce the drag force and improve the flow of cooling air in the aircraft engine. This project was assigned to the Mechanical Engineering final year students of the University of Saskatchewan and Kevlar® 49 fiber reinforced polymer was selected for the rebuild of the cowling [5]. The preference for Kevlar® reinforced epoxy composite over aluminum was due to the difficulties encountered in forming the previously used aluminum plate into the new cowling design. However, detailed thermo-mechanical characterization of the Kevlar® fiber reinforced epoxy selected for this design was not carried out to ascertain its suitability as good replacement for aluminum in this design.

Cessna aircraft are commonly used as recreational aircraft and as crop sprayers in large-scale farming. Exposure of this aircraft's cowling made of FRP to heat fluxes from the aircraft's engine may impair its mechanical integrity and pose danger to the safety of personnel on board. Unforeseen impact load from extraneous objects (e.g. bird strike) are some of the factors that may also pose a threat to the use of FRP used to construct the cowling of the aircraft. The vibrations from the aircraft engine as well as from hydrodynamic shock during flight can create some dynamic loading effect on this material at the same time. It is therefore important to investigate the mechanical integrity of this fiber reinforced epoxy as influenced by thermal exposure and dynamic loading conditions.

1.3 Objectives

The overall goal of this project was to synthesize fiber reinforced epoxy matrix composites using simple hand lay-up method and to assess their suitability for application in fabricating cowling panels of small recreational aircraft such as the Cessna 177. The specific objectives of this research are to determine:

1. The effects of convective and radiant heat exposure on the mechanical behavior of fiber reinforced epoxy matrix composite
2. The effects of type of the applied reinforcing fiber on the mechanical integrity of fiber reinforced epoxy matrix composite.
3. The effects of the applied resin hardener and curing condition on the mechanical response of the composite to dynamic and quasi-static loading.

1.4 Thesis arrangement

This thesis consists of five chapters. An overview of the project, motivation for this work and research objectives are presented in Chapter 1. A review of previous work relevant to the research topic is provided in Chapter 2. Chapter 3 contains detailed discussions on the materials and equipment used and the experimental test method. In Chapter 4, the research results obtained from various thermo-mechanical tests, dynamic mechanical thermal analysis, and microstructural evaluations conducted in the course of this research are presented and discussed. The conclusions drawn from the analysis of the tests results and recommendations for future work are provided in Chapter 5.

2.0 LITERATURE REVIEW

Fiber Reinforced Composites have gained significant recognition as viable alternatives to metallic materials in the transportation industry and in modern building design, where their high specific strength and/or excellent resistance to fatigue failure make them choice materials. Many researchers have continued to work on various subjects that involve their synthesis and characterization for applications in a wide range of engineering structures. Some of these works from previous research that are relevant to the current research project are highlighted and are reviewed in this chapter.

2.1 Composite materials

The words "composite material" is coined out from the phrase "composition material" which refers to material made of two or more constituent materials with different physical and chemical properties. The principal goal of combining the constituent materials in a composite is to create superior and unique materials that combine the desired properties of all the constituents while retaining their identities in the new product. Composite can be defined as a multiphase material that is comprised of two (or more) distinctive materials with dissimilar properties that are separated by a distinct interface. A composite material has a significant proportion of the properties of each of the constituent phases.

In many cases, a desired combination of properties needed for a particular application may not be achievable in a single material. Composite materials are designed to exhibit optimum combination of properties in a way that is not achievable in monolithic materials [7]. They could be naturally occurring materials such as wood and bone or artificially synthesized materials as in the case of fiber reinforced plastic (FRP), ceramic matrix composite (CMC) and metal matrix composite (MMC). Naturally occurring composite materials are relatively less expensive and have lower mechanical strength than the artificially synthesized composites. In artificial composites, some desirable properties from the constituent materials are combined to produce components with uncommon combination of properties. Many composite materials possess unique combination of properties such as low densities, strength, high stiffness and abrasion rate, high impact resistant and high resistant to corrosion or chemical attack [8, 9]. Good fatigue tolerance, high specific strength and specific stiffness favor the choice of FRPs for high performance applications in the defense, automobile, aerospace and recreational industries [10]. In addition, FRPs are also candidate materials for the high-speed robotic hand system, where a combination of

strength and lightweight is desired [11].

Fiber reinforced plastics generally show higher damage tolerance than ceramics and can also exhibit high strength to weight ratio and have wider application in many engineering fields [12]. But the application of polymers is limited by their service temperature, which in most cases can be pegged to a little above 200ºC. Whereas thermosetting polymers are strong and rigid, unreinforced thermo plastics suffer from low strength and poor stiffness. The high strength of fibers is combined with low density and excellent chemical resistance of polymers in FRPs. One of the major problems associated with the use of FRPs is debonding which can occur at the matrix-reinforcement interface due to the difference in coefficient of thermal expansion (CTE) of the reinforced and reinforcing phases when the composite is exposed to elevated temperature. Thermal induced delamination can also occur due to thermal mismatch between the matrix and the reinforcing fibers [12].

2.2 Classification of composite materials.

Composite materials are classified as metal matrix composites (MMC), polymer matrix composites (PMC) or ceramic matrix composite (CMC) depending on the continuous phase. Composites materials are also classified based on the type of reinforcing materials: fibers- particle- or whisker-reinforced composites.

2.2.1 Metal Matrix Composites (MMCs)

MMCs typically comprise of ductile metallic alloys as the matrix phase and a reinforcing phase, which can be ceramic fibers, whiskers or particles. The addition of the reinforcing phase to metallic materials considerably improves their strength, stiffness and possibly creep resistance [1, 9]. The development of MMC has focused mostly on the light-metals matrices such as aluminum alloy. For example aluminum alloys are reinforced with discontinuous SiC particulates (whiskers) to produce isotropic aluminum matrix composites (AMCs) with higher strength, stiffness and wear resistance than their respective monolithic aluminum alloys. Anisotropic, high-performance AMCs are produced by reinforcement of aluminum alloys with continuous elastic monofilaments (e.g. boron) and multi-fiber yarns, such as SiC and Al_2O_3. These combine the low density of the aluminum matrix with the high strength of the reinforcing fibers [1, 13]. The results of various research investigations have shown that reinforcement of aluminum alloys with discontinuous SiC whisker or particulates produces a potentially low cost composite with high specific stiffness, which can be used in mechanical forming techniques [13]. The structural components of many aircraft are made of light-metal MMCs such as boron fiber reinforced aluminum

and graphite fiber reinforced magnesium composites [13]. In some space applications, where very light weight, high specific stiffness and near-zero coefficient of thermal expansion are highly required, magnesium alloys are reinforced with graphite fibers to form MMCs that meet such a stringent service requirement [13]. Improved stiffness and temperature capability is achieved by reinforcing titanium alloys with SiC fibers for aerospace applications [13]. The mechanical properties of MMCs depend largely on the composition and parameters such as the types, size, volume fraction, aspect ratio and spatial orientation of the reinforcement.

High temperature MMCs can be produced by reinforcing superalloys with high strength and high temperature refractory fibers, thereby producing a high performance composite material with a significantly enhanced thermal resistance when compared with unreinforced alloy. As an example, tungsten, SiC and niobium fibers have been used to reinforce superalloys to form a high temperature MMCs, which have an improved creep properties and allowable service temperature range that can be utilized in turbine blades and aircraft engines [13]. A major concern in the use of fiber reinforced superalloy is the possible formation of brittle intermetallic compounds as a result of chemical reaction between the fibers and the matrix at high temperatures [13].

2.2.2 Polymer Matrix Composites (PMCs)

Thermoplastic polymer structures are bonded with covalent and secondary bonding, which are characteristically weak. Polymers have low density and good chemical resistance compared to metallic materials. These make them choice materials for aerospace applications especially in the fabrication of the fuselage and wings. However the low strength and poor stiffness of thermoplastic polymers limits their structural applications in most cases. The poor mechanical properties of polymers are overcome by suitable reinforcement with woven fibers. Most polymer matrix composites (PMCs) consist of thermosetting or thermoplastic polymer matrix reinforced by 2-Dimensional woven fiber clothes. The fibers commonly used as reinforcement for polymers include carbon, glass and aramid fibers. These may be continuous or short fibers. Examples of polymers commonly used as matrices in PMCs include polyesters, epoxy, phenolic, vinyl esters etc. As a result of their superior mechanical properties and better moisture resistance capability compared to vinyl or polyesters resins, epoxies are the most commonly used polymers as matrices in the fabrication of PMCs for aerospace applications [8].

Fiber reinforced plastics have high specific strength and high specific E-modulus and are gaining increasing attention as choice materials for aerospace applications. A PMC was first used as aerospace material in the early

1940's when Fiberglass/polyester composite was developed as radar-transparent materials to protect radar system on the military aircraft during the World War II. There was an expansion in the structural application of FRP after the war with more than 85% of the nearly 1 million kg of the reinforced plastic market in the US being fiberglass/polyester as at 1984 [13]. Following the development of graphite and aramid fibers, fiber/epoxy composites are gaining popularity in the construction of airframe structures. Other examples of PMC application in the aerospace structures include the polyimide matrix composites, which are fast gaining ground in the design and fabrication of aerospace components [13].

2.2.3 Ceramic Matrix Composites (CMCs)

Ceramic matrix composites are composed of ceramics as the continuous phase and ceramic fibers, whiskers or particles as the reinforcements. Although monolithic ceramics have good compressive strength and high modulus of elasticity, they have low tensile strength and poor fracture toughness, which limit their structural applications [7]. Most conventional technical ceramics such as silicon carbide, silicon nitride, alumina and zirconia exhibit very low resistance to cracking, low thermal shock resistance and low fracture toughness, which hinder their applications in areas where their high-temperatures, strength and excellent resistance to corrosion are required. Ceramic matrix composites (CMCs) are developed to address and overcome the intrinsic brittleness and low fracture toughness of monolithic ceramics. The aim is to obtain ceramic materials with an enhanced fracture toughness, good thermal shock resistance and improved dynamic load capability [14]. This is achieved by introduction of new ceramic phase in form of particulates, whisker or fibers as reinforcements. These reinforcements impede the propagation of cracks in the brittle ceramic matrix. For example, improvement in the fracture resistance of ceramic materials by particle reinforcement is made possible by the interaction between dispersed particles, which results in deflection of cracks and eventually crack arrest. Typically, the matrix and reinforced fibers of ceramic matrix composites are made out of monolithic, polycrystalline ceramics and refractory compounds such as silicon carbide (SiC), silicon nitride (Si_3N_4), MgO, ZrO_2, Mullite (Al_2O_3-SiO_2), B_4C, TiC, TiN, Alumina (Al_2O_3) and carbon (C), which provide the best high temperature properties for structural components due to their high stiffness, excellent high temperature strength, thermal stability and good oxidation resistance [13,14]. Examples of CMCs are Al_2O_3/Al_2O_3, SiC/SiC, C/C, C/SiC, Si_3N_4/TiC and Si_3N_4/SiC composites. The reinforcing phase can be in the form of particulate, whiskers, short fibres, continuous or woven fibers (2D or 3D). Generally, CMCs are hard, stiff, strong thermally stable and corrosion resistant. Reinforcing

ceramic matrix with carbon nanotubes produces composite with high temperature stability as well as exceptional toughness and creep resistance [18].

The application of CMCs varies widely in engineering. These include cutting tools and dies, abrasives equipment, components of turbine engine, low weight components for rotary equipment, bearing, seals, brake disks, and brake system components, in which extreme thermal shock is commonly encountered [14]. In the aerospace industry, CMCs find applications in the fuel injection systems and valves, power units, combustors, structures etc. An example is SiC fiber reinforced, Si_3N_4 developed for such application at National Aeronautics and Space Administration (NASA), Lewis research center, Ohio [13]. In the automotive industry, they are used as heat engines, catalyst converters, drivetrain components, fuel injection components, turbocharger rotor, water pump seals etc. In the defense industry CMCs are used in construction of tank power trains, submarines shaft seals, improved armors, propulsion systems, ground support vehicles, military weapon system, military aircraft (airframe and engine) and wear-resistant precision bearings [9]. In biological and chemical engineering field, CMC are used in building artificial teeth, bones and joint, catalysts igniters and refractories [9, 13]. In Nuclear industry, CMCs are finding useful application in nuclear fuels and reactors [9, 13].

2.3 Fiber reinforced plastics

Fiber reinforced plastic (FRP) consist of reinforcing fibers dispersed within a continuous polymeric matrix phase, which can be thermoset or thermoplastic. The fiber is the principal loading-carrying component of the composite while the polymeric matrix phase binds the fibers together and also serves in distributing load within the material. FRPs generally contain between 30% and 70% volume fraction of fibers [15]. Fibers are typically characterized by very high breaking strength. Most common commercial fibers used for reinforcing plastics include E-glass and S-glass, Kevlar®, boron, silicon carbide, aluminum oxide and carbon [16]. The tensile strength of some polymers increases up to about 10 times through reinforcement with fibers. An example is the improvement in the tensile strength of phenolic resin through graphite fiber reinforcement to form a composite, whose tensile strength can compare favorably with that of AA6061 aluminum alloy that ranges between 193 and 290 MPa and compressive strength of 207 and 290 MPa [17].

The development of fiber reinforced polymer is targeted at producing a low-density polymer-based material, which has high stiffness and high strength. The reinforcing fibers and their correspondence matrices are carefully selected

in the development of FRP by considering their respective properties, which have considerable influence on the mechanical properties of the composite. The magnitude of the fiber-matrix interfacial bonding determines the ultimate strength of FRP. Wang *et al*. [19] reported that efficient load transfer between the matrix and the fiber, which result in improved mechanical properties, is promoted by strong interfacial bonding between the fiber and the matrix [19]. Adequate wetting of the fiber with the liquid polymer is very crucial for development of a strong interfacial bonding between the fiber and the matrix [20]. Pesneau *et al*. [21] underscored the importance of good and adequate wettability of fiber mats with the polymer resin during fabrication of FRP composite products, in relation to composite strength and service performance [21]. Gautam [22] also traced the strength of FRP to the strength of the bonding between the reinforcing fibers and the polymer matrices. Another factor that influences the mechanical behavior of FRP is the fiber volume fraction. As the fiber volume fraction (the principal load carrying component) increases, the composite strength and stiffness increases too [22]. When compared with the polymer matrix, which possess a low stiffness, fiber reinforced plastics have high specific strength and modulus in addition to the high corrosion resistance of polymers. This favors the application of FRP in the automobile and aerospace industries [23].

2.3.1 Reinforcing fibers

Fibers are available in different commercial forms. Typical fibers commonly used in composite reinforcement include: E-glass and S-glass, Kevlar®, boron, silicon carbide, aluminum oxide and carbon fibers. Glass, aramid and carbon fibers are the most commonly used fibers in polymer reinforcements to produce high performance FRPs for structural applications [15]. Some of the fiber types commonly used in composites include continuous filament, chopped (discontinuous) strand mat, woven cloth fabric, woven roving etc. Fabrics are produced in different weave forms with different fiber bundle sizes, which could have significant effects on mechanical properties of the FRP. When combined with the polymer matrix to form a composite with low density, high corrosion resistance, high specific strength and modulus is formed, which is finding wide applications in load-bearing structures.

2.3.1.1 Glass fibers

There are three classes of glass fibers: E-glass designated for electrical use, S-glass used for high strength application and the C-glass, commonly used for civil engineering applications [15]. Glass fibers have the advantage of high tensile strength, high chemical resistance and excellent insulating properties over several other fibers. They can easily be manufactured by drawing from molten state into very fine filaments with diameters

ranging between 2 - 13 μm [15]. Polymers reinforced with glass fibers are very useful in a highly corrosive environment due to chemical inertness of glass fibers and the polymer matrix. One disadvantage of glass fibers is that small abrasion or flaws on the surface of glass fiber can reduce its tensile properties and consequently affects the resulting composite strength [8, 24]. Rudzinski *et al.* [24] reported that thermal stability and good design flexibility could be achieved by application of glass fiber reinforced polymer in automotive hoods, an area where design flexibility and resistance to thermal degradation is critical because of continuous exposure to elevated temperatures.

2.3.1.2 Kevlar® fiber

Kevlar® fibers belong to the family of aramid (aromatic polyamide) fibers, which are characterized by very low density and high strength-to-weight ratio [6]. These fibers have higher fracture strengths and modulus than most other polymeric fibers [8]. Kevlar® fibers have excellent fatigue and creep resistance and they are low conductors of electricity [15, 25]. Kevlar® fibers possess unique properties such as lowest specific gravity and high strength-to-weight ratio when compared to most other polymeric fibers [6] and this has enhanced their application in the manufacture of FRPs. Its outstanding strength-to-weight ratio makes it very attractive as the choice fiber for FRP design [26]. When Kevlar® fiber is used as reinforcements for polymers, the resulting composite has very high specific strength and good fracture toughness [16]. As a result of their good resistance to impact failure, Kevlar® fiber reinforced polymers are used for military applications such as body armor and protective clothing used by the fire fighters as well as helmets and gloves [8]. Kevlar® fibers are also used as reinforcement in tires, ropes, gasket, missiles, sporting goods, pressure vessels and sometimes in automotive brake system and clutch linings [16]. The structure of Kevlar® fiber is mostly aligned along its axis, i.e. the chain molecules are oriented along the axis of the fiber as shown in Fig. 2.1. This arrangement greatly enhances the fiber strength and impacts the fiber with desire properties such as good flexibility and abrasion tolerance. The aramid ring provides good thermal stability. Kevlar® fibers are available in the following grades; Kevlar® grade number 29, 49 and 149 [6, 15]. The properties of the various grades of Kevlar®, glass and carbon fibers are compared in Table 2.1.

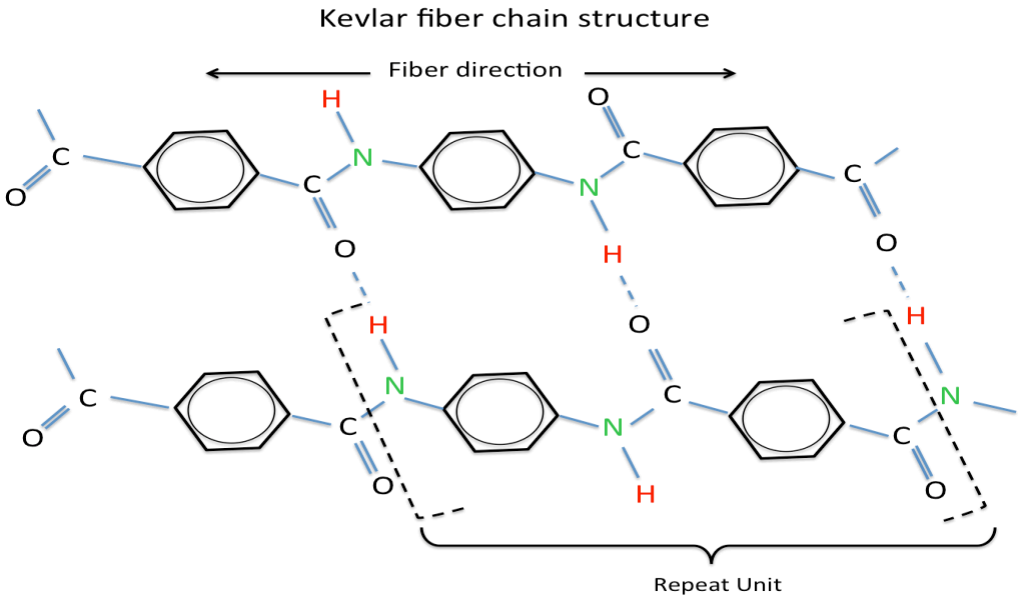

Fig. 2.1. Aramid (Kevlar®) fibers chain structures [adapted from 8]

Table 2.1. Properties of Kevlar®, glass and carbon fibers [15]

Grade	Density (g/cm^3)	Tensile strength (GPa)	Tensile modulus (GPa)	Tensile elongation to fracture (%)
Kevlar® 29	1.44	2.27	83/100	2.8
Kevlar® 49	1.44	2.27	124	1.8
Kevlar® 149	1.49	3.4	186	2.0
E- Glass	2.55	1.72	72	2.4
S- Glass	2.49	2.53	87	2.9
Carbon	2.00	2.48	525	1.1

The two most commonly used Kevlar® in the manufacture of FRPs for structural applications are Kevlar® 29 and Kevlar® 49 [15]. Kevlar® 49 fiber is known to have very low thermal conductivity, but a very high vibration-damping coefficient. Kevlar® 149 which is an improvement of Kevlar® 49 has a tensile modulus that is 40% higher than that of Kevlar® 49, although it possesses a lower strain-to-failure [6]. The tensile modulus of Kevlar® 29 is relatively very close to that of E glass fibers (electrical grade glass) and S glass fibers, yet it possesses a

density that is almost half the density of glass. This implies that Kevlar® fibers is a better choice over glass fibers where lightweight is a major design consideration. The weight can even be further cut down with the use of Kevlar® 49 or 149 if the higher specific strength is desired [15]. Kevlar® filament is made through a process, which involves extrusion of precursor through a spinneret, the process that earns Kevlar® fiber its anisotropic nature i.e. stronger and stiffer in the axial direction than in the transverse direction [15]. Graphite fiber is known to possess similar anisotropic nature too [16, 15]. Optimum reinforcing capability of Kevlar® fibers can only be achieved if the composite is used at temperature below 300^{o}C [16]. They do not melt at elevated temperatures but only degrade.

2.3.1.3 Carbon fibers

Carbon fibers have good thermal conductivity and retain their excellent tensile strength and modulus at elevated temperature in inert environments [8, 7]. They are therefore excellent reinforcements for composite materials intended to have good thermal conductivities or for high temperature use [7]. Polyacrylonitrile (PAN), rayon and pitch are the three major polymer precursors used in producing carbon fibers [15, 27]. Carbon fibers have the highest specific strength and modulus of all the known reinforcing fibers [8]. They are classified into high strength, high modulus and ultra-high modulus grades and possess lower thermal expansion coefficient than both Kevlar® and glass fibers [15]. A major drawback to high temperature use of carbon fibers is their poor oxidation resistance at high temperatures [8]. Carbon fibers are commonly used in advanced polymer-matrix composite used in high performance applications including aircraft structural components (military and commercial), filament-wound rocket motor cases, pressure vessels and recreational equipment [8, 28].

2.3.2 Epoxy matrix

Epoxy is one of the most popular thermosetting polymers used as the matrix in the manufacture of FRP for high performance structural applications [19]. Epoxy basically refers to a chemical group consisting of an oxygen atom chemically bonded to two already bonded carbon atoms [2]. Epoxy was the matrix material used in this study, while glass and Kevlar® fibers were selected as the reinforcing phase. Preference for epoxies is due to its wide range of very useful properties such as excellent chemical and solvent resistance, excellent bonding and proper adhesion to different variety of fillers and fibers (enabled by its inherent polar nature), and absence of toxic volatile by-product during curing [29]. A fully cured epoxy is stronger and stiffer with better durability and a higher

maximum operating temperature when compared to other thermosets [2]. Its electronic characteristics favor the application of epoxy in the electronic packaging industries [30, 19]. Industrial applications of epoxies include its usage as adhesives, laminating resin, sealants, casting compounds, varnishes and paints. The adhesive properties of epoxy, its resistance to water absorption and the accompanying degradation make it ideal for boat building [31]. When reinforced with fibers, the resulting epoxy matrix composite possesses a high strength-to-weight ratio and good resistance to environmental degradation, and finds useful application in aircraft fuselage and components [31]. Epoxy matrix composites can be fabricated with a relatively high degree of dimensional accuracy owing to low shrinkage of epoxy resin during curing [29].

Epoxies are classified into two major categories: glycidyl epoxy and non-glycidyl epoxy as shown in Fig. 2.2. The glycidyl epoxies are produced through condensation reaction of dihydroxy compound, diabasic acid or a diamine and epichlorohydrin in the appropriate proportion. On the other hand, Non-glycidyl epoxies are produced by peroxidation of olefinic double bond. Most commonly used epoxies are glycidyl-ether epoxies e.g. diglycidyl ether of bisphenol-A (DGEBA) and novolac epoxy resins.

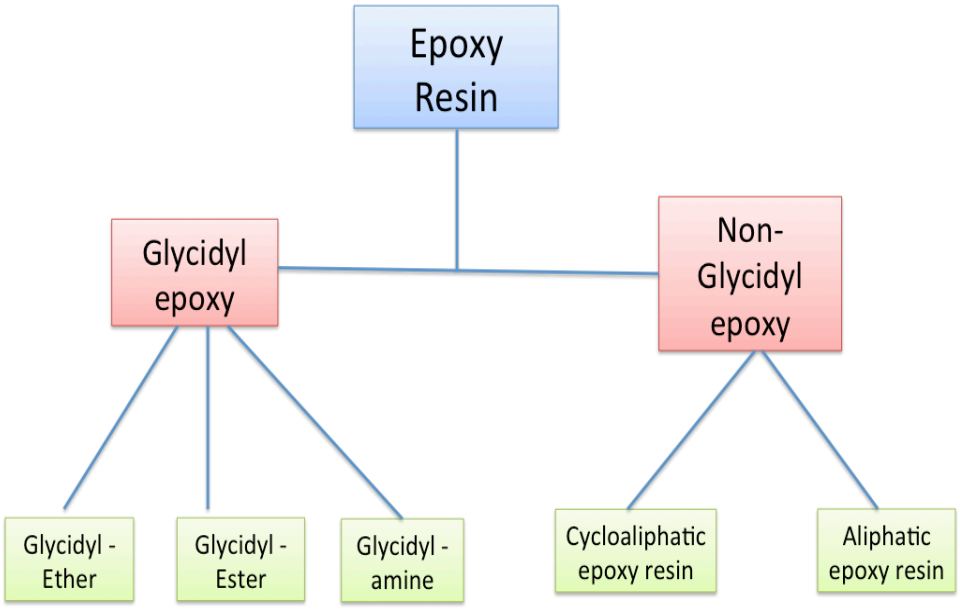

Fig 2.2. Classification of epoxy resin.

The epoxy resin consists of epoxide rings at the ends of its molecules and a curing agent (called hardener), which contain amines or anhydrides [2]. Amines are the most commonly used curing agents for epoxy. Makoto et al. [32] examined the formation of hardeners from different amines and anhydrides families and suggested the cyclic dicarboxylic and polycarboxylic acid to be best suitable for crosslinking epoxy resin. Unlike polyester resins,

which are cured by catalyst, epoxy resins are cured by an amine sites called hardener by the process of additional polymerization reaction in which two epoxy sites are bonded to each amine site in the hardener to form a complex three-dimensional network [31]. The molecular structures of epoxy resins have some similarity with the long chain molecular structure of vinylester, both having reactive sites at either end. The only different is that epoxy group forms these reactive sites in epoxy resin while ester group in vinylester forms the reactive sites. Tetraglycidyl 4,4-diaminodiphenymethane (TGDDM) is an example of a multifunctional epoxy resin, which create a highly crosslinking 3D network [31].

A mixture of liquid epoxy resin and the curing agents have low viscosity and can therefore easily impregnate fiber preforms during composite manufacture. The curing of epoxy can easily and quickly be achieved at temperatures ranging from 5°C to 150°C, depending on the choice of curing agent. Pure epoxy has glass transition temperature (T_g) of about 170ºC [19]. Glass transition temperature (T_g) in polymer is the temperature range over which polymer chains mobility increases significantly, thereby causing the thermosetting polymer to experience change in its rigid or hard state to a more pliable or softer state. The chemical structure of the epoxy resin, the hardener type and the degree of cure are some of the factors that could affect the maximum T_g of a thermosetting polymer [33]. An accelerated curing can be achieved when excessive amount of curing agent (hardener) is used, but this will affect the working life, and thermal stability of the resin. Epoxy is considered to be highly combustible as well. When it is thermally decomposed by exposure to high level of heat flux, it yields a substantial quantity of flammable volatiles [33]. Other polymeric materials used as matrix in a fiber reinforced composite as previously mentioned includes phenolic resin, which is known for its excellence fire retardant property and polyester resin.

2.4 Thermal degradation and flammability of fibers and fiber reinforced composites.

A widespread application of polymer matrix composite (PMC) in load-bearing primary structures is limited by the susceptibility of many polymers to easily catch fire and release large amount of smokes and toxic fumes in the process [66]. In addition to fatigue, the other prominent source of damage to aircraft fuselage structure can be due to impact from extraneous object as in bird strike, impact from hailstones or lightning strike [34]. The use of fiber reinforced epoxy in the design of aircraft fuselage is therefore not without its challenges. A significant problem associated with fiber reinforced epoxy is its poor fire resistance due to its high combustibility. The overall long-term durability of FRP, especially when subjected to harsh environmental conditions poses a concern. This is with respect to the capacity to sustain their high level performance at elevated temperature and under impact loading. Generally, polymers lose their E-modulus (stiffness) and flexural strength when exposed to excessive thermal flux,

especially above their glass transition temperature, which often ranges between 80°C to 150°C. Exposing polymers to a temperature much higher than the glass transition temperature can lead to degradation of chemical structure or decomposition leading to loss of mechanical properties, and combustion [35, 36, 37]. Thermal properties of the disperse phase (fibers) can also play a significant role in determining the thermal and mechanical response of a fiber reinforce plastic on the long run [36]. Karbhari *et al.* [38] recommended that FRPs should not be used in any application that involves exposure to temperatures above their glass transition temperatures. The acceptable practice in structural design requires that the chosen materials should have a T_g of at least 30°C above the maximum expected service temperature to ensure reliability [38].

Glass and carbon fibers are more thermal and fire resistance than combustible polymeric fibers such as aramid fibers and polyethylene fibers, which easily degrade when exposed to fire [33]. Polymer matrix composites made of Kevlar® fiber has ignition time that is shorter than those made with glass or carbon fibers [39]. Studies by Brown *et al.* [40, 41] showed that decomposition of Kevlar® reinforced epoxy begin at relatively low temperature of 150°C to 250°C as combustible gases which can aid quick ignition are formed during the decomposition process. The formation of these combustible gases is delayed for a longer period of time in composites reinforced with carbon or glass fibers [40, 41]. Aramid fibers degrade easily when exposed to strong acids and bases, but relatively inert when exposed to other chemicals or solvents [8]. Another study by Lay *et al.* [42] showed that polyesters based composite ignite faster than the vinylester based composites, however they both exhibit similar rate of heat release in every test condition [42].

There has been extensive research work carried out various techniques to improve the fire resistance of FRPs [3, 17, 39, 42]. In most applications where fiber composites are directly exposed to fire, flame retardant additives such as phosphorus and nitrogen based intumescent and char promoting agents are added to slow down resin decomposition [3]. Resins are mixed with fire retardant additives such as, aluminum trihydrate, antimony trioxide and zinc borate, which can reduce flammability of fiber reinforced composite when exposed to low intensity fires. Polyester resin ignition time is doubled by suitable additions of alumina trihydrate, which consequently improves its post thermal exposure properties [42]. Some of these resins containing fire retardant additives are however very expensive and can release toxic fumes if ignited at elevated temperature [39]. Fire resistance property of FRPs can also be improved by coating the composite with a thermal barrier such as a blanket of ceramic fiber [39, 42]. This is aimed at causing some delay in the onset of combustion. Phenolic resins have inherent fire resistance. Investigations have shown that they have longer ignition period, lower heat release, lower smoke generation and lower rate of flame spread compared most other polymers when exposed to elevated temperatures and flames [39]. Phenolic resins according to several previous studies, when compared to epoxy and polyester resins experienced relative ignition delay due to slower rate of combustible gases release during combustion, which prolongs its

heating time before the gas concentration attains the level of flash point required for ignition to occur [39].

2.4.1 Effect of Thermal Degradation on Mechanical Properties of Fiber Reinforced Plastics

The mechanical properties of fiber reinforced plastics are adversely affected at high temperature by phenomena, which include resin combustion, fiber-matrix debonding, delamination and matrix cracking. Chatys *et al* [37] explained that aging, which have considerable influence of physical-mechanical properties of FRPs, may be accelerated or retarded depending on the intensity of thermal exposure of the composite [37]. The ignition time in composite can also be affected by such factors as the cross-linking density and composition of the resin matrix, the degree of curing and the type of fiber used as the reinforcement [36, 43]. Yasunobu *et al*. [26] reported that for an epoxy resin, the tensile strength decreased by about 80% while failure strain increased 11 times when temperature was changed from -50°C to 80°C. Kandare *et al*. [3] reported that FRPs lose their mechanical strength and flexural stiffness when exposed to a heat source as a result of matrix's depolymerisation [3]. When exposed to high thermal condition over a period of time, a thermoplastic matrix can soften extensively leading to increase in viscoelastic response, which may result in an increased susceptibility to moisture absorption and loss of mechanical integrity [38]. Glass fibers have been reported to have a rapid and irreversible decline in strength with the attendant impact on composite strength at high temperatures, even in the absence of stress [35].

Previous records have shown that severity of the impact of fire-related hazards associated with composite materials is higher in confined spaces such as tunnels and buildings than in open spaces such as roads and bridges [38] The heat released as a result of the heat build up and accumulation of toxic fumes within a confined space could have catastrophic effects. On the fire in an open space may be less damaging because of the release of heat and toxic fumes to the atmosphere. A composite will exhibit corresponding loss of flexural modulus and flexural strength across its depth when it is heated up to temperatures above the glass transition temperature. The loss in modulus is said to be reversible below the temperature at which, chemical degradation will occur. However, an increase in temperature above the glass temperature can result in damage to the chemical structure of the resin matrix and consequently weakens the fiber–matrix interfacial bonding and results in irreversible loss in load bearing capability of the composite [38]. Researchers have observed that physical and mechanical properties exhibited by FRPs exposed to thermal flux are not only functions of temperature but also function of time [44].

When subjected to impact loading, damage tolerance is considered to be one of the most important parameters of interest in FRPs [26]. This property is very crucial in aerospace applications, and can be influenced by service temperature. Hirai *et al*. [26] reported that for a glass fiber reinforced vinyl composite subjected to high-energy impact, a decrease in the composite capacity to resist fracture was observed, which was a consequence of transverse fiber fracture and delamination. Similarly, subjecting a cross-ply laminates of polyethylene fiber /epoxy matrix composite to a high-velocity impact shows that the energy required for damage initiation doubled as temperature was increased from -50ºC to 100ºC. Aramid and glass fiber reinforced epoxy matrix composite are not significantly affected by temperature changes within these range. However, a significant change can occur at temperature above 150ºC [26]. According to Bibo *et al*. [45], temperature increase from ambient temperature to 150ºC has little effect on carbon fiber reinforce polymers.

It has been reported that empirical relation exists between the mass loss at elevated temperature and the strength and modulus of FRPs [44]. Complex physical and chemical processes occurring in the polymer matrix at elevated temperatures accounts for the changes in both physical and chemical properties during thermal exposure [10, 46]. The results of several research efforts have shown that matrix resin behaviour governs the damage tolerance of fiber composite under impact loading [47, 48, 49, 50, 51]. Hirai *et al* [26] reported a correlation between the matrix resin failure strain and the compressive strength under impact loading. Bai *et al* [44] and Mouritz [39] reported that various forms of thermal-induced damage such as matrix cracking, degradation of fiber strength, and delamination would lead to loss of the mechanical properties of FRPs at elevated temperatures. Kandare *et al*. [10] included loss of fiber-matrix bonding strength as one of the developments that lower the stiffness of FRP during exposure to elevated temperatures. Some previous materials tests have also indicated that composite degradation due to matrix hardening, matrix micro cracking and fiber-matrix interfacial bonding can occur when FRPs are exposed to subzero temperature [38]. Also, exposure to temperature above the ambient temperature can result in an initial composite post curing, leading to strength increase and followed by degradation after a prolonged exposure. Karbhari *et al*. [38] asserted that premature debonding could occur. A summary of temperature-dependence on properties of composite materials is shown in the Fig. 2.3. As a result of the heat released during exothermic reaction accompanying decomposition within a composite material, an increase in the specific heat capacity will occur. Unlike specific heat capacity, the thermal conductivity decreases at this stage as a result of thermal resistance from the decomposed gases causing a shielding effect [44]. The E-modulus therefore decreases as shown in the diagram when glass transition occurs and drops drastically at the decomposition temperature [44].

Failure becomes inevitable when a composite made of thermoplastic resin softens excessively as a result of thermal exposure beyond the polymer's Material Operational Limit (MOL). Material Operational Limit (MOL) of a given laminating resin is the temperature at which composite flexural strength experience a decrease in its room temperature value by half. Karbhari *et al*. [38] recommended that this must be clearly factored into consideration in FRP design. Although polymer decomposition and combustion have reported to be majorly responsible for the reduction in the post-fire stiffness and strength of fiber reinforced plastic [57], gradual resin depolymerization has also been reported to occur in FRPs at elevated temperature, which also contributes to loss in strength [10]. Strumpler *et al*. [53] observed that decomposition of polymers used as conductive materials can lead to irreversible changes that affects electrical properties of the composite, when exposed to temperature above 300°C.

Thermal stresses can also develop in fiber reinforced polymer as a result of thermal exposure at elevated temperatures. Shengzu *et al*. [17] in his research observed the formation of micro-cracks at the fiber/matrix interface that was attributed to thermal stress generated during the phenolic matrix composite's exposure to temperatures of up to 300°C. He further showed that debonding occurred between the glass particles and the matrix in glass particles reinforced phenolic resin at temperature above 360°C [17]. Generating induced thermal stress in the fiber reinforced composite is capable of weakening the matrix or induce matrix cracking, and thereby reduce flexural strength and modulus.

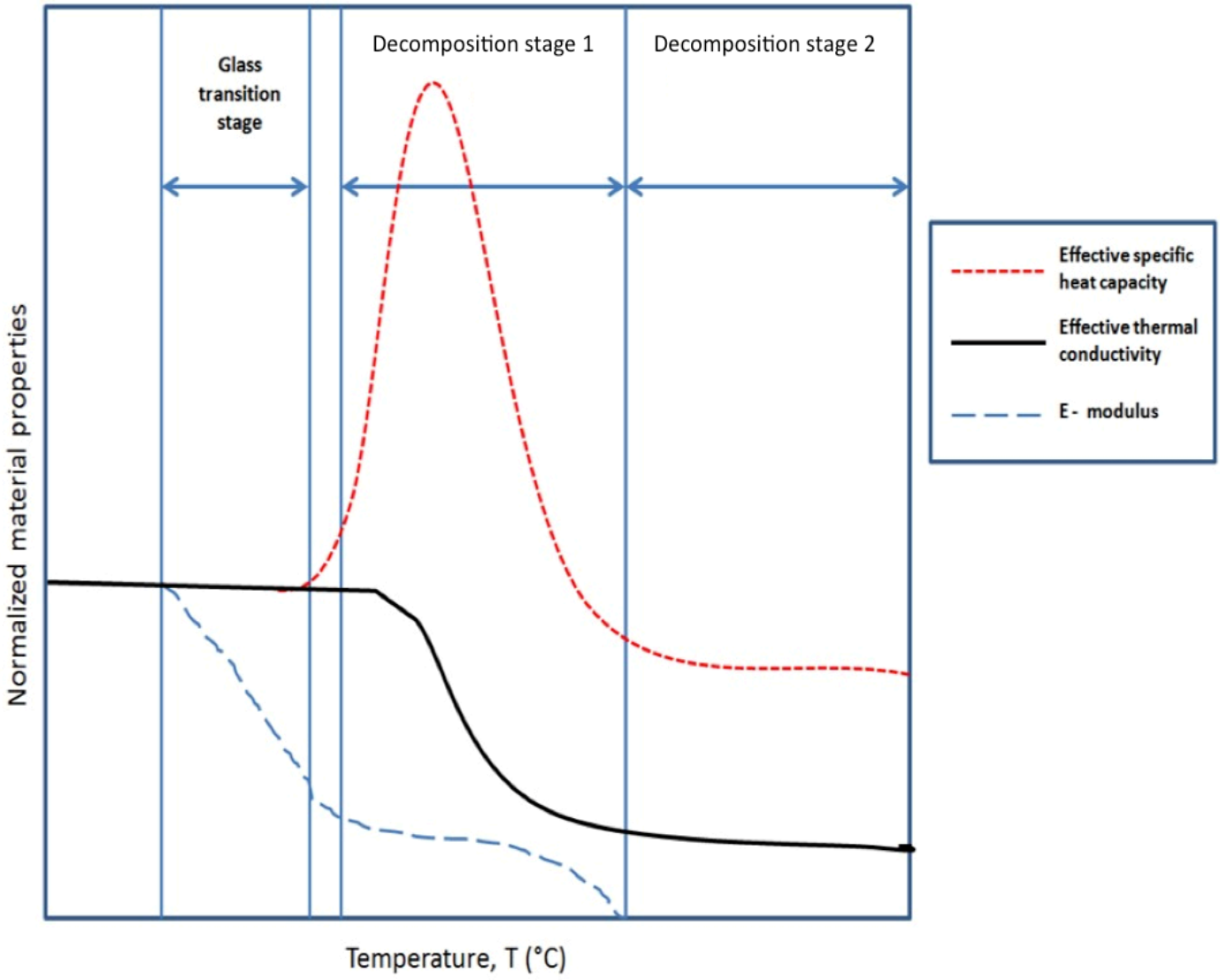

Fig 2.3. Effects of exposure temperature on mechanical and thermal properties of FRPs [Adapted from 44].

2.4.2 Stress distribution and crack generation

Sun *et al.* [54] described the typical stress distribution that occurs within composites during multiple cracking and fiber-matrix interfacial debonding and discussed the micromechanics of matrix cracking, interfacial debonding and matrix crack saturation that are associated with the composites' failure as summarized in Fig. 2.4. The Load-Displacement curve of composite shown in Figure 2.4 represents the typical damage process in the material when subjected to mechanical loading in a direction parallel to the fiber axis. When subjected to a tensile load the matrix crack initiation first occurs at the point A, a region that implies the elastic limit of matrix is reached. The matrix crack propagates in the transverse direction across the fiber. If the interfacial bonding between fibers and matrix are weak or they are frictionally coupled, thus bridged-fibers are created to assist in carrying additional loads

(crack-bridging) which consequently lead to the deflection of the matrix crack at the fiber-matrix interfaces and sliding. Generation of more matrix crack occurs when applied load is further increased and rate of propagation of interfacial debonding increases with a larger sliding zone, this is the non-linear process observed between point A and B. At point B, matrix cracking becomes saturated. Eventually, point C is reached which is the point representing the composite's maximum strength. At this point, lots of fibers within the composite fracture, thereby resulting into loss of load-bearing capacity.

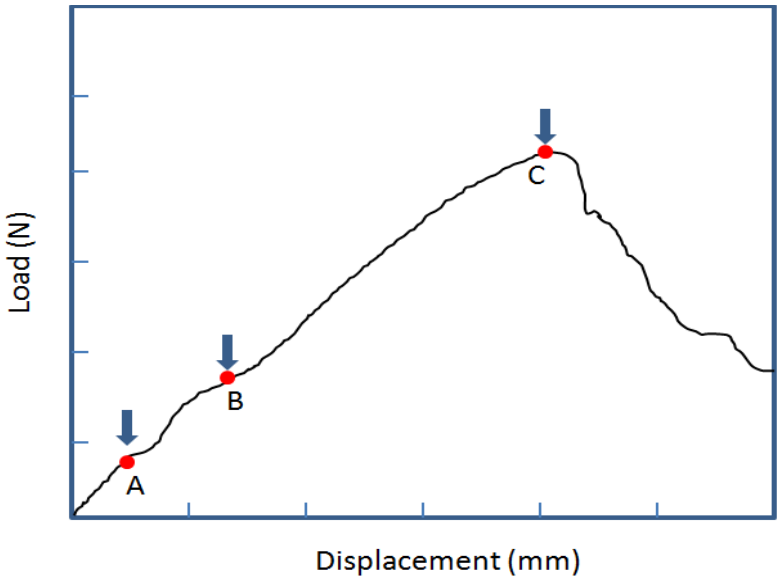

Fig. 2.4. Load-Displacement curve for a SiC fiber reinforced borosilicate glass composite subjected to tensile loading parallel to the fiber direction [54]. (A) elastic limit of the matrix (B) point where matrix cracking becomes saturated, and (C) point C- composite maximum strength)

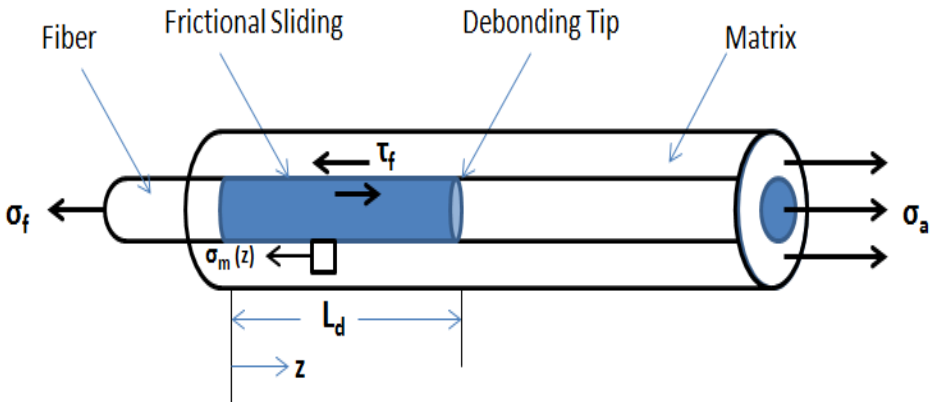

Fig 2.5. Schematic representation of stress distribution around a fiber pullout [adapted from 54].

Figure 2.5 shows stress distribution around a fiber pullout during fracture. The debond length, L_d is determined by the interfacial debond strength, τ_d. τ_f is the interfacial shear strength, σ_f and σ_m are the stress in the fiber and matrix respectively while σ_a is the applied stress and z is the sliding length. As shown in Fig. 2.5 the stress distribution in the cracked area of a partially bonded and debonded interface depends on the debond length, L_d and this is determined by the interfacial shear strength τ_u. The interfacial shear strength is determined by the nature of the debonding that occurs at the interface while the established criterion that determines the type of interface.

τ_f represents the frictional interfacial stress and τ_d is the debond shear stress. The interface is said to be unbonded when τ_d is equal to zero and it becomes strongly bonded when τ_d is greater than τ_f. The force balance in the composite cylindrical unit suggests that the length of debond (L_d) within a composite has a relationship with the applied stress σ_a, and can be represented in the equation 2.2 as shown [54]:

$$\frac{L_d}{r} = \left(\frac{V_m E_m}{V_f E_c}\right)\frac{\sigma_a - \sigma_d}{2\tau_f} \quad \text{.....2.1}$$

V_m and V_f are volume fraction of the matrix and the fiber respectively, E_m and E_c are the elastic modulus of matrix and composite, *r* is the radius of fiber [54]. Initiation of debonding occurs when the applied stress, σ_a, is equal to the debond initiation stress, σ_d, which is the external stress needed to initiate interfacial debonding. When the external stress is increased, there is further increase in debonding until the shear stress, τ_u at the tip of debond becomes approximately equal to the shear strength at the fiber/matrix interface [54].

2.5 Effect of processing technique on composite strength.

The type of the processing techniques used for a FRP has an influence on its fiber-matrix interfacial strength, which determines its mechanical properties [55]. The two of the major techniques used in producing FRPs are Resin Infusion Molding (RIM) and Resin Transfer Molding (RTM). RIM is the process of drawing resin into a mold containing layers of fiber cloth under vacuum whereas RTM involves injection of liquid resin into fiber preform under pressure. Any technique that allows better wetting of the fiber by the polymer is reported to enhance production of composite with better mechanical properties [37]. For example, glass fiber reinforced polymer composite produced using Resin Infusion Matrix method has been reported to possess mechanical properties that are about 59% higher than those produced by Resin Transfer Molding [37]. Heating and cooling cycles during processing could generate thermal stresses in the composite, which are capable of causing development of initial

microcracks that can easily initiate crack even before an external load is applied [56]. Thermal residual stress strongly affects the mechanical integrity of fiber reinforced plastics and are regarded as inherent flaws and may serve as precursor to failure during mechanical loading [57].

During fabrication of fiber reinforced epoxy composite material, curing of the composite is allowed at either room temperature or a regulated temperature environment. Curing the polymer matrix at a specified regulation temperature condition must be carefully controlled because of the possibility of the occurrence of plasticization, especially when the curing temperature is near the polymer glass transition (T_g) temperature. During composite processing, the proportions of resin and harder contents can affect the properties of resulting composite materials, especially when the polymers are not mixed in the right proportion. Reversible and irreversible changes in the polymer structure can occur when epoxy undergoes plasticization or hydrolysis during composite synthesis. These responses to thermal exposure often result in reduction in both the modulus and glass transition temperature of epoxy, and can cause deterioration of the mechanical properties [10]. Addition of fillers (such as silica) in a composite material may encourage formation of cavities, which may lead to poor fillers-matrix bonding and consequently to reduction in the composites impact strength [58]. This indicates that a polymer matrix with high filler loads absorbs less impact energy because matrix continuity is impeded by the fillers, making each particle a site of stress concentration with the potential to initiate microcracking [58].

2.6 Applications of fiber reinforced plastics

Application of synthetic composites dated back to the 1500 B.C., when the Egyptians and Mesopotamian settlers constructed strong and durable buildings used mixture of mud and straw [25]. Straw was the major reinforcement material for synthetic composite material used in the ancient times. The Mongols later invented the first composite bow from the combination of wood, bone and animal glue which was regarded in the ancient times as the most powerful weapon on earth until the invention of gunpowder [25]. In the modern technology, FRP was first applied in the form of boron fiber-reinforced epoxy skins for F-14 aircraft in 1969. This aircraft was first flown in 1970 [6]. Since then, FRP has gained considerable popularity in structural materials for aircrafts as well as in the marine and automotive industries. This is a result of its superior properties such as high corrosion resistance, low density, high impact resistance, good fatigue tolerance, high specific strength and specific stiffness [6, 59]. Interest in the application of FRP composite in civil engineering structures has witnessed considerable growth globally [60, 61].

FRP is preferred in many spacecraft applications because of their high dimensional stability displayed over a wide temperature range. Space temperature can vary between -100^{o}C and 100^{o}C [6]. Fiber Reinforced Polymer is dimensionally stable over this temperature range [6]. It is reported that most of carbon fiber reinforced epoxy laminates can be manipulated to have a coefficient of thermal expansion that is close to zero, which is a very big advantage in space structures [6]. Liren *et al.* [28] reported that fiber reinforced epoxy composites have become very attractive in building some lightweight armor [28]. S-glass fiber reinforced Polyester polymer are receiving favorable considerations for use as one the major component in Composite Integra Armor (CIA) Systems, not only because of its structural stability but also due its high resistance to failure under dynamic shock loading [28]. The application of FRP composites in automobile industries, space vehicles, etc. is aimed at achieving a tangible amount of weight reduction and fuel efficiency. Mallick [6] noted that a total weight saving of 11.95 KN (2688 lb) per vehicle is achievable with the use of FRP composites in the manufacturing of space shuttle. About 80% weight savings was recorded in the automobile industries in 1981 when E-glass reinforced epoxy was used to replace a ten-leaf Corvette rear leaf spring of an automobile chassis component [6]. Thermal protection system is another area of modern technology where fiber reinforced plastics has gained attention. Such systems include space heat shields for atmospheric re-entry, rocket motor nozzle lines, blast defectors and missile magazines where fiber reinforced phenolic resin composites is used [17].

In this chapter a brief overview of properties of FRPs, as influenced by the constituent, thermal exposure is presented. A summary of review on reinforcing fibers and epoxy resin is included. Applications of FRPs and the influence of thermal exposure on their mechanical behavior are also highlighted.

3.0 MATERIALS AND METHODS

The relevant information on the materials used and the experimental methods adopted in the course of this research are presented in this chapter. Procedures for sample fabrication, convective and conductive heat exposure of the samples, Thermogravimetric Analysis (TGA) and Dynamic Mechanical Thermal Analysis (DMTA), Flexural test, dynamic impact tests and microscopic analysis are outlined and explained.

3.1 Materials

Fiber reinforced plastics were synthesized in this study for application in the cowlings of small recreation aircraft such as Cessna 177. The reinforcing materials used are woven roving fabrics made of Kevlar® 49, E-glass and S-glass fibers. Kevlar® fibres with three different fabric styles, Kevlar® # 120, Kevlar® # 281 and Kevlar® # 285 were used. Their weave types and mechanical properties are summarized in Table 3.1. S-glass and E-glass have different chemical formulation. S glass is made up of magnesium and aluminum silicate. Its breakage strength is approximately 40 % higher than that of other types of glass fibers such as E glass fiber. E glass fibers, on the other hand, possess excellent electrical insulation properties. It is made of low alkali glass based on aluminum borosilicate [29]. The matrix is made of Aeropoxy PR 2032 epoxy resin manufactured by PTM & W Industries. Epoxy belongs to the ether group containing three-membered epoxide ring that originates from monomers and with curing agent containing amines or anhydrides [2]. Two types of hardeners, manufactured by PTM & W Industries, PH3665 and PH3660 were used to accomplish the polymerization reaction of the resin during curing. As indicated by the manufacturer in the Material Safety and Data Sheet (MSDS), PH 3665 hardener was developed to provide a longer working time for larger and/or more complicated laminates when necessary, while PH 3660 was designed for just one hour working time; hence it cures faster than PH 3665. The type of hardener used as catalyst for the polymerization of epoxy resin may affect the degree of curing and consequently influence the mechanical properties of fibre reinforced epoxy. Apart from the difference in working time, the two hardeners vary in specifications and properties. The mechanical and physical properties of the reinforced fibers as well as the physical properties of the applied epoxy resin and hardener, as provided by the manufacturer, are summarized in Tables 3.1 and 3.2.

Tables 3.1. Mechanical properties of the fibers

Manufacturer Fiber Style nomenclature		Kevlar® #285	Kevlar® #281	Kevlar® #120	E-glass #120	S-glass
Breaking strength	Warp	4344	4309	1792	862	1124
(kPa)	Fill	4482	4482	1723	827	952
Weave type		Crow	Plain	Plain	Crowfoot	Plain
Thickness (inch)		0.01	0.01	0.0035	0.004	0.009
Weight (oz. /Sq. Yd.)		5.0	5.0	1.8	1.45	5.8
Width (inch)		38	38	38	50	60

Tables 3.2. Physical properties of the applied epoxy resin and hardeners

	Resin	Hardeners	
	PR 2032	PH 3660	PH3665
Color	Light amber	Amber	Amber
Viscosity at 77 °F, centipoise	1,650 cps	190 - 200 cps	200 – 250 cps
Specific Gravity, gms. //cc	1.15	0.96	0.95
Pot life at 77 °F	N/A	1 hour	2 hours
Epoxy mixture density (g/cm^3)	2.1	2.1	2.1

3.2 Manufacture of the fibre reinforced epoxy composites.

The investigated fiber reinforced plastics were fabricated using hand lay-up technique. The fiber fabrics were cut into sheets of 252cm^2 sizes. The epoxy resin was mixed with a hardener in the recommended resin / hardener weight ratio of 100:27 at room temperature. The hardener is a modified amine consisting of diamine molecules, which react chemically with epoxy molecules to form a rigid 3D network structure when the additional polymerization reaction is completed. The amine molecules react with the epoxy molecules in a fixed ratio, it is therefore essential that the correct mix ratio of the resin and hardener be used to ensure a complete polymerization reaction. If more or less amine is added to epoxy than required to complete polymerization reaction, unreacted

resin or hardener will remain within the matrix, which will affect the final properties of the cured epoxy. To assist with the accurate mixing of the resin and hardener, the manufacturer provided the optimum mix ratio that was used in this study.

Thin coatings of the resin (epoxy mixed with hardeners) in the B-stage were applied on the cut fiber fabrics using a soft brush. The resins were allowed to crosslink to the *B-stage* before coating on the fiber fabrics. The epoxy resin becomes viscous enough at this stage such that it cannot run off the fiber sheets during the hand laying process. The weight of the fiber sheets before application of epoxy resin was determined using a KILOTECH KHA5001R series Laboratory weighing scale. Before the polymerization reaction was allowed to complete and produce a fully cross-linked resin matrix (C-stage), coated fiber mats were stacked on one another. They were pressed together using a roller to ensure a uniform distribution of the polymer on the fiber surface and in the void spaces between single fibers and fiber bundles, strong adhesion of fiber layers and elimination of air bubbles trapped within the laminates. The number of stacked layers needed to obtain any desired thickness of composite plate was determined by the thickness of the applied woven fiber fabric. For example, in order to produce a plate of an average thickness of 3.2 mm, the number of laminates and corresponding average fiber volume fractions are presented on Table 3.3.

Table 3.3. Fiber volume fractions of the synthesized fiber reinforced epoxy composite

Fiber	Type	Density (g/cm3)	Number of fiber layers	Fiber volume fraction
Glass	S-Glass	2.49	18	71 %
	E-Glass	2.55	29	66 %
Kevlar®	Kevlar® #285	1.44	9	69 %
	Kevlar® #281	1.44	11	65 %
	Kevlar® #120	1.44	27	62 %

A dead weight of 3.5 kg was placed on the stacked fiber layers to exert pressure of about 1400 Pa on the laminate during the final stage of the polymerization to promote good adhesion of the laminates. In addition, application of pressure would aid the escape of any air bubble trapped in the polymer and reduce porosity. Curing was done at room temperature and the applied pressure was removed after 12 hours, when the polymer has completely reached the C-stage. The cured composite was also weighed to determine composite final density as well as volume

fractions of its constituents as presented in Table 3.3. The average weight fraction of fiber in the composite for all specimens in the study varies depending on the fiber bundle size and the weave type.

The composites laminates were cut into the required various sizes required for the subsequent tests using rotating silicon carbide disc. The geometry and sizes of the test specimens are shown in Fig. 3.1. The mechanical behavior of the composites were evaluated using flexural test, impact test, Dynamic Mechanical Thermal Analysis (DMTA).

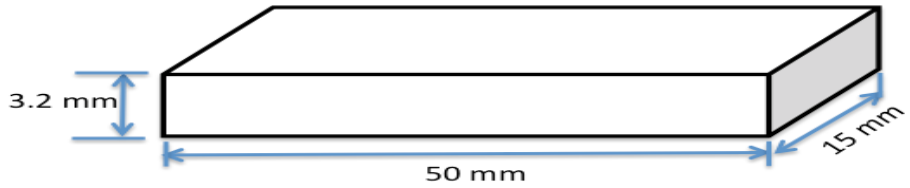

a. Flexural test specimen

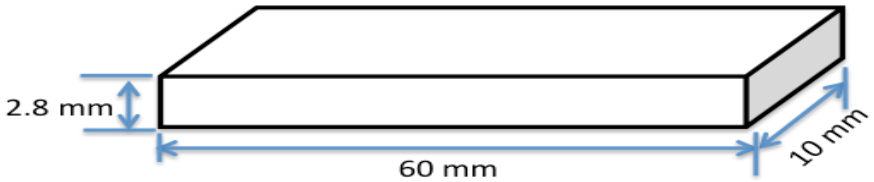

b. DMTA test specimen

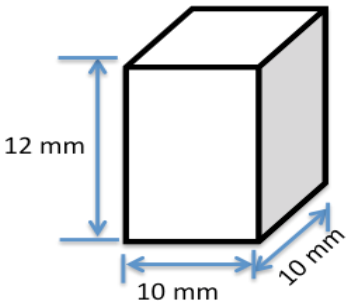

c. Dynamic impact test specimen

Fig 3.1. Schematic diagram of test samples geometry

In order to determine the effects of thermal exposure on the mechanical integrity of the composite, the sectioned test specimens were exposed to various degrees of heat fluxes or temperature in cone calorimeter (at 4, 5 and 7 kW/m^2) and in an electric furnace (at 100ºC, 150ºC, 200ºC, 250ºC and 300ºC) for varying period of time. In

addition to the mechanical tests, the synthesized composites were subjected to microscopic evaluation to investigate porosity, fiber-matrix-bonding and delamination in the materials prior to and subsequent to thermal exposures. Composite failure mechanism under impact loading was also evaluated to examine the failure pattern in both glass and Kevlar® fibers reinforced epoxy under dynamic shock loading condition.

3.3 Microscopy

Both of Optical Microscopy (OM) and Scanning Electron Microscopy (SEM) were used for microstructural evaluation of the manufactured fiber reinforced plastic composited before and after exposure to mechanical load or thermal flux. The higher magnification of SEM was utilized in determining the extent of wetting and bonding between the fibers and matrices. Region of delamination, fiber-matrix interfacial debonding and matrix cracking within the composite as a result of thermal exposure and loading were carefully examined using scanning electron microscopy. Sample preparation before microscopy involved sample sectioning, cold mounting using acrylic and grinding using 120 Grit SiC paper and polishing. At different polishing stages, different grades of polishing clothes were selected and used with corresponding polishing solutions as shown in table 3.4.

Table 3.4. Polishing cloths and corresponding solutions

Polishing Cloth	**Corresponding Solution**
9 η MD Allegro	9 η MD Allegro solution
3 η MD Mol cloth	3 η MD Mol solution
1 η MD Nap cloth	1 η MD Nap solution
0.5 η Ops cloths	0.5 η Ops solution

A Nikon 100 MA Eclipse inverted optical microscope was used to carry out the optical microscopic examination of the specimens. Images were taken and analyzed with the aid an image processing software known as *Pax-it.* Microscope lens of various magnifications (x50, x100, x500 and x1000) were used in taking the optical micrographs. A JOEL JSM-6010LV Scanning Electron microscope was used to carry out the SEM investigations using both backscattered and secondary electron imaging techniques. The specimens were imaged using acceleration voltage ranging between 15 kV and 20 kV.

3.4 Flexural test

The flexural properties of the composites were determined using 3-point bending test for a rectangular cross section samples according to ASTM standard D 7264/D7264M as shown in Fig. 3.2. This is the standard test method for determining the flexural properties of polymer matrix composite materials [59, 62]. The test method stated in procedure A is the standard applicable in this research and is commonly used for continuous-fiber-reinforced polymer matrix composites with minimum span-to-thickness ratio of 16:1 for the test specimen. The flexural test was conducted using Instron 5500 universal testing machine. The dimension of the cuboid-shaped specimens for the bending test is 50 mm x 15 mm x 3.2 mm and support span was 40 mm. The test was conducted using a 5 kN load cell with loading done at a cross speed of 10mm / min. The data acquisition system generated the test data and plotted it to a load-displacement curve from where the flexural modulus, flexural stress and flexural strain of the composites were determined using equation (3.1) to (3.3) [59, 62]. For every test sample, the load was applied on the surface of the specimen directly exposed to heat source during thermal treatment. Five samples were tested for each test condition and the flexural moduli and strength reported represent the average values of the five tested samples under similar experimental condition. The uncertainty provided in the results (Chapter 4) represents the value of standard deviation for the five tested samples.

$$E_f = \frac{L^3 m}{4bd^3} \quad \text{.....(3.1)}$$

$$\sigma_f = \frac{3PL}{2bd^2} \quad \text{.....(3.2)}$$

$$\epsilon_f = \frac{6Dd}{L^2} \quad \text{.....(3.3)}$$

where: σ_f = Stress in outer fibers at midpoint, (MPa)

E_f = Flexural Modulus of elasticity, (MPa)

ϵ_f = Strain in the outer surface, (mm/mm)

P = Load at a given point on the load deflection curve, (N)

D = maximum deflection of the center of the beam, (mm)

L = the support span, (mm),

b = width of test beam, (mm),

d = depth of tested beam, (mm) and

m = slope of the initial straight-line portion of the load deflection curve, (P/D), (N/mm).

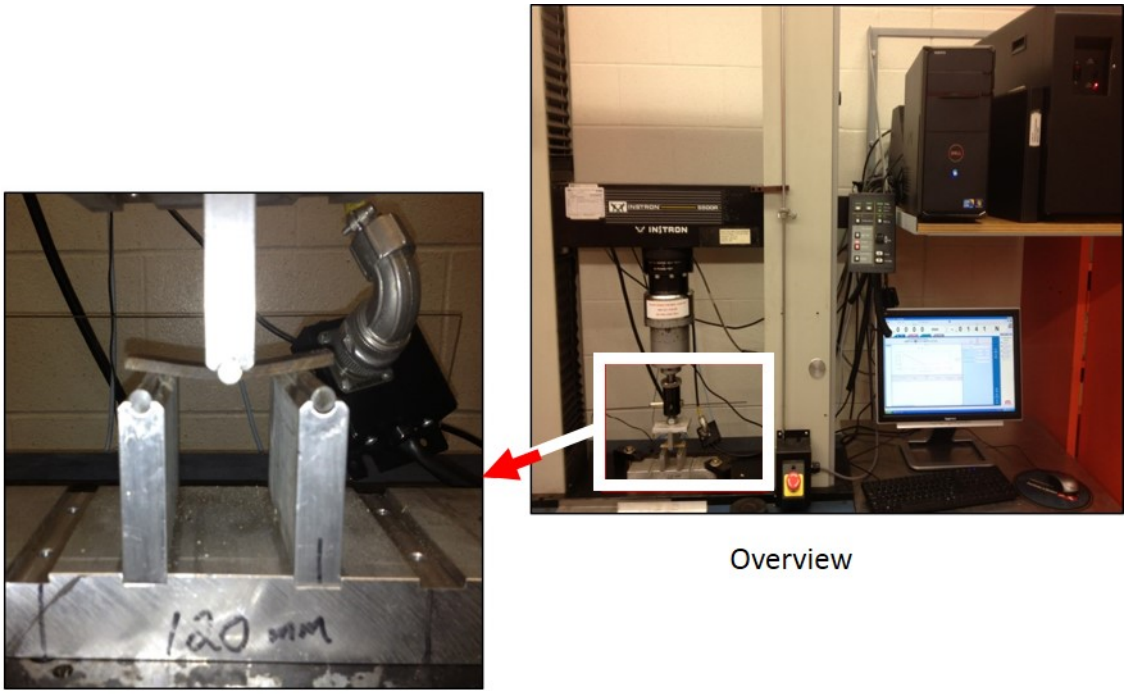

Fig. 3.2. Photograph showing the setup for the 3-point bending test.

The bending test provides information on the strength and the stiffness of the synthesized composites. Flexural strength is measured at the convex or tensile side of the specimen surface. It is described as the maximum stress on the uttermost fiber of the test specimen corresponding to the maximum applied force before failure [62]. The slope of the initial linear portion of the stress versus strain curve gives the flexural modulus, which is a measure of the specimen's stiffness. The deflection is measured by the crosshead position.

3.5 Dynamic mechanical test

Dynamic impact test and dynamic mechanical thermal analysis (DMTA) are the dynamic test methods adopted in this research work. Each test method and the procedures adopted during this research are explained in the subsections 3.5.1 and 3.5.2.

3.5.1 Dynamic Impact Test.

The test specimens with dimension 10 mm x 10 mm x 12 mm were subjected to dynamic impact test using split Hopkinson pressure bar (SHPB). This equipment was designed and fabricated at the University of Saskatchewan. A schematic diagram of the equipment is shown in the Fig. 3.3.

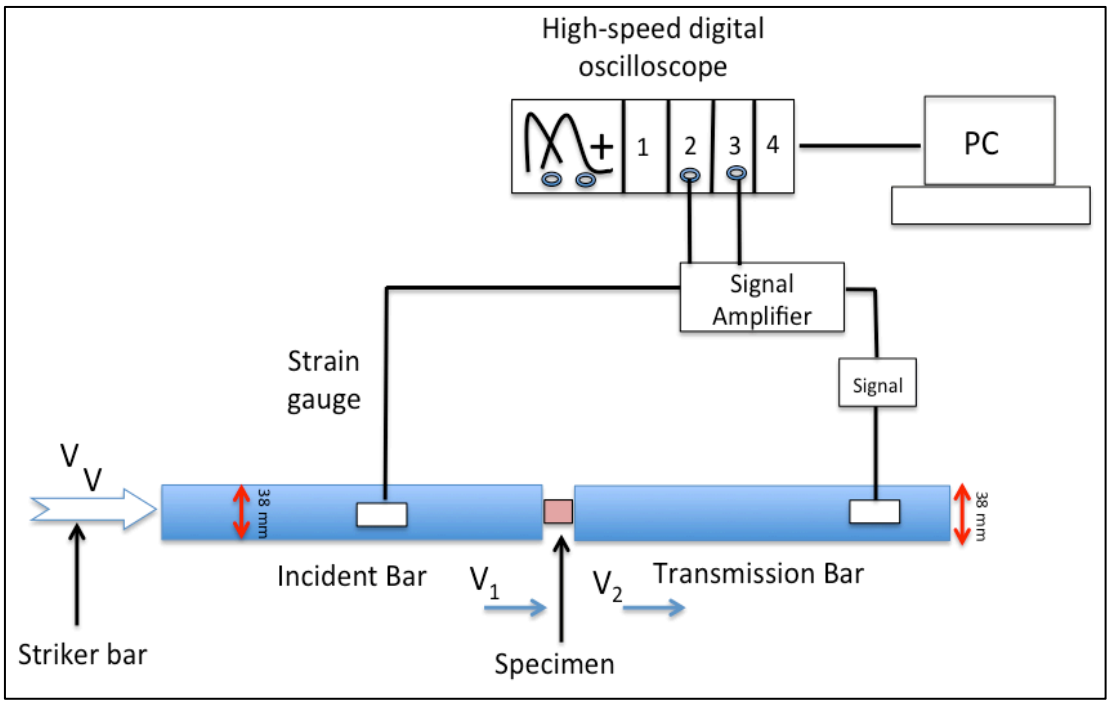

Fig 3.3. Schematic diagram of Split Hopkinson pressure bar equipment.

Split Hopkinson pressure bar (also known as Kolsky Bar) is the conventional equipment used to characterize the dynamic mechanical response of materials under high strain-rate loading (10^2 - 10^4 s^{-1}). Such rapid deformation is generated under dynamic shock loading (also called dynamic impact loading). Typical examples of such loading condition include, helmet impact on hard surfaces and bird impact on the aircraft body structure. There are three major components in this equipment: a loading device, bar components and a data acquisition system. The bar components consist of two bars; input and output bars. Strain gauges attached to each of these bars were connected to the data acquisition system, which consist of signal conditioner and amplifier and an oscilloscope. The loading device consists of a light gun with a long gun barrel through which a fired projective travels gaining velocity before impacting the incident bar. Compressed air in pressure vessel drive the projectile gaining kinetic energy as it travels through the gun barrel. The sensor attached to the end of the gun barrel measures the impact velocity of the projectile.

Figure 3.4 shows photographs of the Hopkinson pressure bar equipment used in this study. A test specimen sandwiched between the input and output bars before an impact test is shown in the insert for Fig. 3.4a while the firing chamber is shown in the insert for Fig. 3.4b. A projectile fired by a light gun strikes the input bar generating

elastic wave, which travels through the bar and rapidly deform the specimen sandwiched between the input and the output bars. Test samples were impacted using firing pressure ranging between 100 and 160 kPa. This generated impact momentum that ranged between 21.3 and 38.3 kg m/s^2. The applied range of firing pressure produced strain rates of between 700 s^{-1} and 1400 s^{-1} in the specimens, depending on the impact momentum and the intensity of thermal exposure of the test specimens before the impact test. The elastic wave signals were captured by the strain gages attached to the input bar as incident and reflected waves, and strain gauges on the output bar as transmitted waves. These strain signals are conditioned and amplified by signal conditioning and amplification system connected to the strain gages. A mixer's signal digital oscilloscope connected to the signal conditioner records and stores the elastic wave signals. The incidence wave is the wave propagating through the input bar towards the specimen. A fraction of the waves is expended in deforming the specimens, fraction transmit through specimen and propagate through the output bar as transmitted waves.

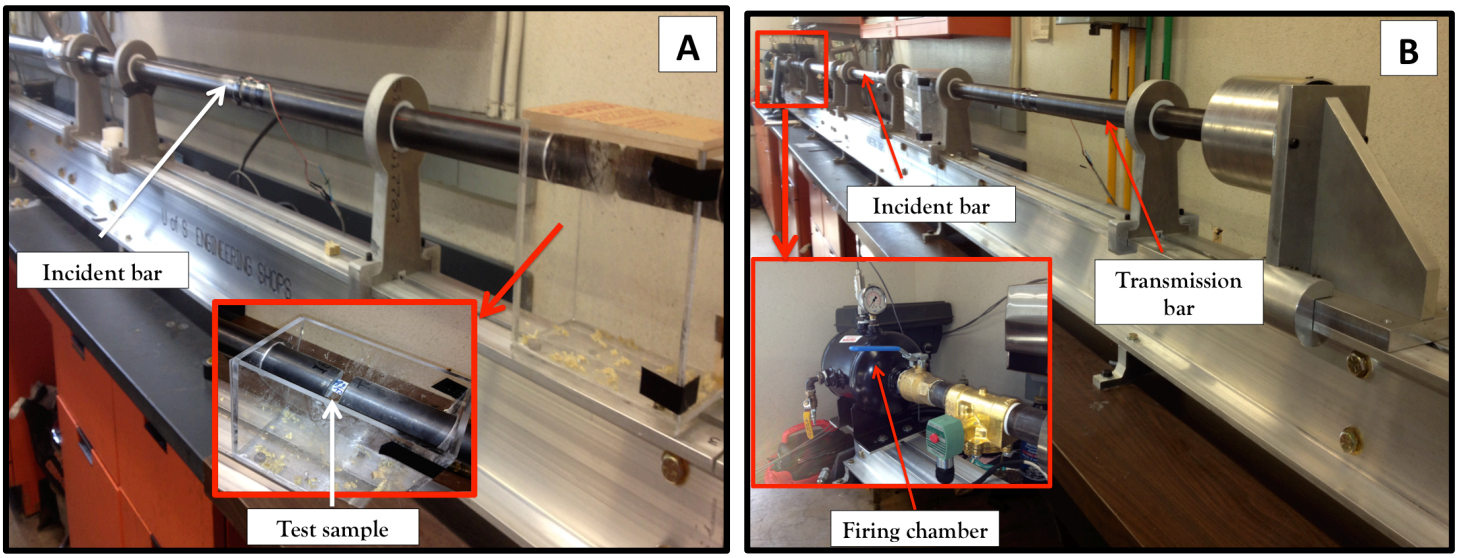

Fig 3.4. Photograph showing the Split Hopkinson pressure bar used in this study.

Reflected waves are those that are reflected back at the interface between the test and the input bar interface, and they are captured by the strain gage on the input bar. The strain gauges on the incident bar measure the incident and reflected pulses while strain gauge on the transmission bar measures the transmitted pulse. Equation 3.4 shows the equation used in calibrating the bars expressing the relationship between projectile velocity and strain [65].

$$\varepsilon_I = \frac{1}{2}\frac{v_{st}}{C_B} \quad \text{.....(3.4)}$$

where:

σ_I, and ε_I represent the stress and strain amplitude of the incident pulse produced by the striker impact; C_B, ρ_B,v_{st} represent the elastic wave speed in the bar, density and the striking velocity of the bar respectively. The obtained data from oscilloscope in voltage were converted to stain values using the conversion factor obtained from the equipment of calibration. The strain rate ($\dot{\varepsilon}$), strain (ε) and stress (σ) values were computed using equations (3.5) to (3.7) respectively [65].

$$\dot{\varepsilon} = -2\frac{C_B}{L_s}\varepsilon_R \quad \text{.....(3.5)}$$

$$\varepsilon = -2\frac{C_B}{L_S}\int_0^t \varepsilon_R dt \quad \text{.....(3.6)}$$

$$\sigma = \frac{A_B}{A_S}E_B\varepsilon_T \quad \text{.....(3.7)}$$

where the subscripts *I, R,* and *T* represent the incident, reflected and transmitted pulses respectively and , E_B, is the Young modulus of the bar material, A_B and A_S are the cross sectional areas of the bars and the specimen while L_S is the specimen's length.

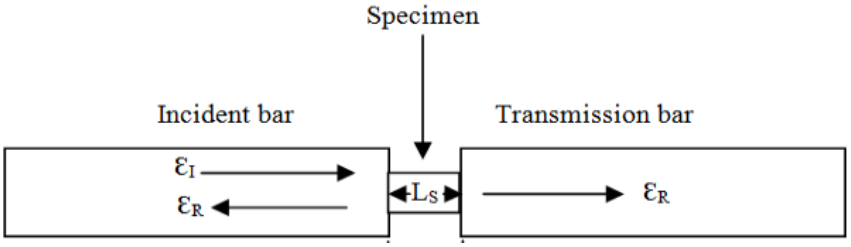

Fig 3.5. Test-specimen section of a Split Hopkinson pressure bar showing direction of elastic wave propgation [Adapted from 65].

3.5.2 Dynamic Mechanical Thermal Analysis

Polymers demonstrate both elastic and viscous behaviour and they are therefore described as viscoelastic materials. The viscoelastic properties of the manufactured fiber reinforced epoxy matrix composites were investigated using Dynamic Mechanical Thermal Analysis (DMTA). The test samples were rectangular in shape with a size of 60 mm x 10 mm x 2.8 mm. In this research, the DMTA was carried out through a collaborative research arrangement with GABO QUALIMETERS TestanlagenGmbH, Germany, a DMTA equipment manufacturer, using their newly introduced DMTA equipment - 500N Eplexor system, EPLEXOR 25N to 500N model. Fig 3.6 represents a typical

experimental set up during the DMTA test in the laboratory. The test temperature was set within the range of -80ºC to 250ºC depending on the factor(s) under investigation. The specimens were heated at rate of 10ºC/min. When the effect frequency of vibration was not under investigation, a fixed frequency of 10 Hz was used for the tests. The obtained data from these measurements are storage modulus, loss modulus and mechanical loss factor. The mechanical loss factor (tan δ) is the ratio of the loss modulus to the storage modulus, which gives a measure of the material energy dissipation during dynamic mechanical loading [63].

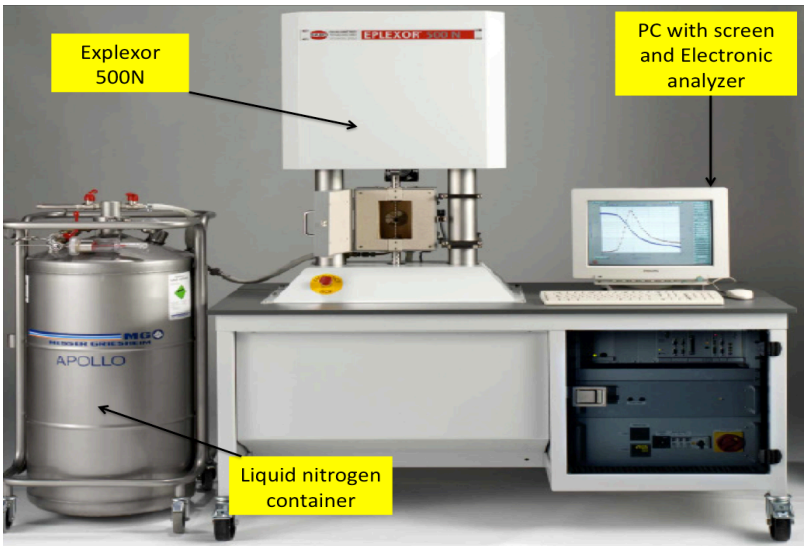

Fig 3.6. Experimental setup for DMTA. (Source: DMTA hand book by GABO QUALIMETERS TestanlagenGmbH, Germany).

3.6 Evaluation of service condition for Cessna aircraft cowling.

In the course of this research, a visit was made to the hangar of a commercial flight operator in Saskatchewan; Air Champion, Estevan. The company has been in operation for close to 30 years, and currently has over 15 Cessna aircraft in its fleet. Cessna aircraft are rented out for mainly recreational and other purposes daily. The company's operation is guided by the government flight operative regulations and Cessna aircraft manufacturer's manual. Useful information from flight maintenance reports was obtained from the maintenance department of the company, and this provided some data that give insight into the thermal condition of a typical Cessna aircraft chamber during flight trips. Fig 3.7 shows the cowling panels of a Cessna aircraft, while Fig. 3.8 shows the thermal condition of the cowling chamber. The information derived from this field application helped in the simulation of experimental thermal conditions adopted in the laboratory examination investigation of the test specimens in this study.

Fig 3.7. Cessna aircraft cowling component and cowling panels.

The cooling air is forced into the chamber through the air outlets on the nose cover (see Fig 3.7) of the cowling. This enhances cooling effect of the aircraft engine during flight, thereby reducing heat generation within the chamber and consequently reduced the amount of convective heat to which the cowling surface (upper and lower housing) is exposed to.

The schematic representation of the heat transfer analysis within the cowling chamber is shown in figures 3.11 and 3.12. According to aircraft manufacturing standards and guide, the maximum allowable temperature of the engine block of an aircraft is 260°C and oil inlet temperature is 118°C. During field application, a typical Cessna aircraft exhaust gas temperature is between 649°C – 816°C while the cylinder head temperature is between 177ºC to 204°C. Field measurement of the heat transfer within the cowling chamber records the maximum temperature inside the cowling during operation at an estimated values between 65°C and 70°C. Based on a maximum aircraft engine surface temperature of 260°C, the radiative and convective heat flux to the surface of the housing (cowling) would be approximately 4.7 kW/m^2 (see details in Appendix 1). Therefore, a heat flux of 5 kW/m^2 was adopted in this study. Heat fluxes of 3.7 and 7.0 kW/ m^2 were also used to provide data on additional operating conditions.

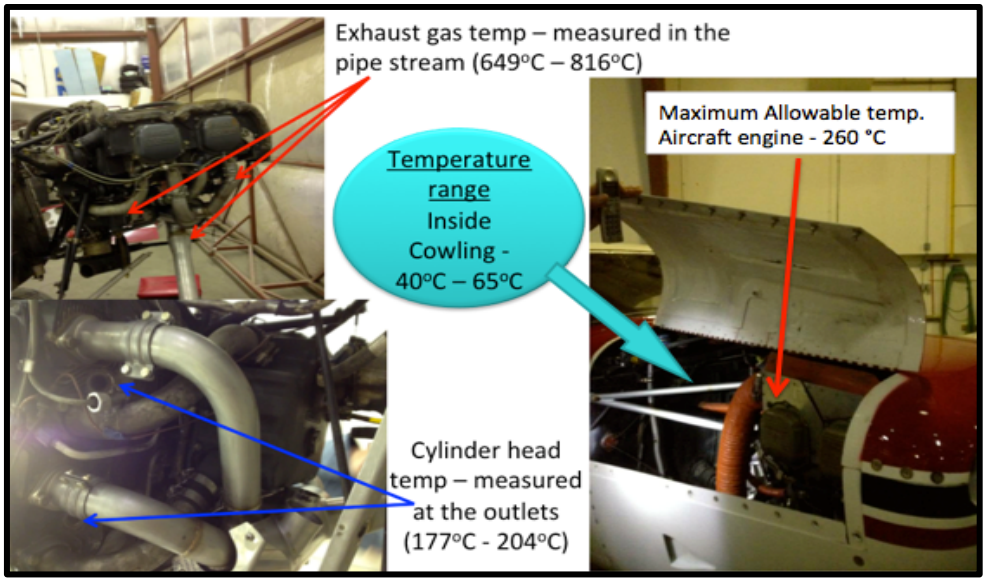

Fig 3.8. Temperature distribution in the cowling chamber.

In reference to the Cruise and Range performance manual for the Cessna-Cardinal aircraft [64], the maximum cruise is normally limited to 75% of its power while the total fuel capacity is 49 gal. At 5.8 hours (348 minutes), the total fuel consumption according to the cruise performance specification would be 48 gal, which implies that the total fuel capacity would be completely consumed in less than 355 minutes. Therefore, the maximum flight time possible for this aircraft model is less than 300 minutes; hence the test samples were subjected to maximum radiative thermal condition time of 360 minutes before further flexural testing. Observing the field application and analysis of the heat fluxes generation during use, it can be established that the temperature and heat flux the material will be exposed to in service is very low, compared to the selected temperature and test variables.

3.6.1 Thermal Exposure

Thermal exposure of the test specimens was carried out in an electric furnace and cone calorimeter to simulate convective and radiative thermal exposure. Five test samples were selected from the various investigated materials and tested for each test condition.

3.6.1.1 Radiative Thermal Exposure

The laboratory radiative thermal exposure of the fabricated composite samples was carried out in a cone calorimeter, manufactured by Fire Testing Technology (East Grinstead, West Sussex, UK). The temperature of the conical heater on the cone calorimeter was set so as to produce an incident heat flux of 5 kW/m^2 on the surface of the sample, as shown in Fig. 3.9. This heat flux was measured using a water-cooled Schmidt-Boelter heat flux gauge. It was assumed that the gauge and the specimen surface have similar values of emissivity, which is the

relative ability of the material surface to emit radiation energy. The temperature of the specimen surface was measured using the infrared thermometer (Minolta Land Cyclops 300bAF) focused directly on the heated surface of the specimens. The heat fluxes and corresponding temperature incident on the samples surface are presented in Table 3.5.

The flux meter gauge was aligned directly opposite to the radiant cone within a recommended spacing of 25 mm to take readings for each experiment. At this cone-specimen spacing the incident heat flux over the exposed surface of the specimen should be fairly uniform. At the start of each experiment heat shutter was placed in front of the radiant cone as a barrier as shown in Fig. 3.10 in order to prevent heat flux radiation from reaching the samples until incident flux level attained before samples were exposed to the predetermined thermal condition. Once the required steady state heat flux was attained, the shutter was removed and the test specimens exposed for a given period of time as given in Table 3.5. Once the surface of the sample reached a steady-state temperature, this temperature was recorded.

Table 3.5. Heat flux and the corresponding temperature – Radiative thermal condition.

Sample	Exposure time	Heat flux (From the radiant cone)	Cone Heater Temperature	Sample Surface temperature (steady state)
Fiber reinforced epoxy	360 mins	3.7 kW/m^2	300ºC	170 - 174ºC
Fiber reinforced epoxy	360 mins	5.0 kW/m^2	340ºC	178 C – 180ºC
Fiber reinforced epoxy	360 mins	7.0 kW/m^2	400ºC	246 – 248ºC

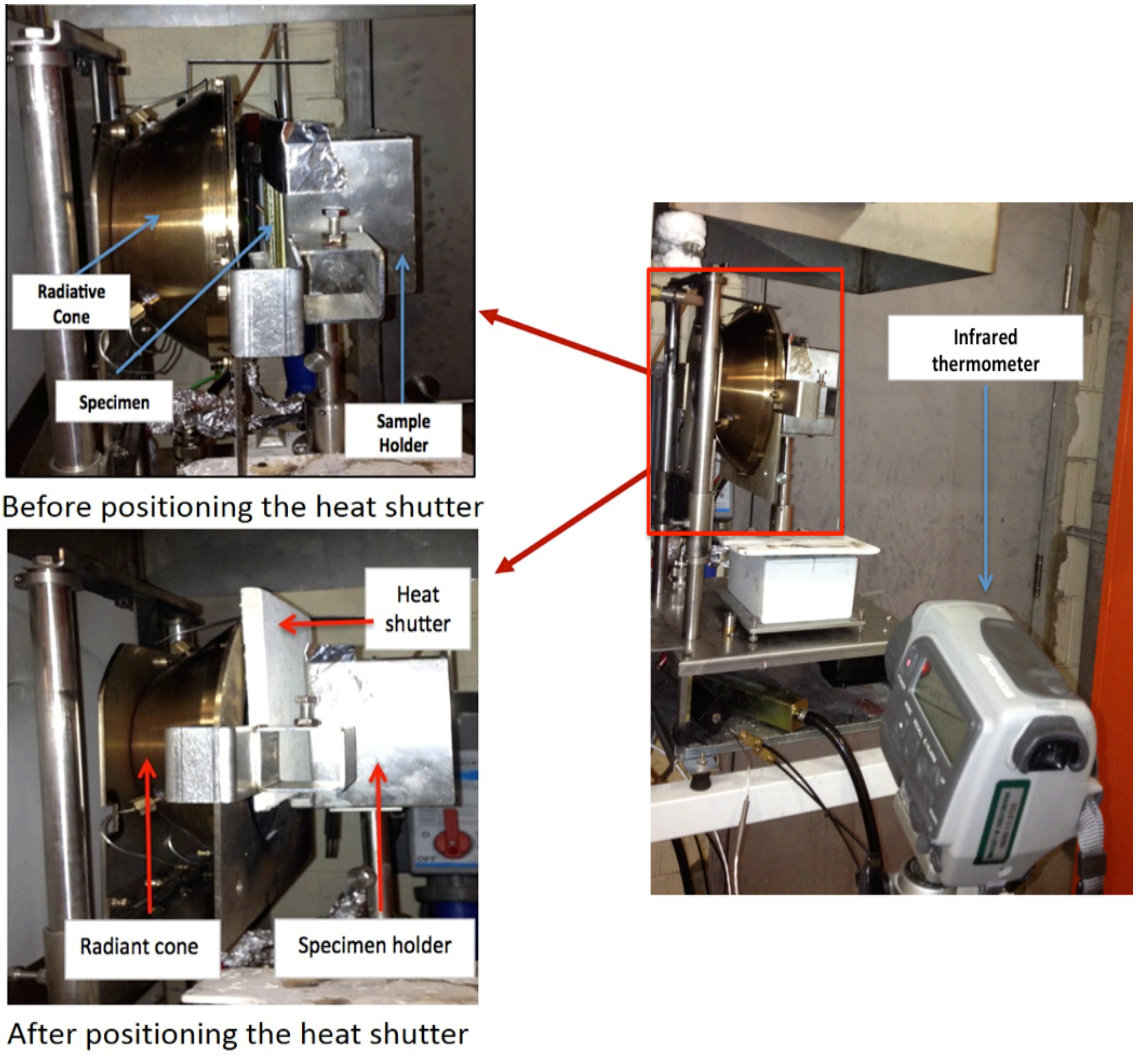

Fig. 3.9. Photographs of the cone calorimeter setup used in this study (Vertical orientation).

3.6.1.2 Convective Thermal Exposure.

Laboratory convective thermal exposure of the test specimens was carried out in an enclosed Thermoscientific Lindberg Blue M Furnace, shown in Fig. 3.10. The required temperature for every test condition, as shown in Table 3.6, was achieved by heating up the furnace chamber to a steady state before specimen were placed inside the furnace and allowed to stay for a predetermined period of time of up to 2 h. Samples were taken out and allowed to cool to an ambient temperature. Post thermal mechanical behavior of specimen, the flexural strength and flexural modulus were evaluated by subjecting the exposed specimen to 3-point bending tests and impact tests while response to dynamic impact load was determined using split Hopkinson pressure bar as mentioned earlier.

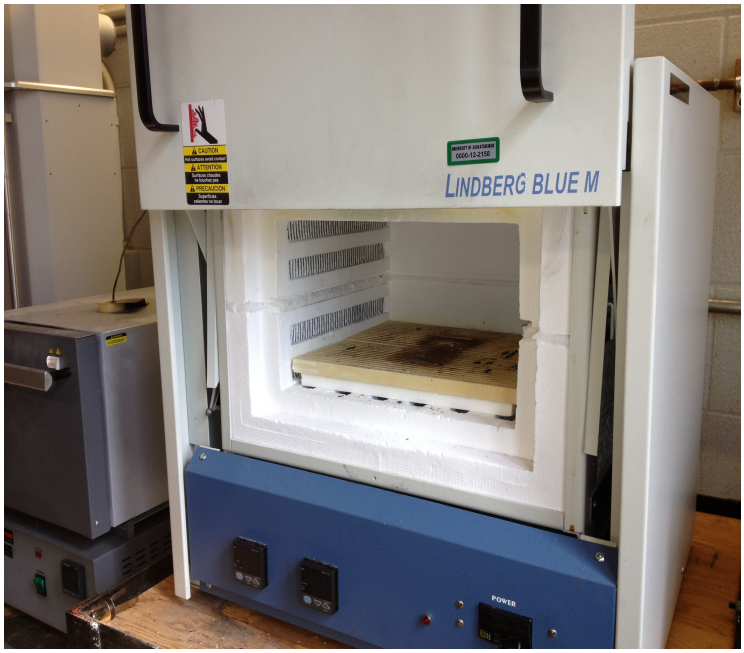

Fig 3.10. Lindberg Blue M electric furnace.

Table 3.6. Experimental condition for convective thermal exposure.

Composite	Hardener type	Furnace temperature (°C)	Exposure time (mins)
Woven Kevlar® / epoxy	PH3665	100, 120, 150, 200, 250, 300	30, 60, 90, 120
Woven S-glass / epoxy	PH3665		
Woven E-glass / epoxy	PH3665		
Woven Kevlar® / epoxy	PH3660	100, 120, 150, 200, 250, 300	30, 60, 90, 120
Woven S-glass / epoxy	PH3660		
Woven E-glass / epoxy	PH3660		

Considering the heat transfer analysis as stated in the previous paragraph, convective heat transfer in the field application was assumed to be negligible relative to the radiation transfer from the engine surface. However, in order to gather information on the performance of these materials under a wider range of conditions, convective exposures of up to 300°C were used in this study. Nevertheless, the simulated convective test was conducted in respect to exposure time and temperature to determine their influence on the mechanical behavior of the fiber reinforced epoxy. The physical changes that occurred in the composite including fiber-matrix interfacial bonding

and delamination at different elevated temperatures in the furnace were observed and documented. Data collected from the field application over a period of time shows that the average temperature attained on the inner side of the cowling panel during aircraft operation ranges between 40°C to 70°C. The chamber experiences consistent cooling by the forced flow of air through the openings at the cowling frontal cover plate as shown in Fig. 3.11, thereby providing cooling effect to the aircraft engine.

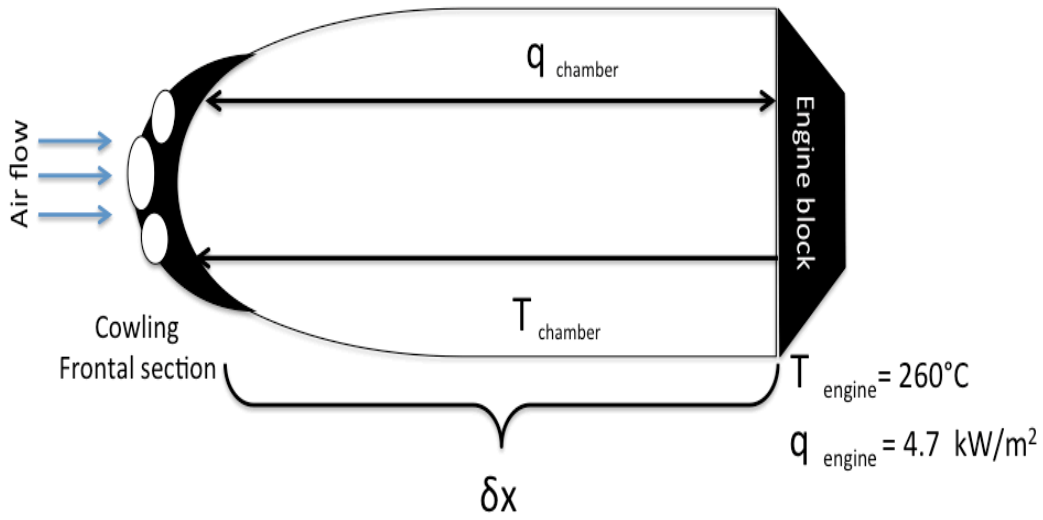

Fig 3.11. Schematic diagram of heat transfer analysis in the typical cowling chamber of Cessna aircraft.

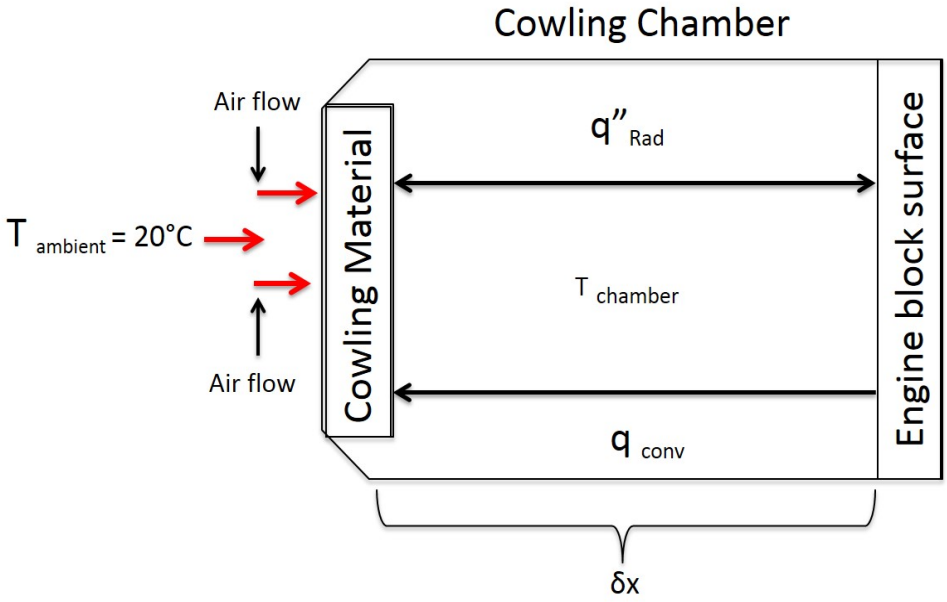

a.

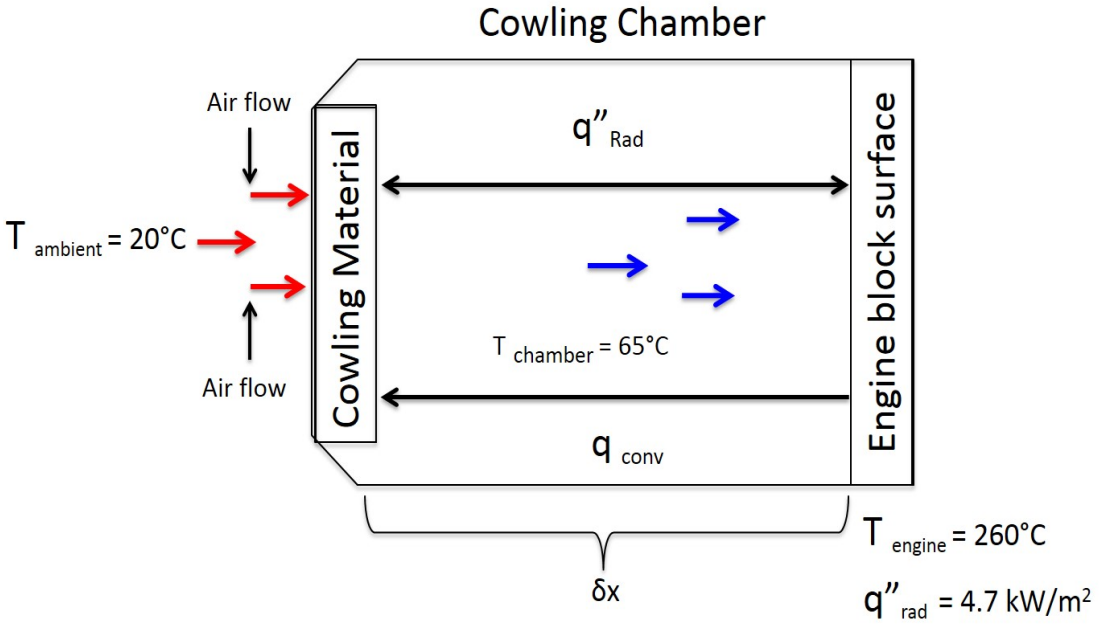

b

Fig 3.12. Heat transfer analysis in the cowling: (a) heat transfer (b) temperature and air flow.

The convection furnace in which samples heat exposure was carried out in the laboratory has relatively low convection heat transfer coefficient values due to much smaller air flow in the furnace chamber when compared with the rate of air flow that occurs in the Cessna aircraft chamber during service. This consequently may have some impact on the sample's mechanical properties when subjected to convective thermal test condition in the laboratory than what occurs in the intended field application of the material. Simulating convection heat transfer field application in the laboratory is however not a major concern as it is assumed to be negligible. As shown in Fig. 3.12, field application data and Cessna aircraft manufacturer manual give the maximum allowable cylinder head temperature of the engine block as 260ºC while convectional temperature flow in the cowling chamber is less than 70ºC. Samples were subjected in this study to test condition more severe than the anticipated service. This was aimed at testing the samples under very stringent test conditions to observe their performance in case anything goes wrong with the air cooling of the engine in flight.

3.7 Thermogravimetric analysis (TGA)

Thermogravimetric analysis (TGA) is used to determine the weight change that occurs in a material as a function of temperature and time in a controlled environment (nitrogen, helium, air, or in vacuum). The amount of weight change occurring in a material is measured either as a function of increasing temperature or isothermally as a function of time following ASTM D2584 standard [62]. TGA provides useful information on the thermal stability of a material in different environment (e.g. inert or oxidizing). The test temperature range in a TGA experiment can

vary from room temperature to as high as 2400ºC depending on the equipment used. Rate of vapour generated in any analysis can also be identified and measured by Thermogravimetric analysis interfaced with a mass spectrometer RGA. When equipped with a gas analysis accessory, TGA equipment can allow for independent gas mixture flow control.

TGA was conducted for four different samples: (i) glass fiber reinforced epoxy, (ii) Kevlar® fiber reinforce epoxy, (iii) unreinforced epoxy cured with hardener PH 3660 and (iv) unreinforced epoxy cured with hardener PH 3665. The specimens were analyzed using TGA Q5000 IR. 15 Build 263, universal V4.5A TA Instruments. The equipment setup for this experiment is shown in Fig. 3.13. The temperature range under which the test was conducted was between 25ºC to 350ºC at the heating rate of 10ºC /min in nitrogen gas atmosphere. The TGA temperature range covered the glass transition temperature range of the composites material up till the temperature at which degradation is expected to occur within the material. The gas inflow and outflow rates were both set at 10 mL/min and the ramp at 5ºC/min. The experimental test condition for the specimen is given in the Table 3.7. The onset temperature of degradation, $T_{d,\ onset}$, was determined as the temperature at which the specimen experience loss in mass of 5% while the point at which there was rapid rate of mass decrease (deduced from the curve derivative) is referred to as T_d (subscript d represents degradation). This also was similar to the parameter used by Mouritz, *et al.* [52] in their study of TGA of a carbon fiber reinforced plastic (CFRP).

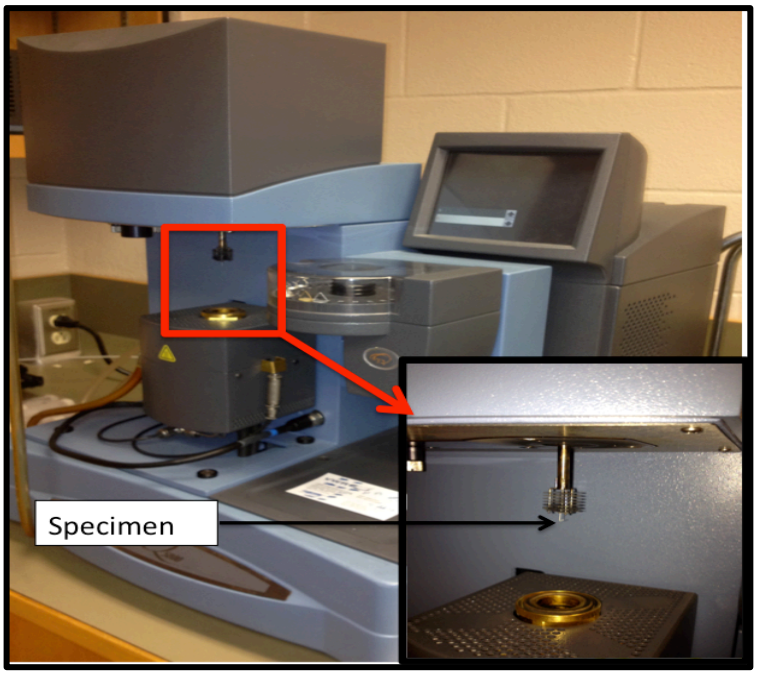

Fig. 3.13. Thermogravimetric analyzer (TGA Q5000IR - TGA analyzer manual).

Table 3.7. Experimental test condition for TGA.

Specimen Type	Specimen size	Temperature range	Specimen description
Woven Kevlar®	108.77 mg	25°C to 350°C	Kevlar® reinforced composite
Woven S - Glass	139.025 mg	25°C to 350°C	S – Glass reinforced composite
Epoxy – PH3665	95.76 mg	25°C to 350°C	Unreinforced epoxy with hardener 1
Epoxy – PH3660	106.23 mg	25°C to 350°C	Unreinforced epoxy with hardener 2

Materials preparation and composite fabrication procedure are discussed in this chapter. The equipment set up for thermal exposure and the test procedures for various mechanical and thermal analyses conducted are highlighted. The results of a fact-finding visit to an operator of Cessna 177 light engine aircraft in Saskatchewan and a thermal analysis of heat transfer analysis between the cylinder head and cowling panels are presented. In the subsequent chapter, an overview of the experimental results will be provided as well as discussion of these results.

4.0 RESULTS AND DISCUSSION.

The results of microstructural evaluation of the fabricated fiber reinforced plastics before and after thermal exposure are presented and discussed in this chapter. Results of the thermal analysis and mechanical tests conducted on the composite materials are also presented and discussed.

4.1 Thermogravimetric analysis (TGA)

Thermogravimetric analysis (TGA) was carried out on the composites in a nitrogen gas atmosphere. Percentage weight loss as a function of temperature was measured for glass and Kevlar® fibers reinforced epoxy prepared using hardener PH 3665) and unreinforced epoxy polymer cross linked using both hardeners PH 3660 and PH 3665. The percentage weight loss, as shown in Fig. 4.1 gives an indication of the extent of decomposition reaction in the composite as temperature was increased. It can be observed from Fig. 4.1 that significant weight loss did not occur in either reinforced or unreinforced epoxy until when the temperature exceeded 300°C. The weight loss in Kevlar® reinforced epoxy became more noticeable than that for unreinforced or glass fiber reinforced epoxy at temperature above 150°C. This weight loss is however very small and could be due to loss of volatile matter such as water vapor on the surface of the composite. Above 300°C, rapid drop in weight occur due to intense decomposition of the epoxy matrix. At an elevated temperature, chain scission in the microstructure of the composite material occurs leading to loss of volatile matter content and reduction in weight which can result into loss in strength and heat resistance of a polymer [22]. General observation implies that for all tested samples, no significant weight loss occur in the reinforced and unreinforced epoxy up to 300°C.

The effect of fiber reinforcement on the weight loss of the epoxy resin is not significant. This underscores the importance of matrix thermal behavior in the decomposition of polymer matrix composites. Matrix degradation determines to a very large extent, the rate of weight loss experienced in the composite material. The effect of using different matrix resin hardener (PH3660 and PH3665) on decomposition of the matrix is very negligible from the TGA analyses.

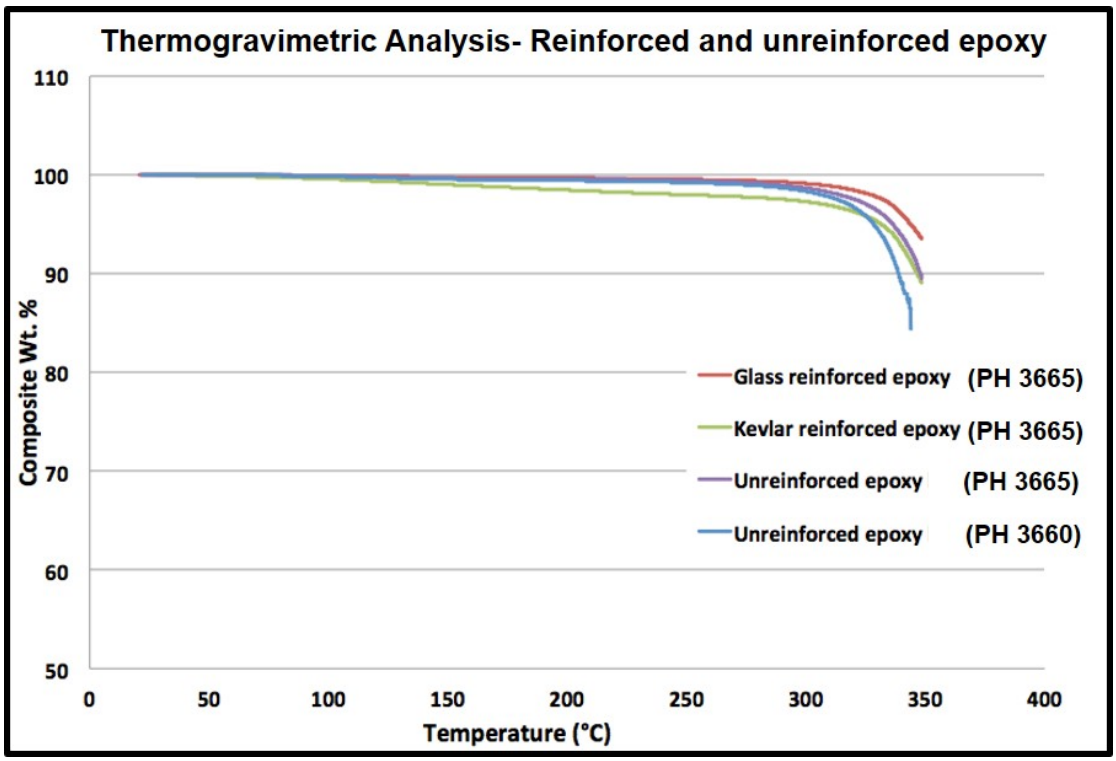

Fig. 4.1. TGA curves showing a comparative decomposition profile of reinforced and unreinforced epoxy. The resin hardeners used are enclosed in brackets.

4.2 Visual examination of composite

The epoxy-hardener mixture exhibited noticeable changes in its physical properties with time as soon as crosslinking takes place in the epoxy resin mixture. The epoxy mixed with PH 3660 resin hardener has a darker opaque color when compared with the epoxy mixed with PH 3665, which is clear and semitransparent. The difference in mixture color however, does not have any significant impact on the composite fabrication process other than the faster curing time experienced while using PH 3660 hardener. Curing of the resins proceeded over time at room temperature leading to increased viscosity, while the epoxy resin mixed with PH 3660 cured faster (under 12 h), the resin mixed with PH 3665 took a much longer time to completely cure. Figure 4.2 shows typical Kevlar® and glass fibers reinforced epoxy plates obtained after the epoxy resin (mixed with hardener PH 3665) was fully cured to the c-stage before cutting into sizes and shapes required for the heat treatment and mechanical tests.

Visual inspection of composites before and after thermal exposure to elevated temperatures revealed different levels of color change. Physical changes in typical glass and Kevlar® fibers reinforced epoxy during thermal exposure at temperature ranging between 150°C and 300°C for 30 minutes are documented in Fig. 4.3. Similar

color change occurred in samples exposed to radiative heat flux in the cone calorimeter. The color changed from yellowish for unexposed Kevlar® fiber reinforced composite specimen and from greyish color for glass fiber reinforced composite to brown and finally to black as the exposure temperature increased beyond 250°C. The brown and black color of the specimens exposed at high temperature is attributed to decomposition of materials to temperatures in excess of 200°C. A significant change in color was not visible in the thermally exposed sample until temperature exceeded 100ºC for both Kevlar® and glass fiber reinforced epoxy composite.

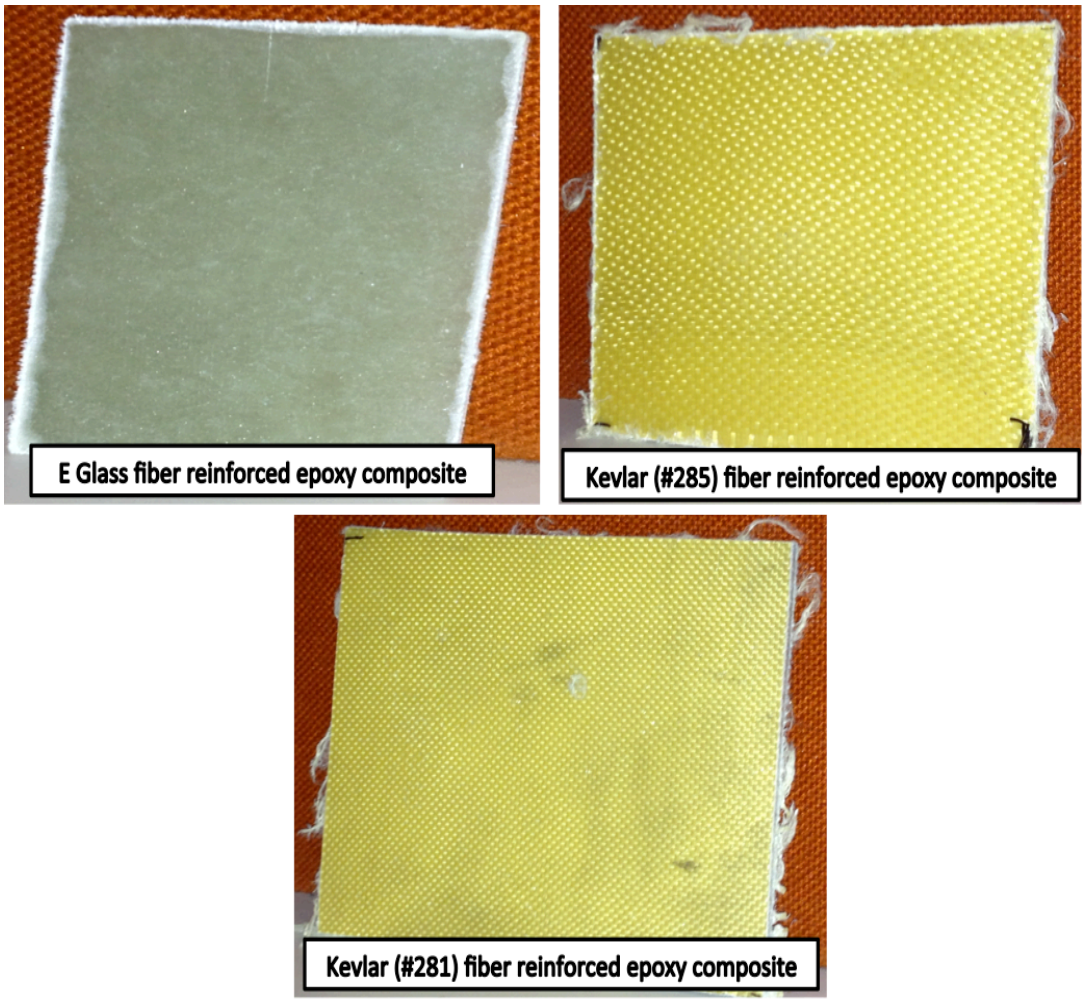

Fig 4.2. Photographs of Kevlar® and glass fibers reinforced epoxy composite plates obtained for room temperature curing of the epoxy/hardener mixture.

Observation based on visual examination shows no delamination until when the temperature exceeded 200°C for Kevlar® fiber reinforced epoxy and 250°C for glass fiber reinforced epoxy. The delamination is expected to result in loss of modulus and strength of composite when subjected to mechanical tests. This may also affect the failure mechanism.

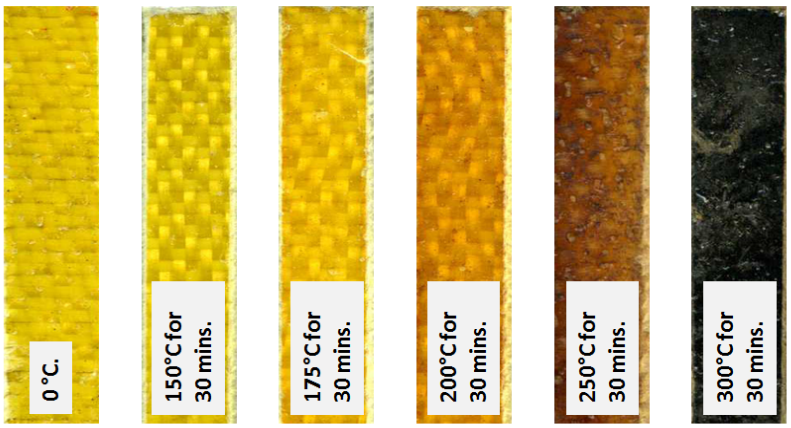

(a) Kevlar® # 285 exposed to convective heat in the furnace.

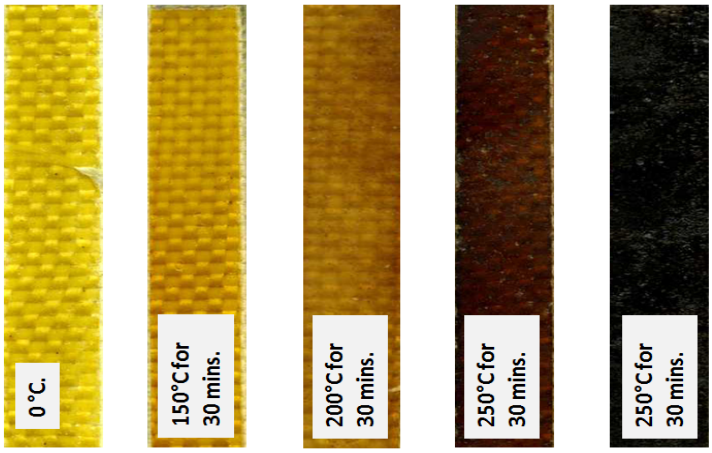

(b) Kevlar® #281 exposed to convective heat in the furnace.

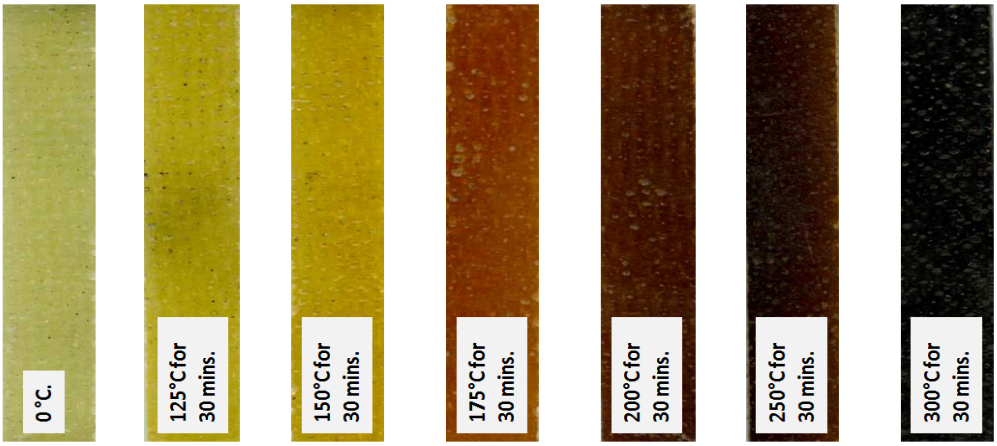

(c) S-Glass exposed to convective heat in the furnace.

Figure 4.3. Photographs showing different level of color changes in the fiber reinforced epoxy composites after thermal exposure in the furnace. (a) Kev #285, (b) Kev. #281 (c) S- glass

Different degrees of delamination were observed during visual observation of glass and Kevlar® fibers reinforced epoxy composite thermally exposed to a temperature of 250°C and above. Figure 4.3 shows the difference in the extent of delamination and damage that occurred in Kevlar® and glass fiber reinforced epoxy composite exposed to a temperature of 250°C for a period of 1 hour. It showed that under the same thermal condition, delamination occurred more rapidly in Kevlar® reinforced epoxy composite than for composite reinforced with glass fibers. This may not be unconnected to the higher possibility of thermal damage to glass fibers at these temperatures than Kevlar® fibers. The Kevlar® matrix bonds may, as result, be more prone to deterioration at temperature above 250°C.

Visual examination of the composites after thermal exposure at 200°C for a period of 1 hour shows no evidence of physical damage to the glass reinforced epoxy composite and delamination was not visible to the naked eyes, unlike the case in Kevlar® fiber reinforce epoxy composite where damage to the reinforced composite was very evident and occurrence of delamination is physically observed which could lead degradation of mechanical properties Further test will confirms the mechanical integrity of the reinforced epoxy under this extreme condition of thermal exposure.

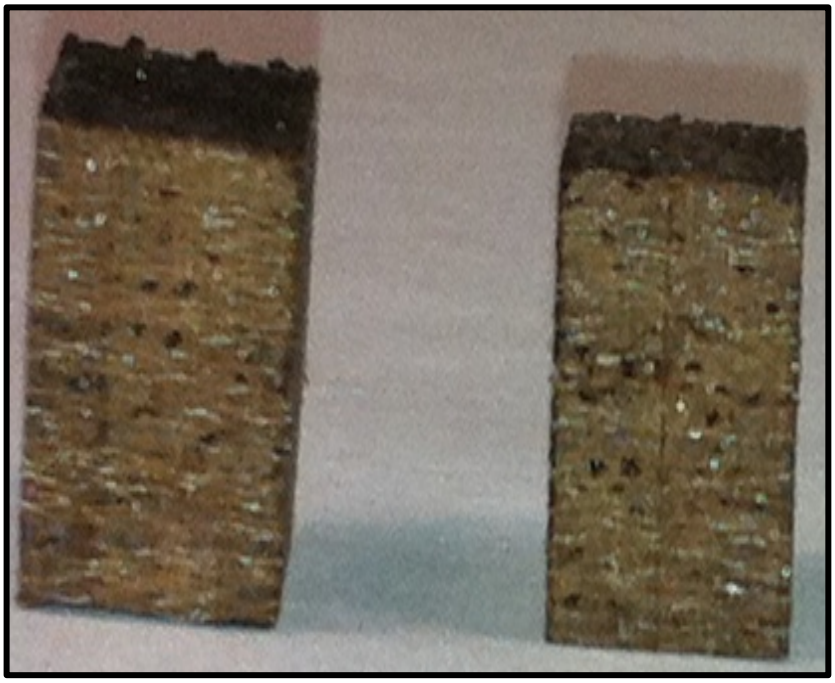

Fig. 4.4. Photographs of S-glass fiber reinforced epoxy composite after exposure at 250°C for 1 h.

Fig. 4.5. Photographs of Kevlar® #285 fiber reinforced epoxy composite after exposure at 250°C for 1 h.

4.3 Microscopic analysis of composites test samples.

Typical micrographs obtained from the microstructural evaluation of the fiber reinforced epoxy produced in the course of the current investigations before thermal exposure or mechanical test are presented in Fig. 4.6 and Fig 4.7, for composites reinforced with glass fibers and Kevlar® fibers, respectively. The micrographs indicate a good impregnation of the fiber bundles and good wettability of the fibers by the epoxy resin. Micrographs of the reinforced epoxy composite show very low porosity with no visible sign of debonding or delamination at the fiber-matrix interface. This result is similar for every composite material investigated irrespective of the type of Kevlar® or glass fibers used as the reinforcement. Application of pressure during the final polymerization stage of the epoxy resin was very effective in eliminating air pockets in the viscous resin hardener/mixture before reaching the c-stage. Good wettability of both fibers as well as the dense structure of the matrix is expected to translate into good mechanical properties of the resulting composite material.

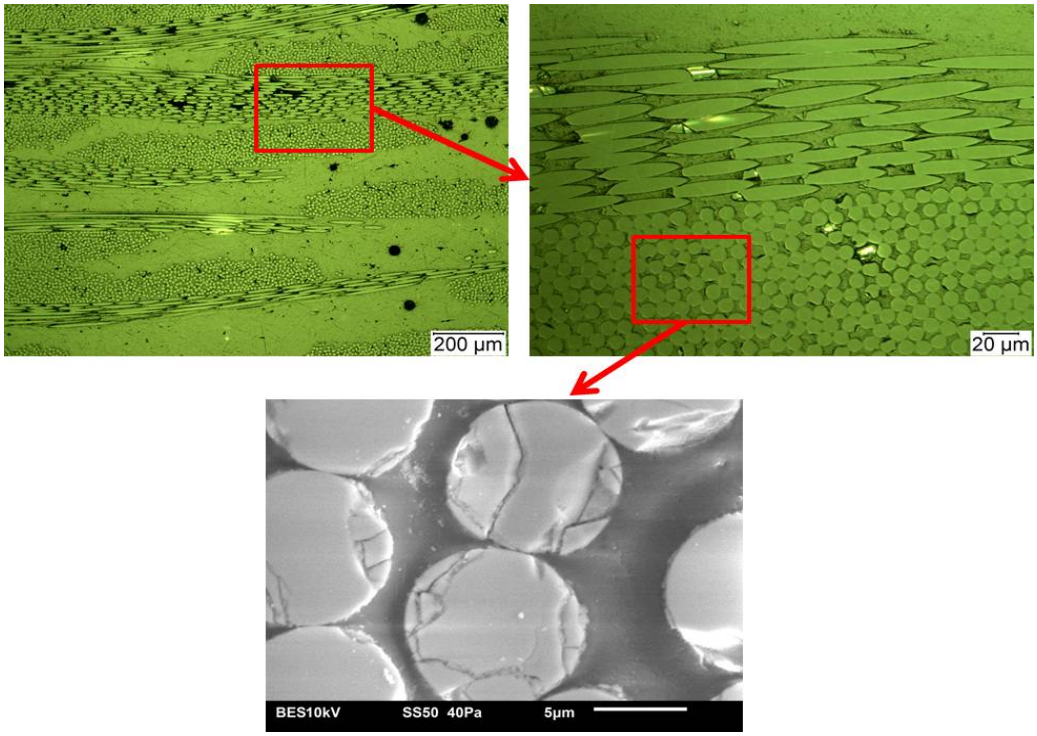

Figure 4.6. Optical and SEM micrographs of glass fiber reinforced epoxy matrix composite showing microstructure after curing at room temperature.

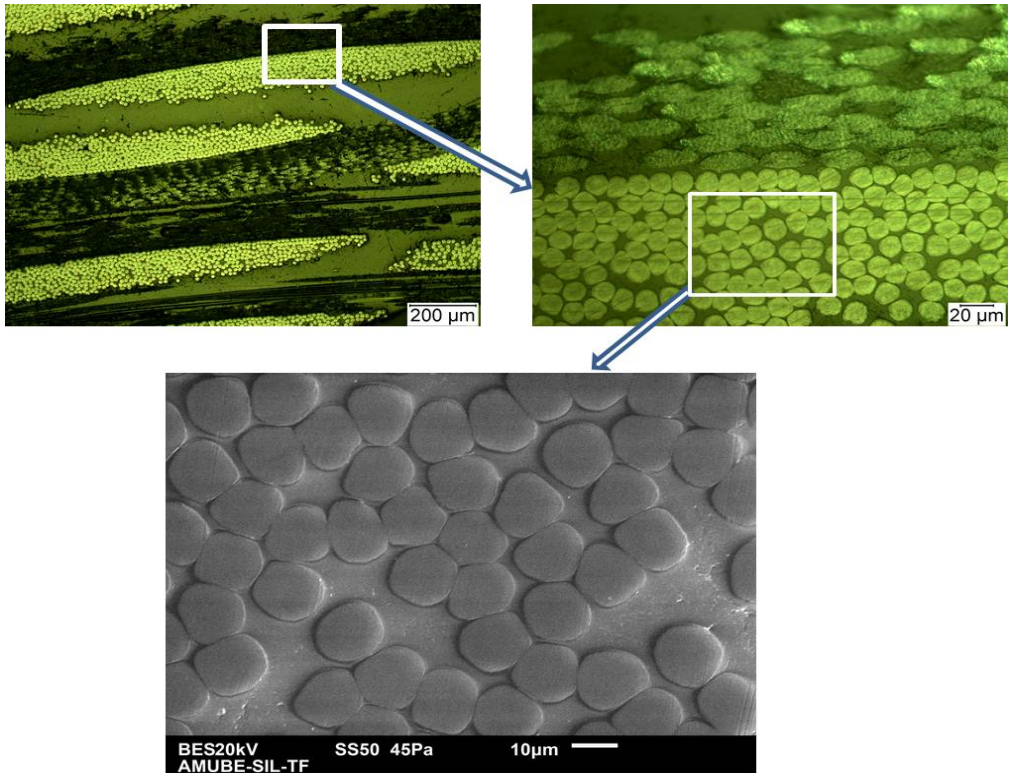

Figure 4.7. Optical and SEM micrographs of Kevlar® fiber reinforced epoxy matrix composite showing microstructure after curing at room temperature.

An overview of the effects of thermal exposure on the microstructure of glass and Kevlar® fiber reinforced epoxy are shown in Fig. 4.8 and 4.9, respectively. The good adhesion between the single fibers and the matrix is retained up to 250°C for both composite materials. This confirms a very strong bonding between the reinforcing and the reinforced components of the epoxy-based composite. This observation also suggests that there is no significant thermal mismatch between the fibers and the matrix, at least up to 250°C. Also there is no evidence of matrix cracking in both composites. However, delamination within fiber bundles at the interface between fiber bundles and the matrix region were observed in Kevlar® fiber reinforced composite when exposed to 250°C for 1 h. These are indicated by arrows as shown in Fig. 4.9. Such visible delamination was not observed in glass fiber reinforced epoxy exposed to 250°C for the same period of time. There was no evidence of matrix cracking, matrix degradation or fiber degradation in the microstructure of both glass and Kevlar® fiber reinforced epoxy for and exposure times of up to 2 hr. exposure temperatures of up to 250°C. This observation is in line with the results of TG analysis, which indicates that no significant decomposition (depicted from weight loss) occur in both the composites and unreinforced matrices until exposure temperature exceeded 300°C. Loss of volatile matter during matrix decomposition would have led to matrix shrinkage. Free matrix shrinkage would have been hindered by the fiber leading to matrix cracking and delamination. Thus lack of any significant matrix cracking up to 250°C can also be an indication of no matrix decomposition at this temperature as observed in the TG analysis. Significant damage due to delamination was observed to occur in both glass and Kevlar® fiber reinforced epoxy when exposed to 300ºC for 1 hr. as documented in Fig. 4.10 and 4.11, respectively. While the glass fibers appear to become more brittle and broke significantly during polishing, the Kevlar® fibers appear to fuse together within each fiber bundle.

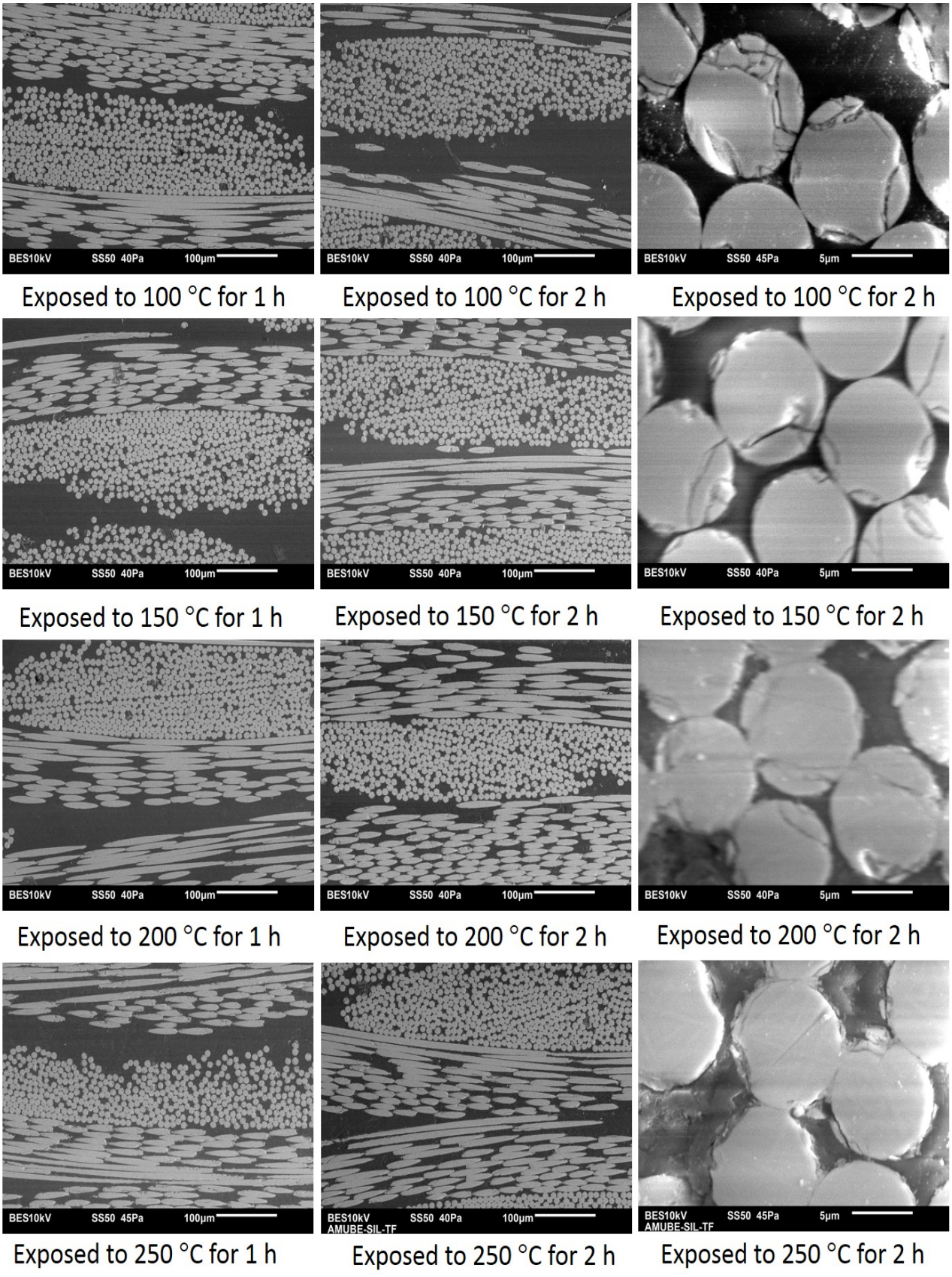

Fig. 4.8. SEM Microstructure of glass fiber reinforced epoxy after thermal exposure in a furnace

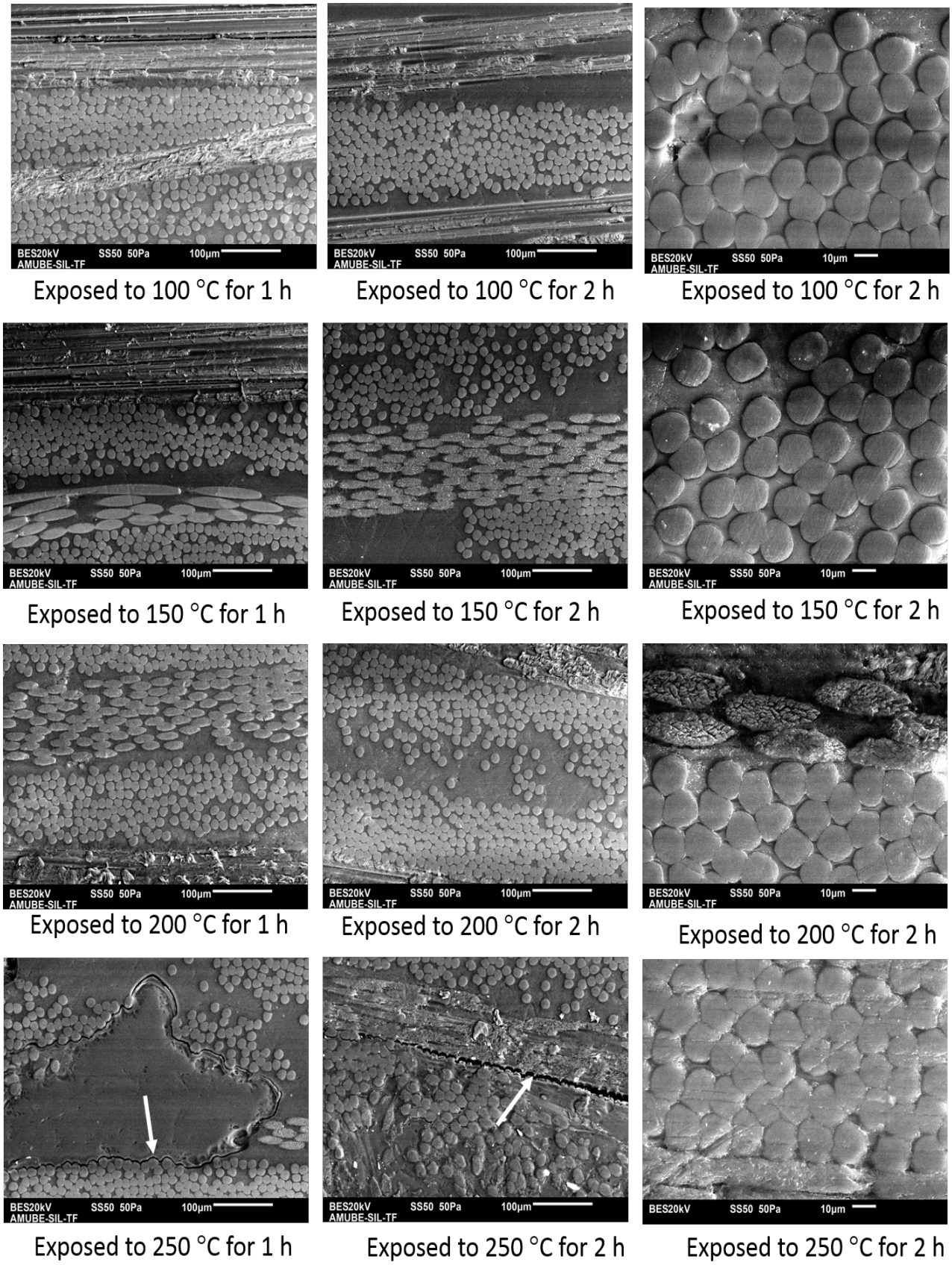

Fig. 4.9. SEM Micrographs of Kevlar® fiber reinforced epoxy after thermal exposure in a furnace – SEM (Arrows indicate delamination).

Matrix degradation due to decomposition occurred extensively in the composite at 300ºC as predicted by the results of the TG analysis. At this temperature it was evident that formation of char occurs at the surface and within the composite. The epoxy matrix became brittle at the exposure temperature as chunk pieces of the matrix fell off during polishing leaving big cavities on the polished surfaces of the composites as shown in Fig. 4.10 and 4.11. This is similar to the result reported by Bhavesh *et al*. [10], that the early stages of composite degradation is a continuation of crosslinking which ultimately results in formation of brittle carbonyl char due to chains scission [10]. Although the microstructure of both glass and Kevlar® fibers reinforced do not show significant damage during thermal exposure to up to 200°C, microscopic investigation of the thermally exposed composites suggest that glass fiber reinforced composite has a better resistance to damage at temperature in excess of 200°C. Thus it is anticipated that glass fibers reinforced epoxy will exhibit superior mechanical performance at elevated temperature. The superior performance of the glass fiber reinforced composite might be due to higher stability of glass than Kevlar®. As indicated in the thermal analysis of the radiative heat flux from the engine of a Cessna aircraft, a cowling made of epoxy reinforced with any of the fibers will not experience temperature rise near the maximum 200°C, where considerable polymer degradation can occur.

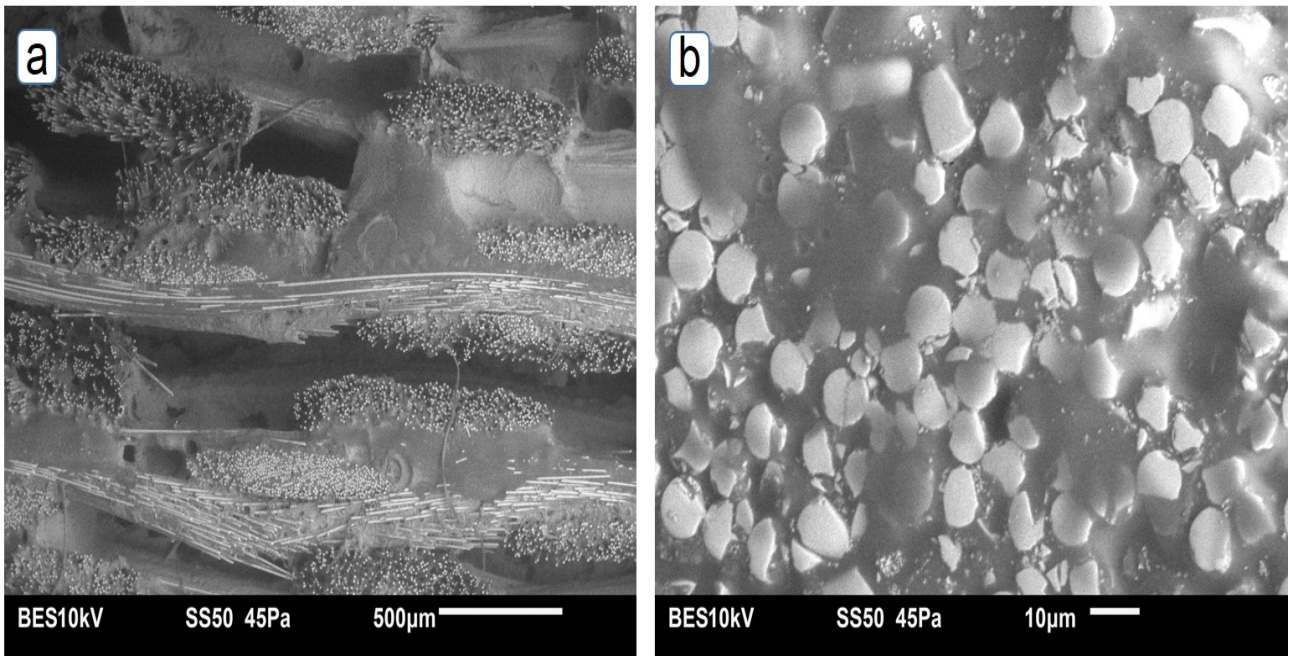

Fig. 4.10. SEM micrographs of glass fiber reinforced epoxy after thermal exposure at 300ºC for 1 h (a) overview and (b) fiber bundle.

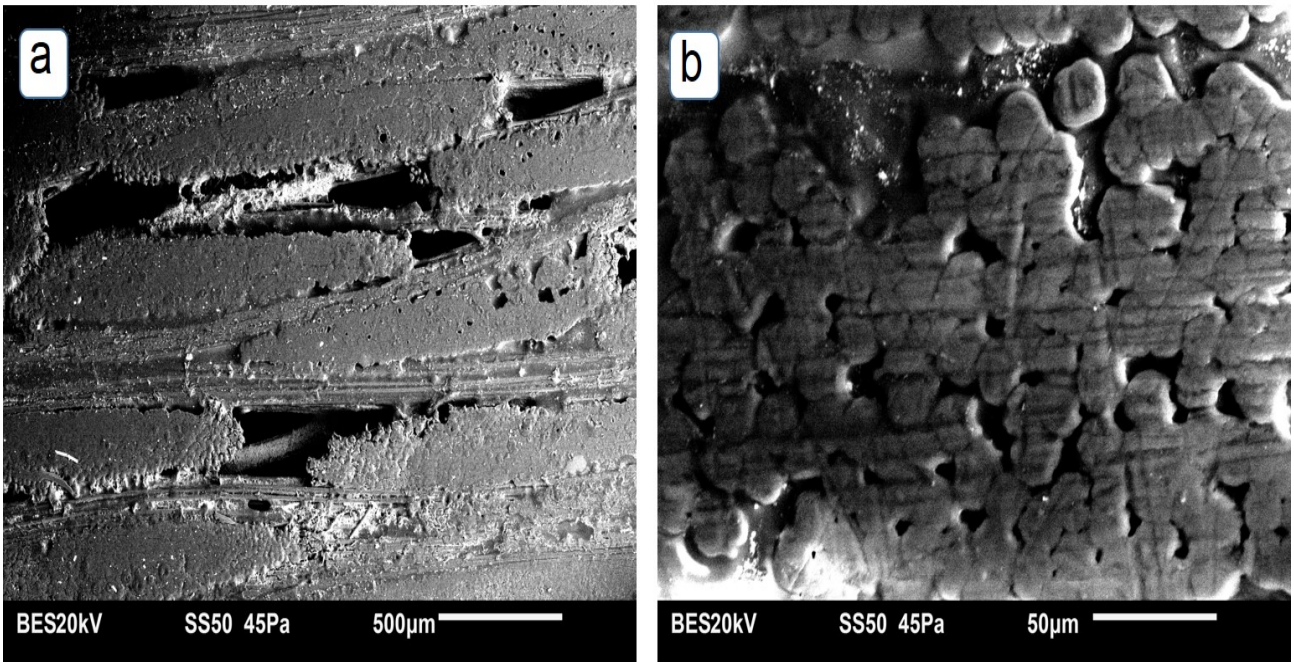

Fig. 4.11. SEM micrographs of Kevlar® fiber reinforced epoxy after thermal exposure at 300ºC for 1 h (a) overview and (b) fiber bundle.

This result indicates that glass and Kevlar® fiber reinforced epoxy composite are not threatened by excessive thermal decomposition when exposed to an elevated temperature below 200°C in service. However, a service condition in which the composites can be exposed to temperature above 200°C without thermal insulation is not recommendable. Intended field application of these composite materials requires far less temperature range, hence, composites of both Kevlar® and glass fibers are considered suitable for this purpose.

4.4 Dynamic mechanical thermal analysis (DMTA)

The dynamic mechanical thermal analysis (DMTA) was carried out to evaluate the damping behavior of both the manufactured glass and Kevlar® fiber reinforced epoxy matrix composites when subjected to dynamic loading at different temperature and under different loading conditions. Each tested sample was subjected to required test condition once per sample. Though some test were repeated two to three times, but the report presented represent sample behavior per test condition. DMTA provides the storage modulus (E′) loss modulus (E′′) and mechanical loss factor (tan δ) of the composite samples under dynamic loading as a function of dynamic strain or static strain, frequency, time and temperature depending on the test sweep mode, which could be strain sweep, frequency sweep, temperature or time sweep. Whereas the storage modulus is a measure of the stored energy in the specimen, the loss modulus is a measure of the energy dissipated in the material during dynamic loading. The mechanical loss factor provides a measure of the damping capacity of the materials under dynamic mechanical

loading. Time temperature scan in DMTA is very useful in determining the glass transition temperature of a polymer. When glass transition occurs in polymers the storage modulus drops very rapidly while loss modulus and mechanical loss factor increases to a maximum value and then drop. Peak values in mechanical loss factor of polymers signifies occurrence of transition in the polymer. Fig 4.12 and Fig 4.13 show the results of the temperature-time sweeps for glass fiber reinforced epoxies as a function of the hardener used in curing the resin matrix. From this figure it can be observed that the glass transition temperatures for the glass fiber reinforced epoxy matrix composites ranged between 80°C and 100°C. This is slightly above the maximum temperature the cowling of a Cessna aircraft will be exposed to in service.

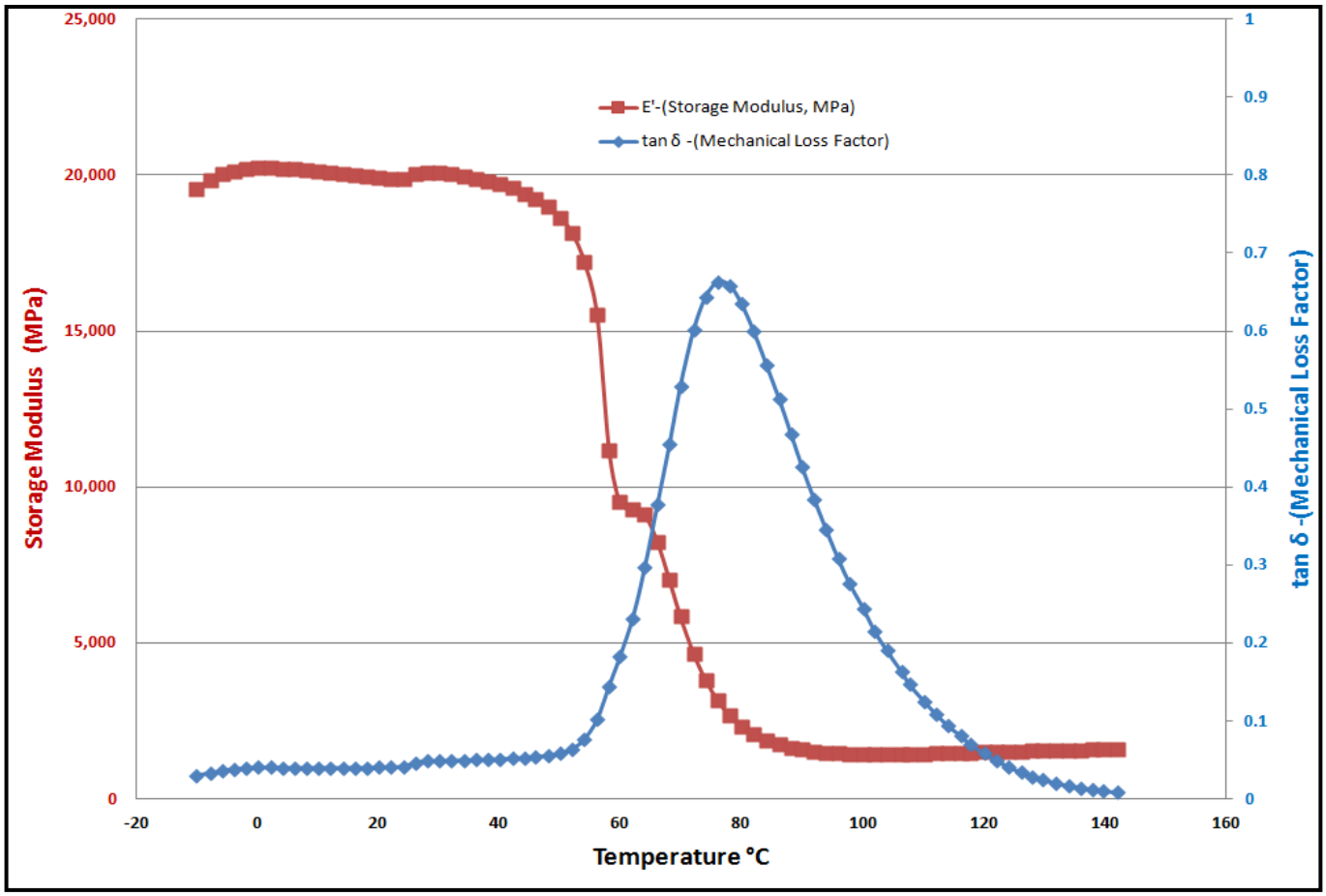

Fig. 4.12. DMTA; Temperature-time sweep on S-glass fiber reinforced epoxy (hardener PH 3660, Frequency = 10Hz, Static Load = 80 N, Dynamic Load = 69 N).

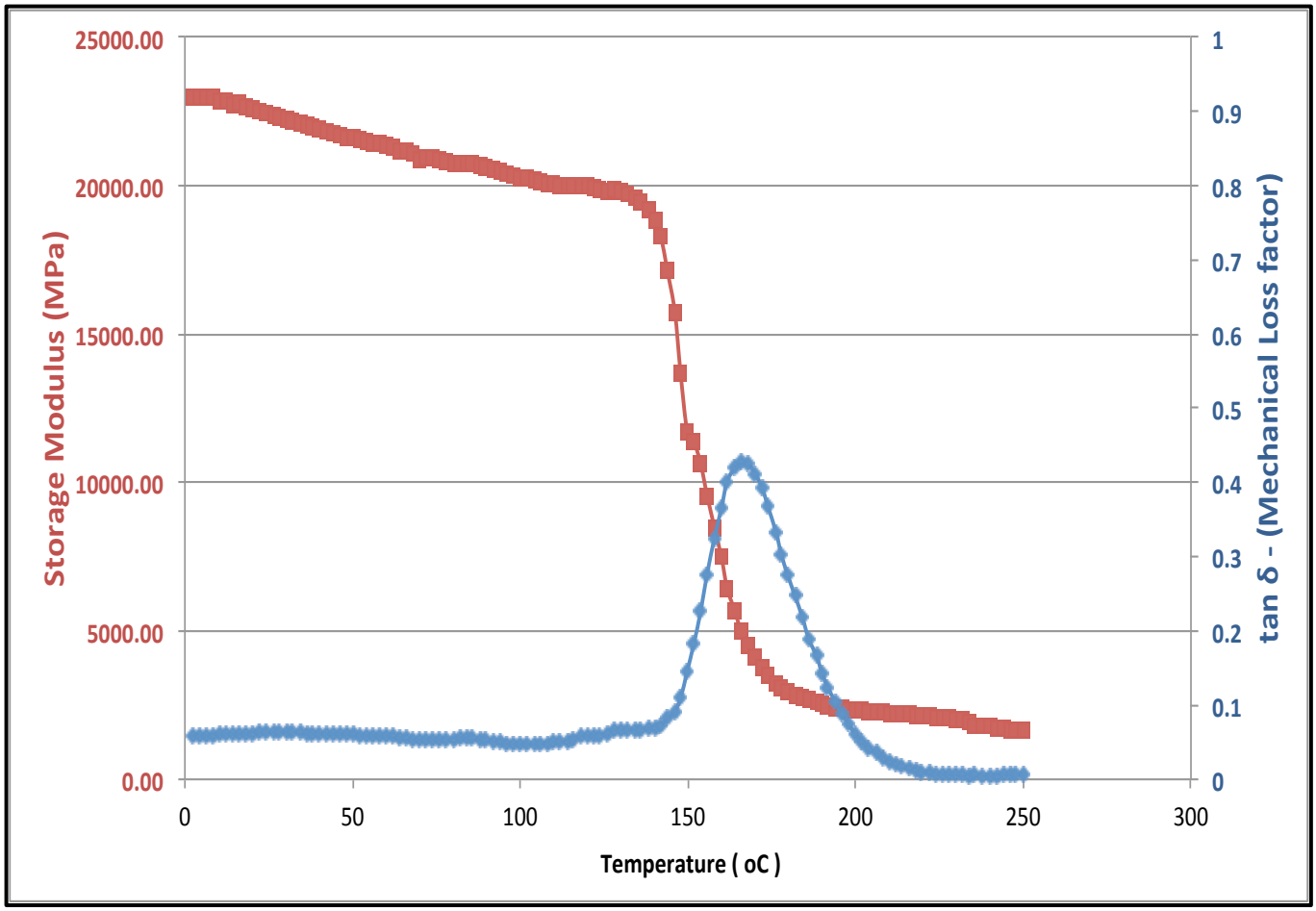

Fig. 4.13. DMTA; Temperature-time sweep on S-Glass fiber reinforced epoxy (hardener = PH 3665, Frequency = 10Hz, Static Load = 80 N, Dynamic Load = 69 N).

The effects of increasing dynamic strain and the applied resin hardener on storage modulus and mechanical loss factor of S glass fiber reinforced epoxy composites are shown in Fig. 4.14. The results show some level of reduction in storage modulus as dynamic strain increased while the mechanical loss factor slightly increased. This agrees with a previous similar result [22] that also revealed that storage modulus experienced a rapid descent as loss modulus rose to its maximum value. Decrease in storage modulus and increase in mechanical loss factor can be due to increase in energy dissipation at the fiber matrix interface as the dynamic strain increased. It has been suggested that storage and loss moduli in a composite are influenced by the extent of elastic energy losses at the fiber-matrix interface during cyclic loading [67]. The increase observed in the mechanical loss factor (tan δ) with decreasing dynamic strain can imply an increase in the damping capacity of the composite. The results of a previous study showed that the value of tan δ for a delaminated composite is higher than for the one in which delamination had not occur [22]. This suggests the existence of possible correlation between mechanical loss factor and tendency for debonding (or delamination) in a composite.

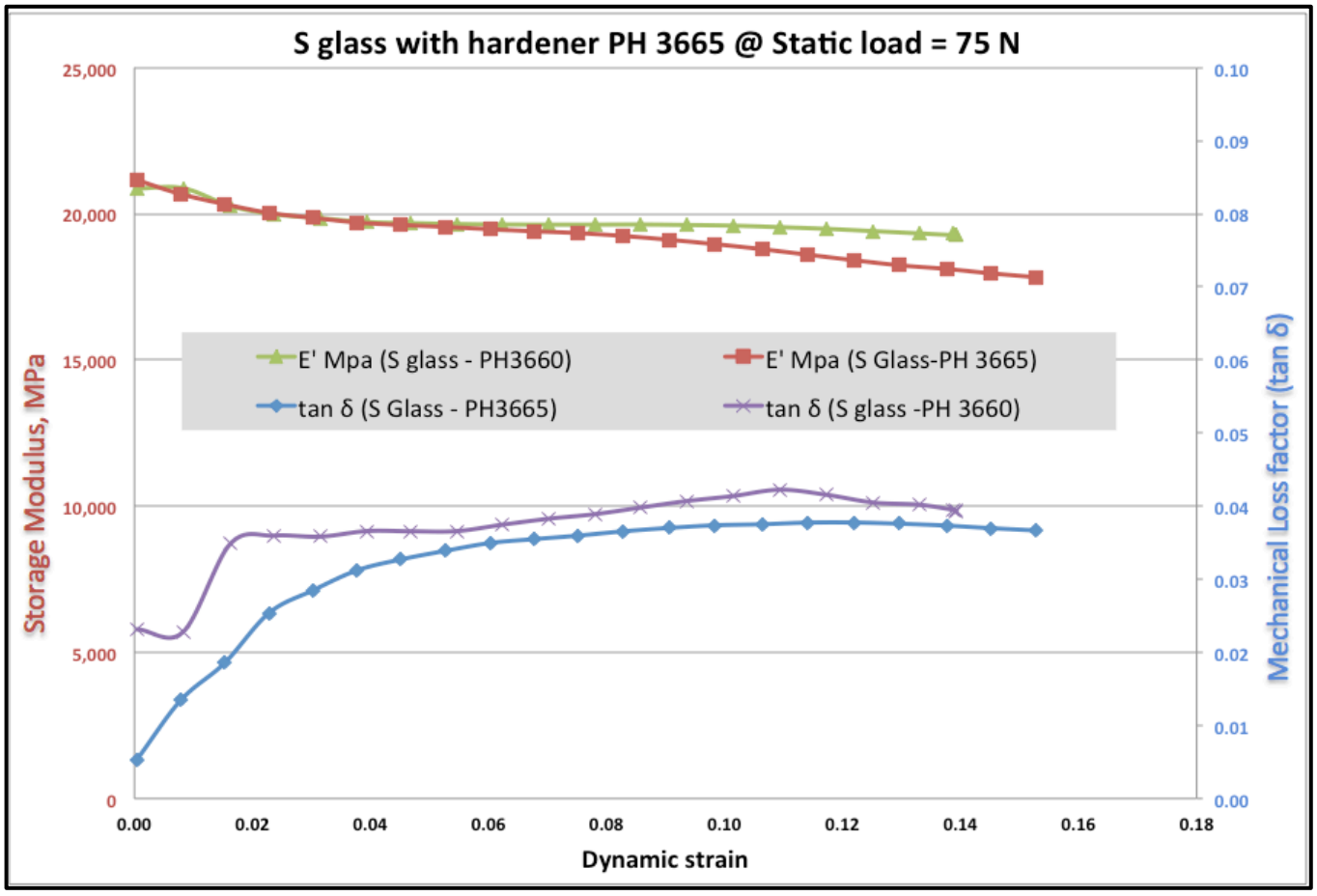

Fig 4.14. The effects of increasing dynamic strain at constant static strain on the storage modulus and mechanical loss factor of S Glass fiber reinforced epoxy matrix composite (Frequency = 10 Hz, T = 25ºC).

Dynamic Mechanical Analysis of two different samples with different hardener resin tested under similar test condition show no significant difference in their storage modulus and mechanical loss factor. The slight difference observable in Fig. 4.14 may be due to inhomogeneity in the structure leading to slight variation in the dynamic mechanical response of the composites. It may also be as a result of a slight variation in the strength of the fiber matrix interfacial bonding, which may affect the extent energy dissipation at the fiber-matrix interface. Figures 4.15 and 4.16 show the results of static strain sweep (at constant dynamic strain) on the Kevlar® fiber reinforced epoxy. As in the case of static strain sweep (Fig. 4.15) the storage modulus decreased while mechanical loss factor increased as dynamic strain increased. Loss in mechanical factor with static strain can also be attributed to energy dissipation at fiber matrix interface.

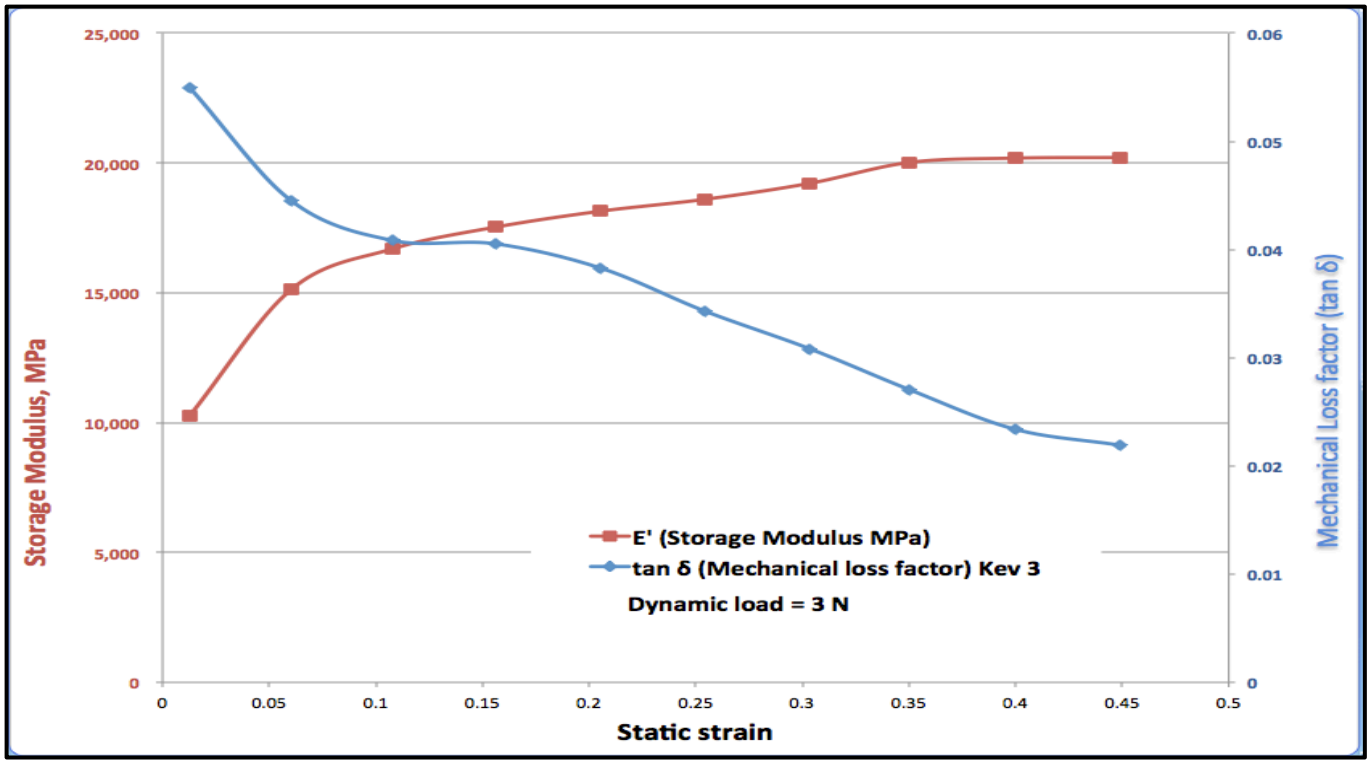

Fig. 4.15. Static strain sweep test on Kevlar® # 120 fiber reinforced epoxy.

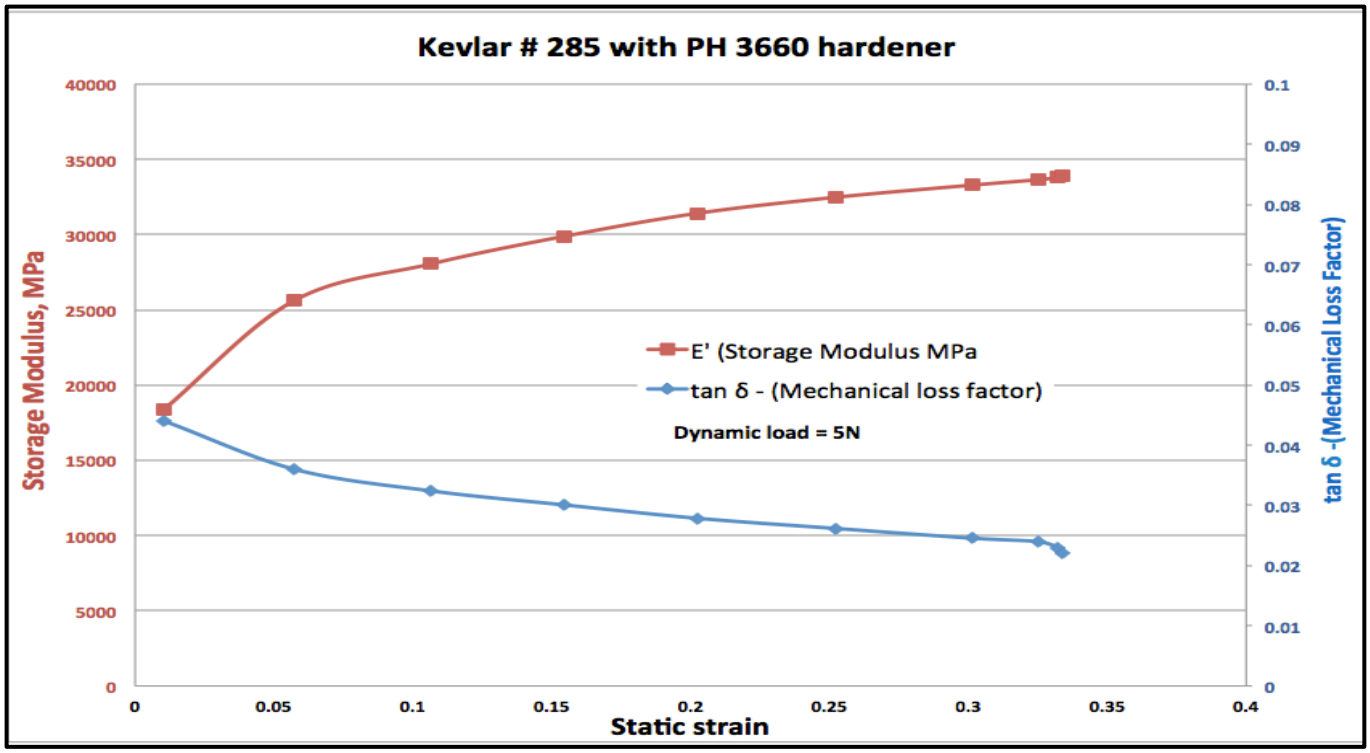

Fig. 4.16. Static strain sweep test on Kevlar® # 285 fiber reinforced epoxy.

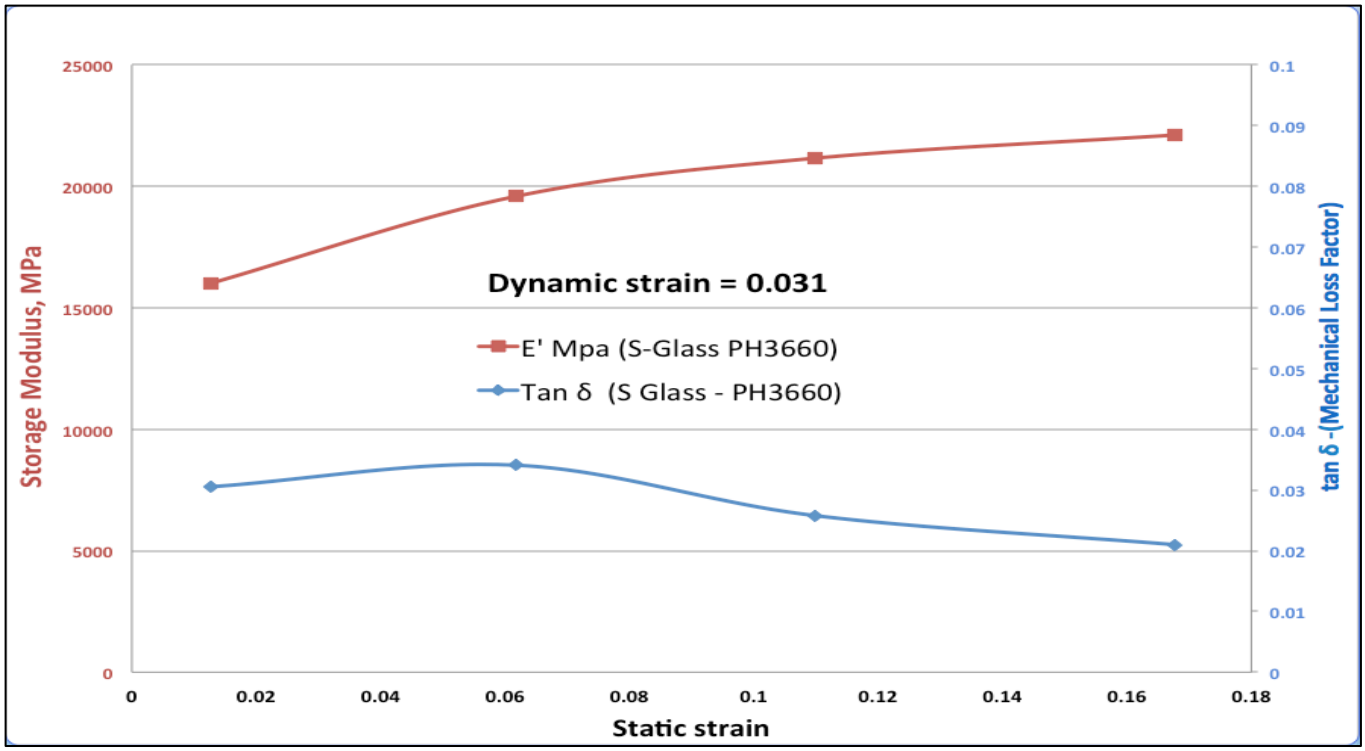

Fig 4.17. DMA: Static strain sweep test on S – Glass fiber reinforced epoxy (PH 3660)

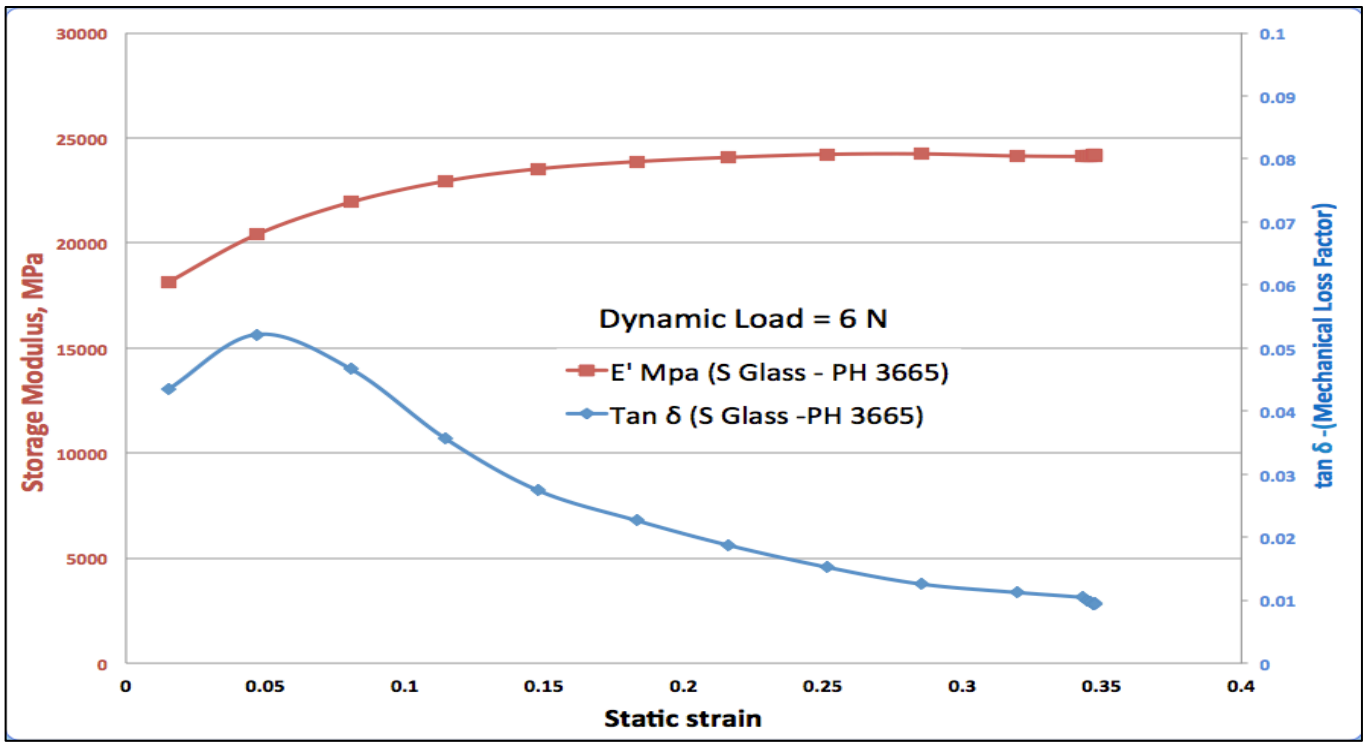

Fig 4.18. DMA: Static strain sweep test on S – Glass fiber reinforced epoxy (Hardener PH 3665).

In the static strain sweep tests, a comparison of the dynamic response of resin cured with different hardener show a higher storage modulus and mechanical loss factor for the composite cured with hardener PH 3665 than those cured with PH 3660 (Fig. 4.19 and 4.20). The difference in storage and loss modulus might be due to a slight difference in the bonding strength between the fibers and the matrices for the two composited obtained from different hardeners. The results of some previous studies have also shown that the storage and loss modulus of fiber reinforced polymers are dependent on the strength of the bonding between the fibers and the matrix [68, 69]. The results of frequency sweep show that both the storage modulus and the mechanical loss factor are largely unaffected by the frequency of the cyclic loading as documented in Figs. 4.21 and 4.22 showing typical results for Kevlar® #285 and Kevlar® #120

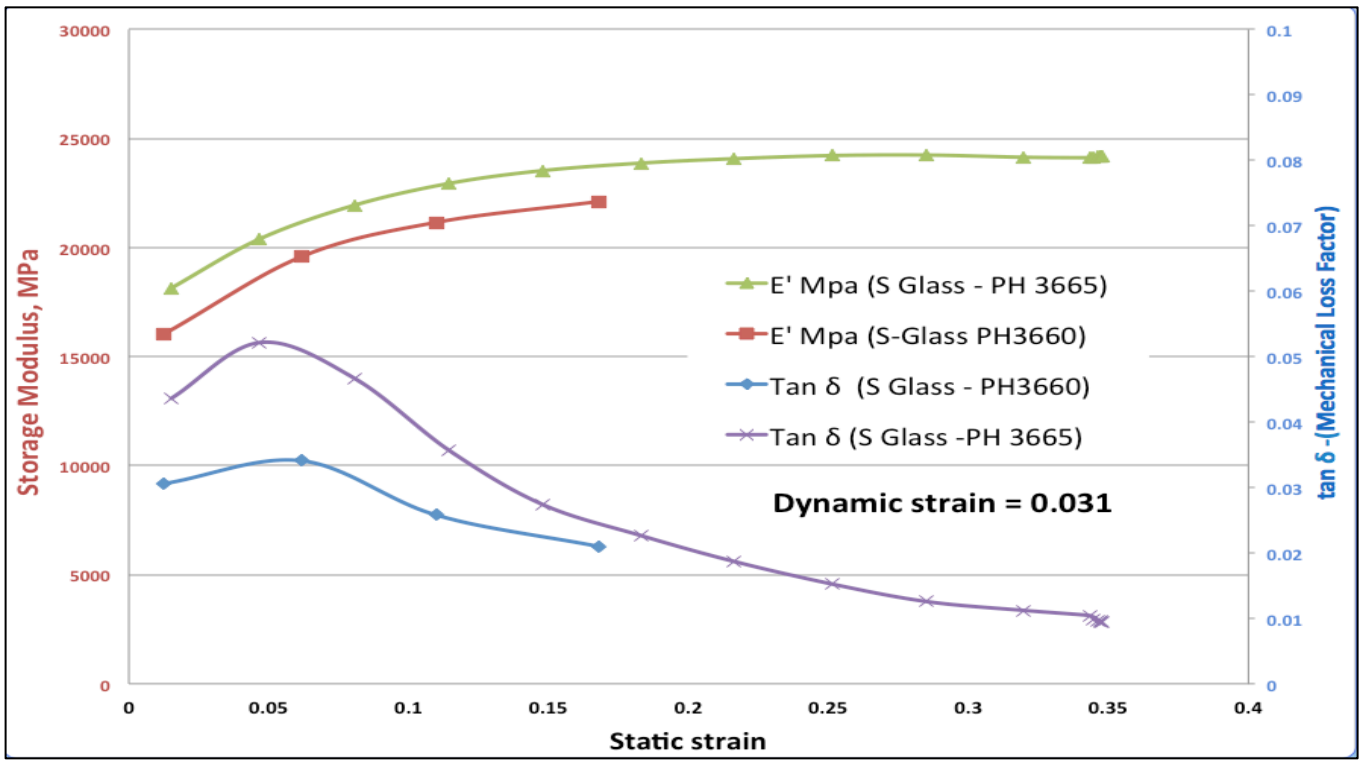

Fig. 4.19. DMA: Static strain sweep test showing the effects of the applied resin hardener on storage modulus and mechanical loss factor of S-glass fiber reinforced epoxy

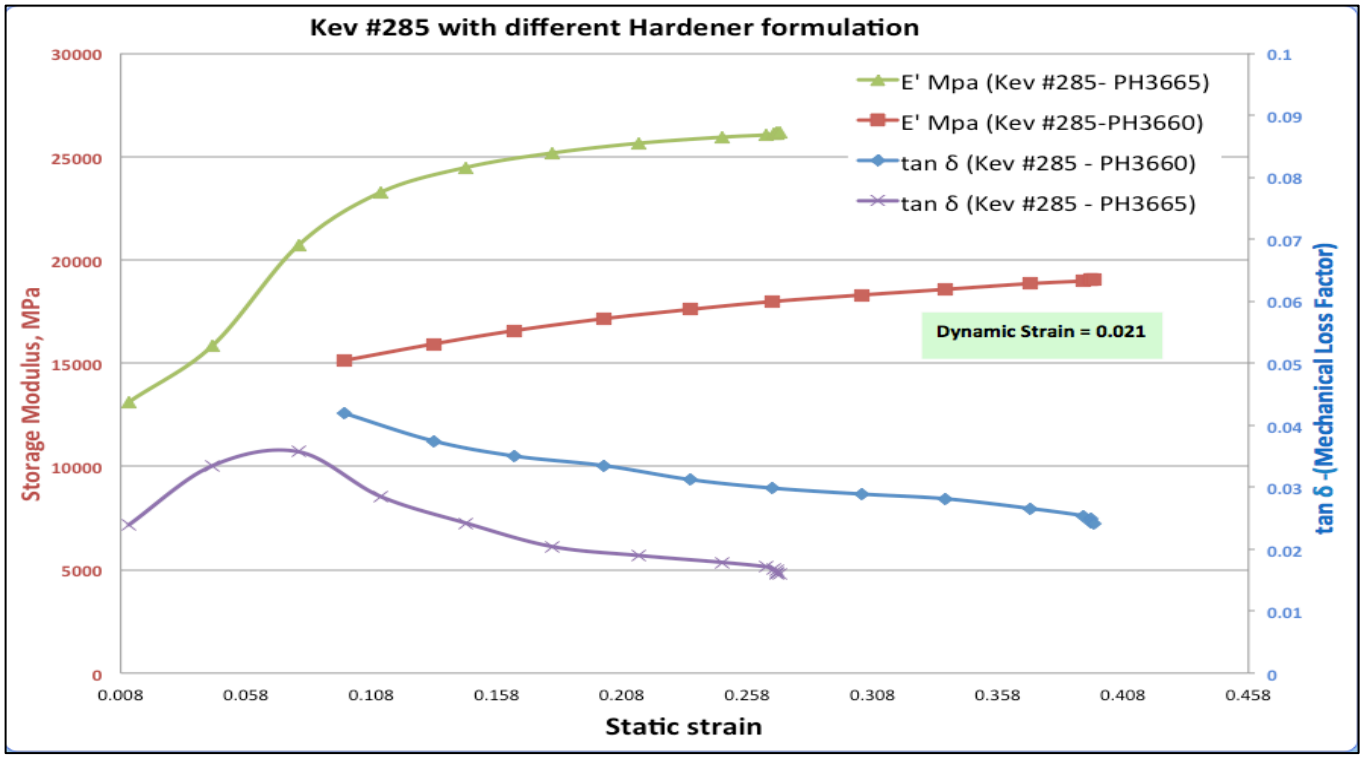

Fig 4.20. DMA: Static strain sweep showing the effects of applied resin hardener on storage modulus and mechanical loss factor of Kevlar® 285 fiber reinforced epoxy

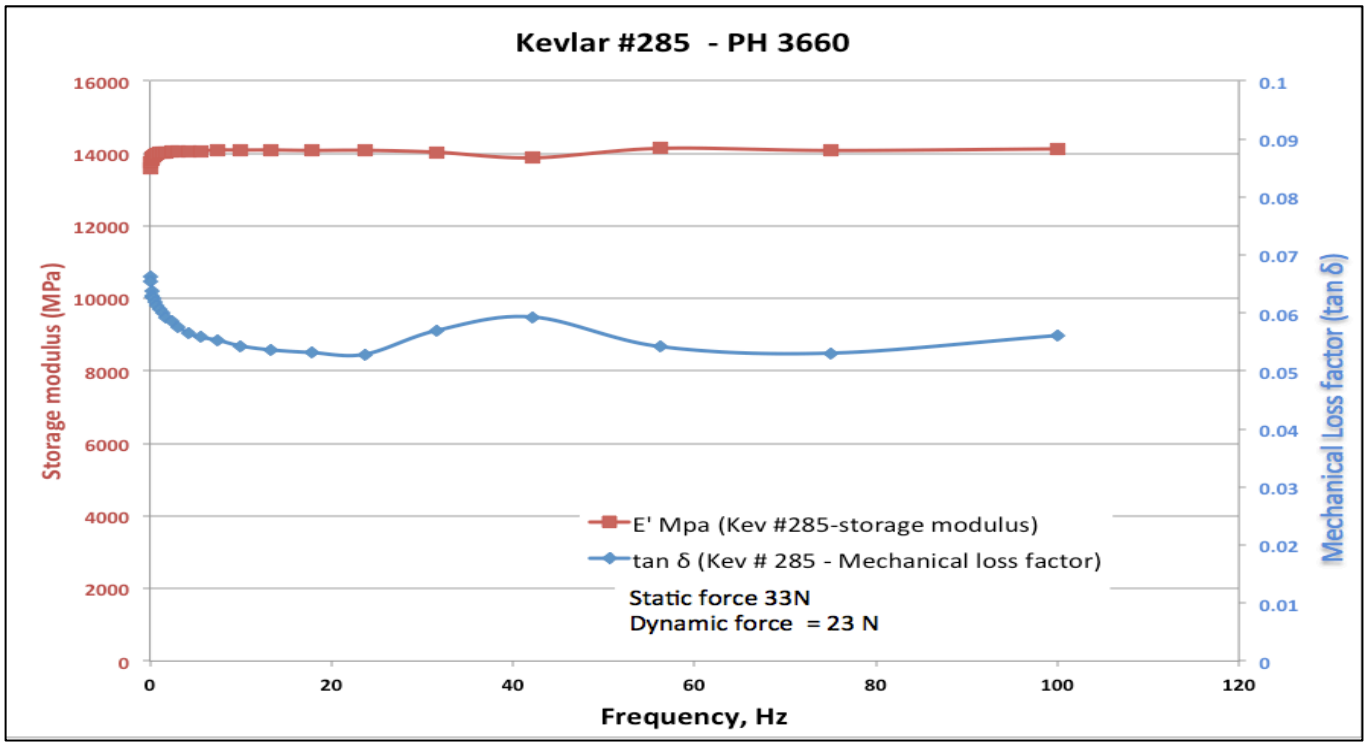

Fig. 4.21. DMA: Frequency sweep on Kevlar® # 285 fibers reinforced epoxy composite

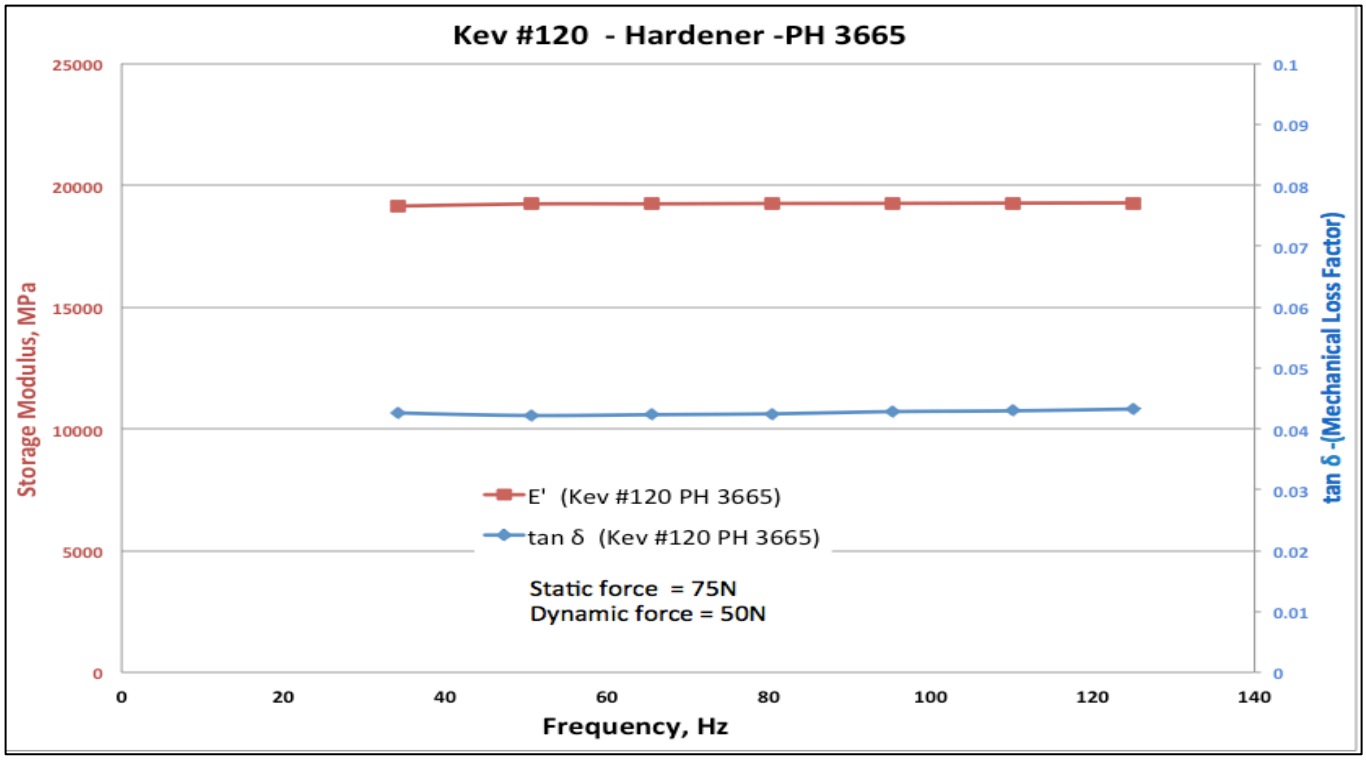

Fig. 4.22. DMA: Frequency sweep on Kevlar® # 120 fibers reinforced epoxy composite

4.5 Quasi-static and dynamic mechanical tests

Fiber reinforced composite materials, as discussed in the previous chapters, exhibit some unique properties that determine their importance in structural applications. These properties can change with change in the service conditions under which a composite is used. Such change in properties under a different service condition can subsequently impair the mechanical integrity of the composite material. The results the effects of thermal exposure on the response of the fiber reinforced epoxy to both quasi-static (three point bending) and dynamic mechanical (impact) loading are discussed. The goal is to ascertain the effects of thermal exposure on the mechanical performance of the material in service.

4.5.1 Three point bending test

Typical stress strain curves obtained during flexural loading of the glass and Kevlar® fiber reinforced epoxy before and after thermal exposure (at 200°C for 2 h) are shown in Fig. 4.23. Epoxy reinforced with glass fiber was observed to have higher flexural strength than that reinforced with Kevlar® fibers. However glass fiber reinforced epoxy exhibited less damage tolerance when compared with Kevlar® fiber reinforced epoxy. While Kevlar® fiber reinforced epoxy showed evidence of plastic deformation before failure, the composites reinforced with glass

fibers fracture within the linear portion of the stress strain curves. Whereas there was no significant difference between fractures strain of glass fiber reinforced epoxy exposed to 200ºC for 2 h. and the one with no thermal exposure, the Kevlar® fiber reinforced epoxy with no thermal exposure (virgin sample) exhibits a more distinct damage tolerance than that exposed to 200°C for 2 h. Comparing the two experimental conditions for both Kevlar® and glass fibers reinforced epoxy composites as shown in fig 4.23, there was no significant difference noticed in the flexural strength for samples at their original state (virgin samples) and after exposure at 200ºC for 2 h. This further confirms the stability of composite's mechanical properties at temperatures of up to 200ºC for 2 h. exposure.

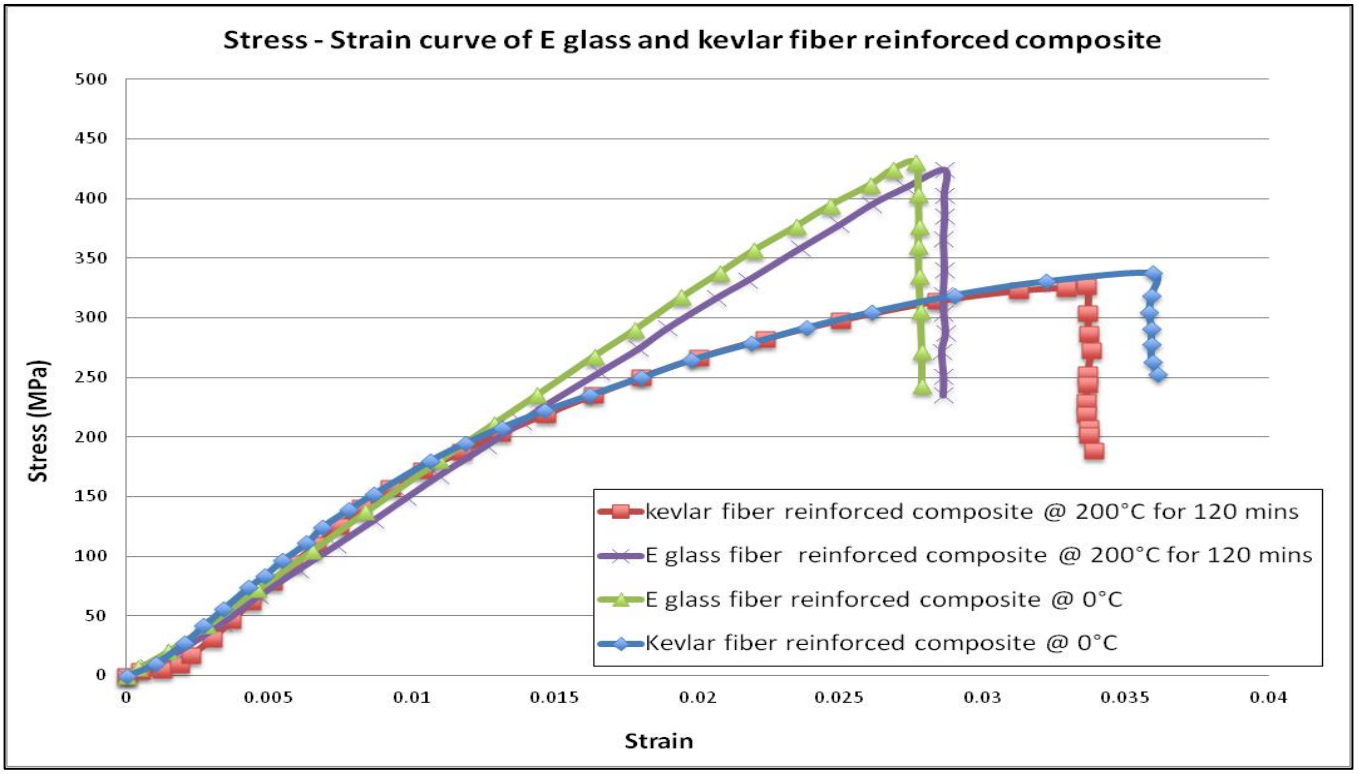

Fig 4.23. Flexural stress-strain curve comparing samples of E glass and Kevlar® #281 reinforced composite before and after exposure at 200ºC for 120 min.

Figures 4.24 and 4.25 show the typical flexural stress-strain curves for glass and Kevlar® reinforced composites after exposure to various thermal conditions. The result confirms further that no significant change occurred in the flexural properties of the composite made of both glass and Kevlar® fibers when exposed to temperature of up to 200ºC and exposure time of up to 120 minutes. But at 300ºC, rapid loss of strength and modulus is observed in both Kevlar® and glass fiber reinforced composites, even for 30 mins exposure. This can be associated to degradation of epoxy resin at temperatures above 250°C as recorded in the results of TGA of the reinforced and

unreinforced epoxy. The resin matrix binds together the reinforcing component (Kevlar® or glass fibers) of the composite. When thermal degradation occurs, it affects the resin matrix significantly and can also affect the fiber matrix interfacial bonding with the attendant consequence of causing deterioration of the mechanical integrity of the composite.

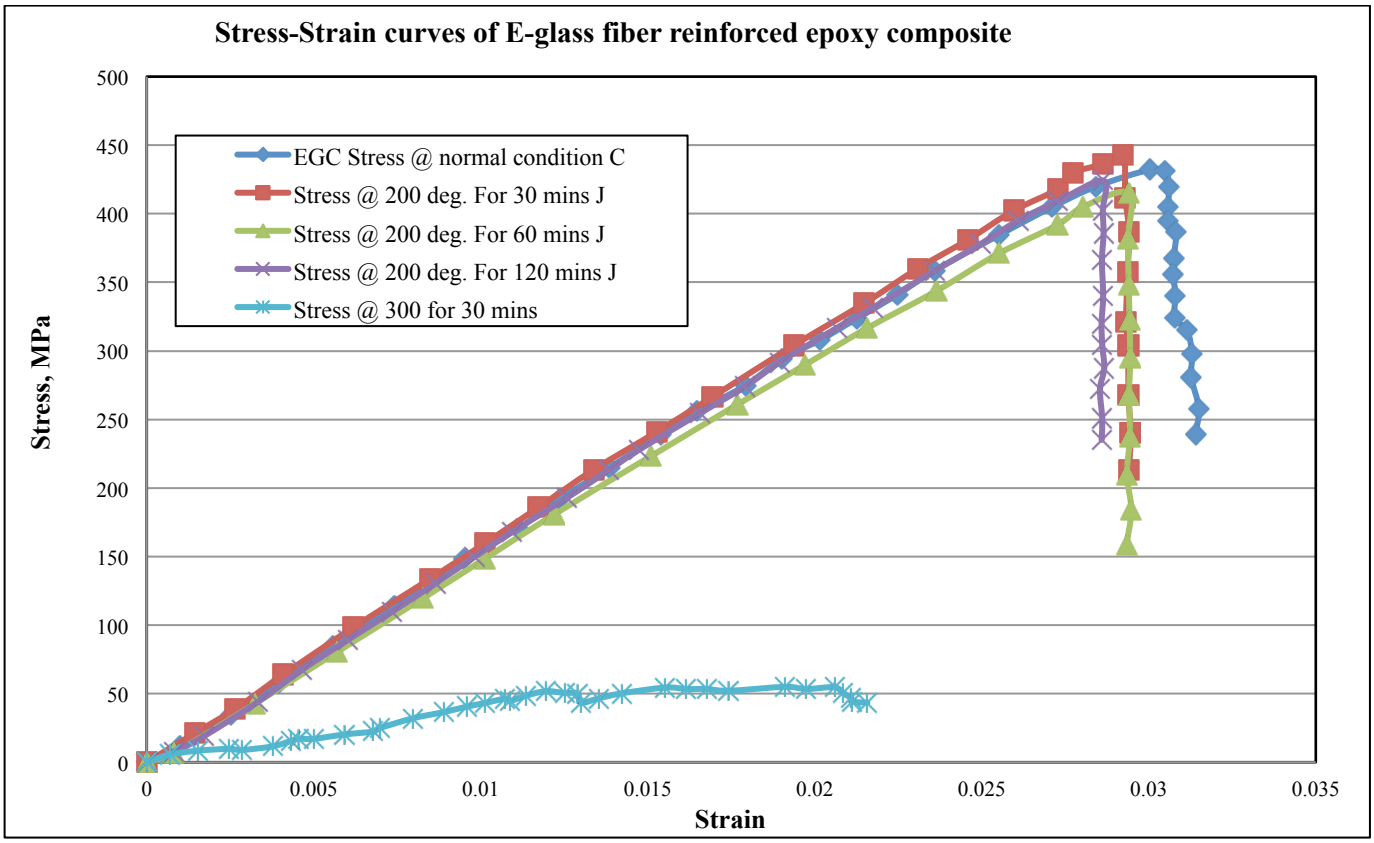

Fig 4.24. Flexural stress- strain curves of E Glass fiber reinforced epoxy composite showing typical effect of temperature on the flexural strength and modulus (PH3665).

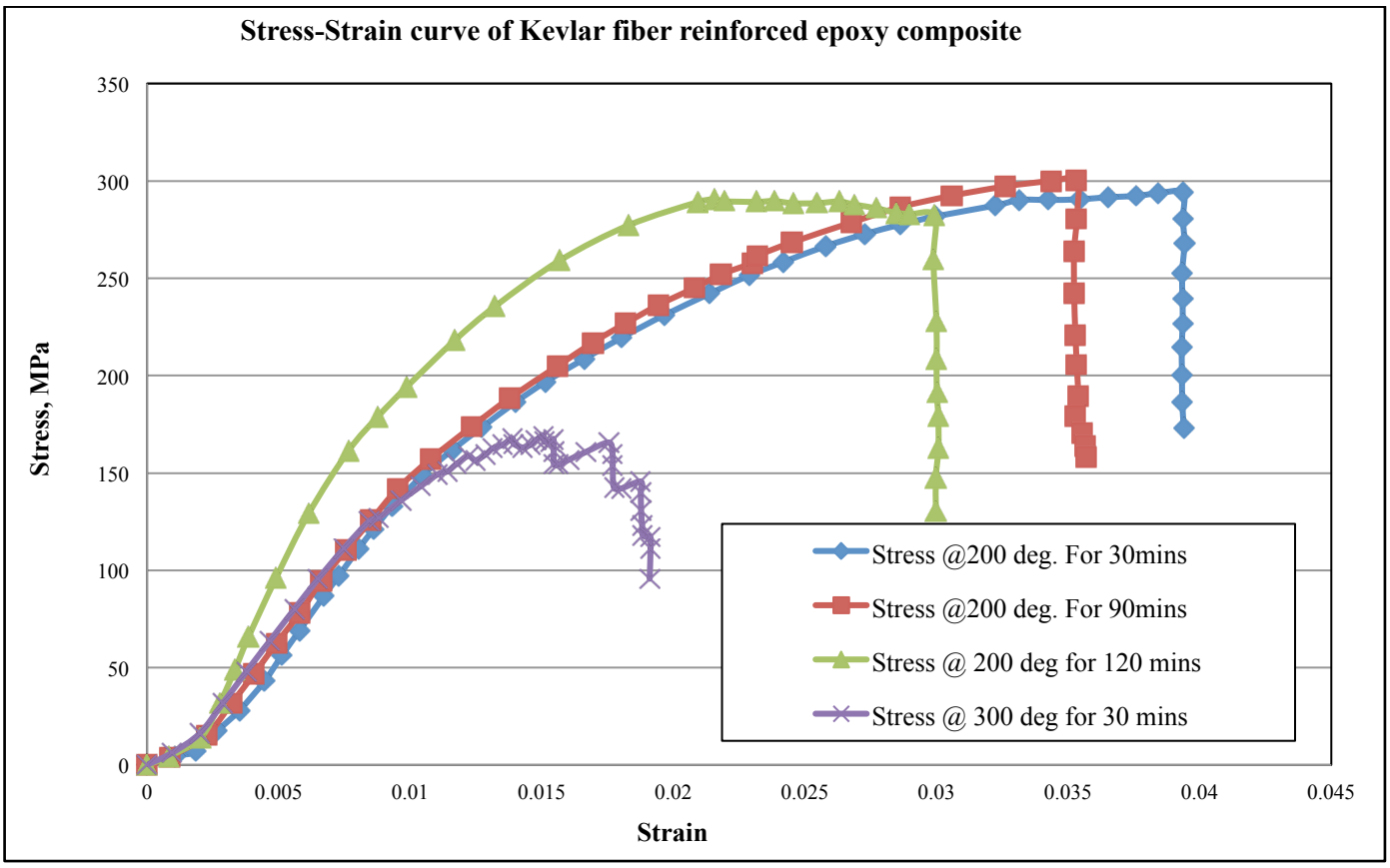

Fig 4.25. Flexural Stress–strain curves of Kevlar® #285 fiber reinforced epoxy composite showing the effect of temperature on flexural strength and modulus (PH 3665).

Fig. 4.26 – 4.29 show the effect of exposure time on flexural strength and flexural modulus of the glass and Kevlar® fibers reinforced epoxy as a function of exposure time at elevated temperatures. For Kevlar® fiber reinforced epoxy (Fig. 4.26), there was no change in the flexural strength as the exposure time increased at 100°C up to the maximum exposure time of 2 h, whereas the flexural strength of the composite started to show noticeable decrease after 1.5 h. exposure at 200 and 250°C. For Kevlar® fiber reinforced epoxy composite exposed at 250°C the flexural strength began to drop rapidly after 1 h exposure time. Fig. 4.27 shows the effect of exposure time on the flexural strength of s-glass fiber reinforced epoxy exposed to convective thermal flux at 100, 200, 250 and 300°C. Unlike in the case of Kevlar® fiber reinforced composite in which drop in flexural strength was observed after 1½ h exposure time at 200 and 250°C in the furnace, the glass fiber reinforce composite did not show any considerable drop in flexural drop in strength as exposure time was increase to 250°C. However, for samples exposed to 300°C, the strength of glass fiber reinforced began to significantly drop at exposure time of 30 minutes against the 1hr. observed for Kevlar® fiber reinforced epoxy. The change in flexural modulus for glass and Kevlar® fiber reinforced epoxy with exposure time at elevated temperature during prior heat treatment (Fig. 4.28

and 4.29) follow a similar trend as observed in the variation of flexural strength with time. It was however observed that flexural modulus the composite reinforced with glass began to drop at an earlier exposure time for all the temperatures compared to the Kevlar® reinforced composite. This suggests that the flexural modulus of the glass fiber reinforced epoxy is more sensitive to thermal exposure than the flexural strength. This may be due to the different effects of thermal exposure on flexural strength and modulus of the reinforcing fiber, i.e. the flexural modulus of the glass fiber reinforced epoxy showed the tendency to degrade more readily at elevated temperature than its flexural strength. It can also been deduced from Fig. 4.26 and 4.29 that as the exposure time increases the rate of matrix decomposition and fiber matrix degradation increases, as expected of most chemical reactions.

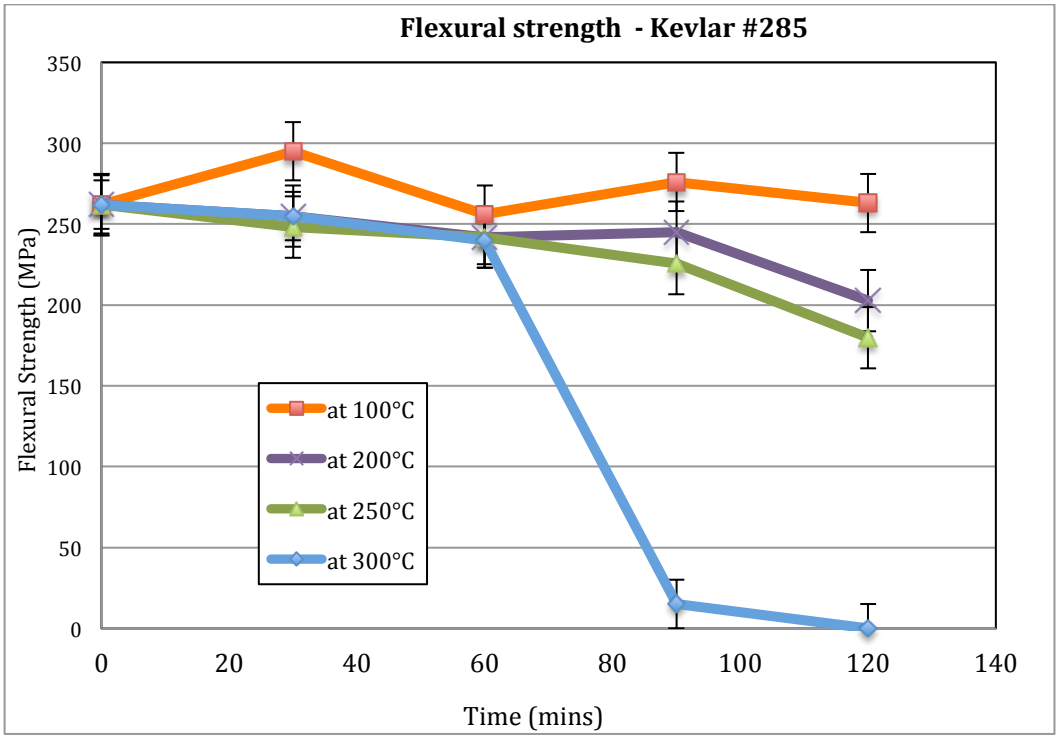

Fig. 4.26. The effects of exposure time on the flexural strength of Kevlar® fiber reinforced epoxy (Resin hardener is PH 3665) at different temperatures.

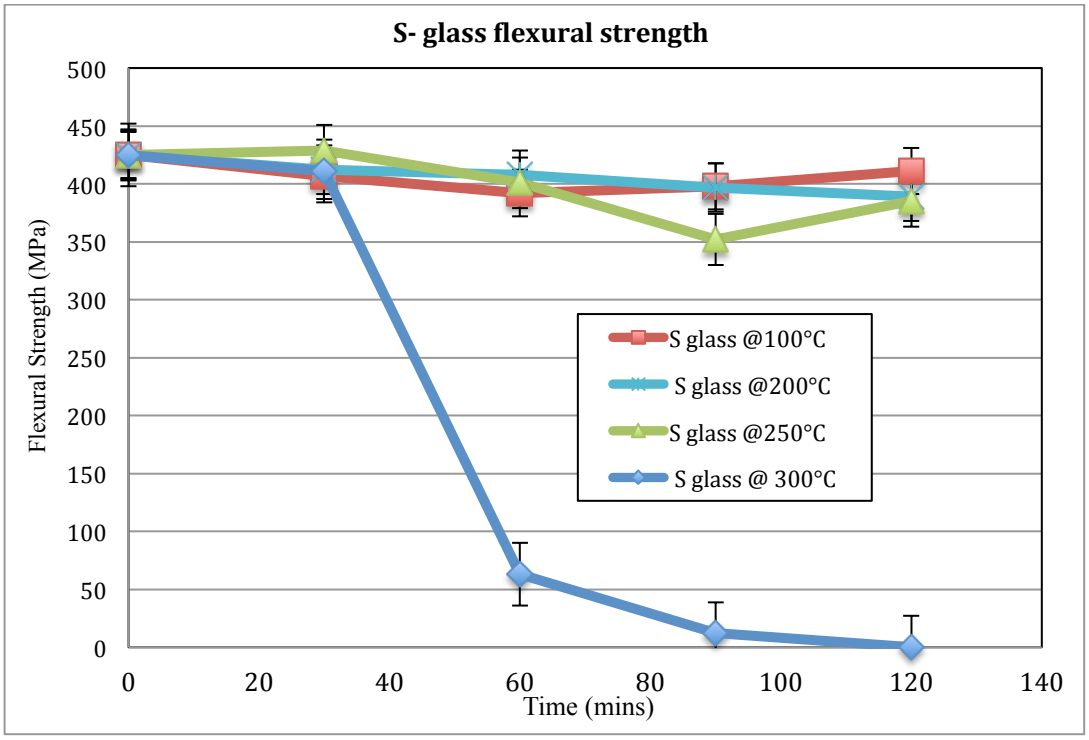

Fig. 4.27. The effects of exposure time on the flexural strength of fiber reinforced epoxy (Resin hardener is PH 3665) at different temperatures.

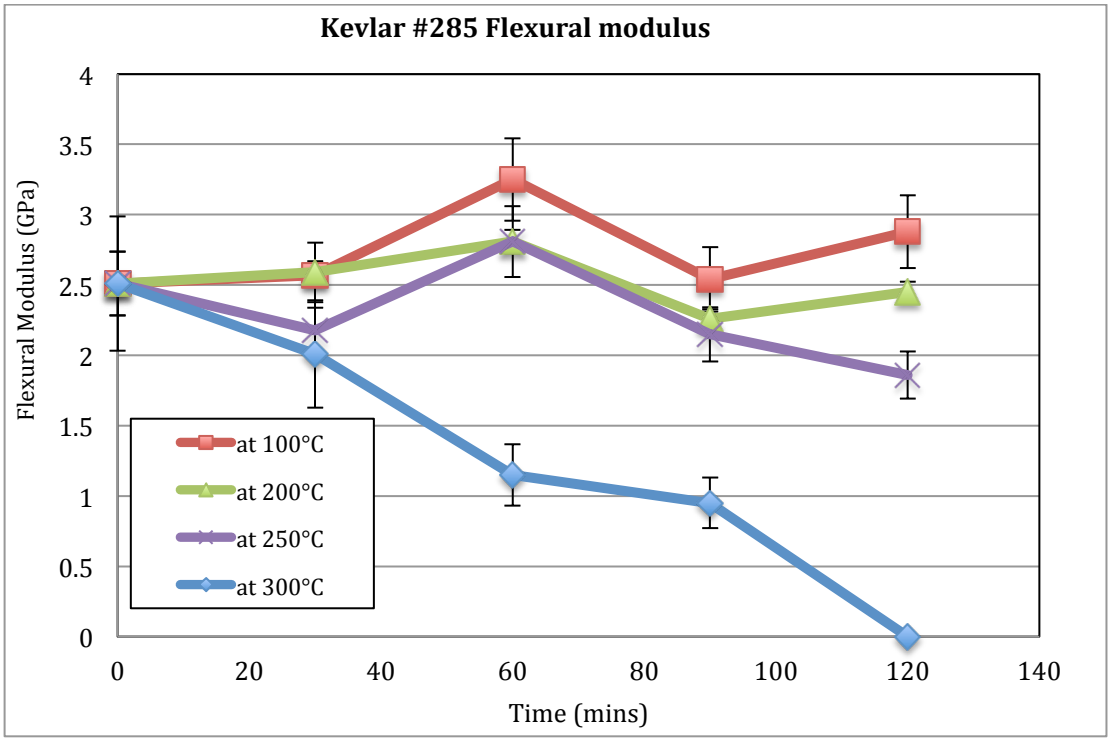

Fig. 4.28. The effects of exposure time on the flexural modulus of fiber reinforced epoxy (Resin hardener is PH 3665) at different temperatures.

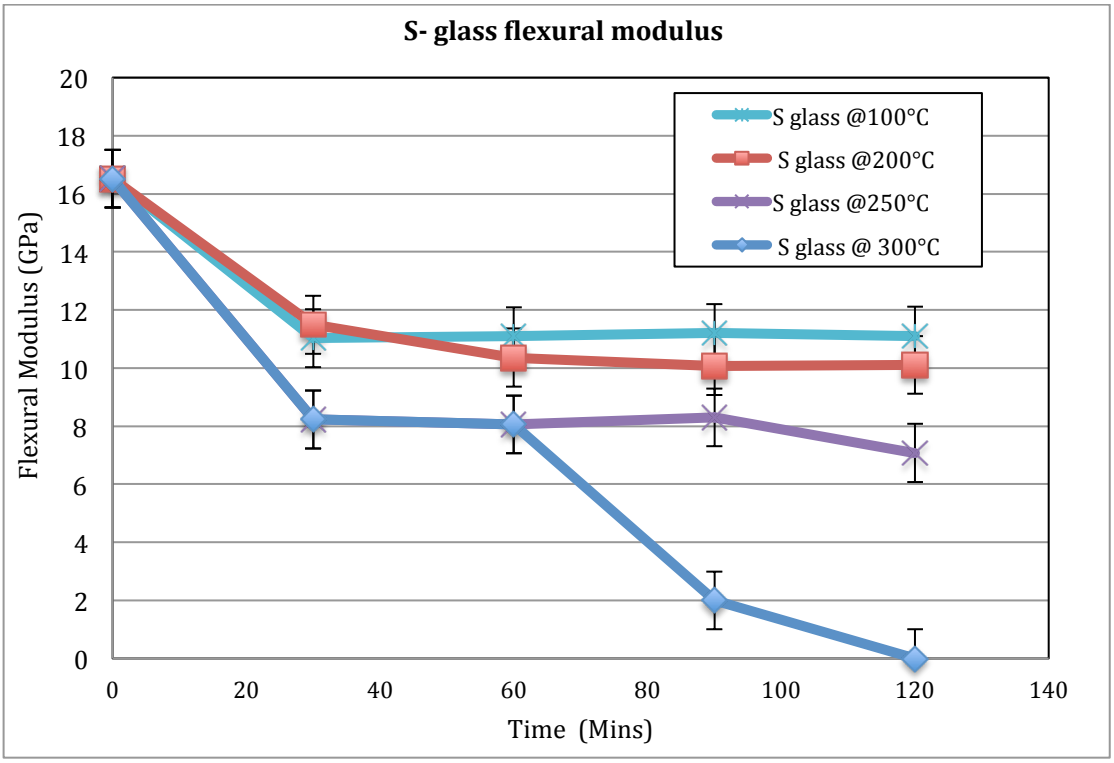

Fig. 4.29. The effects of exposure time on the flexural modulus of S-glass fiber reinforced epoxy (Resin hardener is PH 3665)

The mechanical properties of composites produced with the two different resin hardeners used in this study are compared in Tables 4.1, 4.2, 4.3 and 4.4. The values provided in these tables are averages for five samples with their respective standard deviations. The result presented in Table 4.1 represents composite mechanical behavior under convective thermal exposure. This shows no significant difference in the properties of composite made with these two hardeners irrespective of the type of fibers used in reinforcing the epoxy resin. The slight differences observed in the average values of the strength and modulus for the composites cured with different hardeners can be attributed to inhomogeneous nature of composite materials. Moreover this slight variation is within the limit of experimental error. This suggests that the major difference in this hardener is their effect on rate of polymerization reaction with no significant effect on mechanical properties. Once polymerization is completed, the properties of the composites obtained using these hardeners are the same.

The results presented in Fig. 4.30 show the effects of increase in exposure temperature on flexural strength and modulus of both glass and Kevlar® fiber reinforced epoxy. Whereas for all composites and for most exposure time, flexural strengths are retained as exposure time was increased up to 250°C, while the values of flexural

modulus dropped. This result also agrees with previous result obtained on the effects thermal exposure on the mechanical behavior of a similar FRP [17].

Table 4.1. Effect of the applied resin hardener on the flexural strength (FS) and flexural modulus (FM) of Kevlar® and glass fibers reinforced epoxy

Fiber in composite	Hardener	Temp. ºC	Exposure time (min)	Flexural Strength (MPa)	Flexural Modulus (GPa)
Kevlar® #285	PH3665	No Exposure		288±10	2.28±1.5
Kevlar® #285	PH3660	No Exposure		275±11	2.15±1.5
Kevlar® #285	PH3665	200	120	321±10	2.75±1.2
Kevlar® #285	PH3660	200	120	315±11	2.68±1.2
S-Glass	PH3665	No Exposure		425±12	16.52±2.3
S-Glass	PH3660	No Exposure		415±12	15.20±2.5
S-Glass	PH3665	200	120	410±12	11.11±2.7
S-Glass	PH3660	200	120	394±12	13.19±2.1

The flexural strength and flexural modulus of the fiber reinforced epoxy made from Kevlar® and glass fibers are compared in Figs. 4.31 and 4.32. As can be observed from these figures, the composite made from glass fibers have higher flexural strength and modulus than the composite made from Kevlar® fibers. From the specification provided by the supplier of these fibers (Table 2.1) and from the literature [15], the Kevlar® 49 fibers used in this study have higher breakage strength and breakage modulus than the applied S and E glass fibers. Despite the lower strength of the glass fibers compared to Kevlar® fibers, the epoxy matrix composites made from these fibers are much stronger than those made from Kevlar® fibers. From Table 3.3 there is no significant difference between the volume fractions of the fibers for epoxy composite reinforced with S glass and with Kevlar® #285 (71 % and 69 %) respectively. Also, the difference between the fiber volume fraction in the epoxy reinforced with E glass fibers and with Kevlar® #281 is marginal (66 % and 65 %). The composite made with Kevlar® fibers #120 is the least of all. This result suggests higher fiber strength utilization in the glass fibers reinforced epoxy than in Kevlar® fibers reinforced epoxy. One of the very important factors controlling the strength of fiber reinforced plastic is the strength of the fiber matrix interface [67]. The higher strength of glass fiber reinforced epoxy is attributable to a stronger bonding between the glass fibers and the epoxy matrix. It can thus be concluded that the strength of fiber matrix interface has more impact on composite strength than the strength of the reinforcing fibers. The lower

damage tolerance of the composites made of glass fibers under both flexural and bending loading is due to the brittle nature of the glass fibers compared to the rather the tough Kevlar® fibers. Moreover Kevlar® fibers are known for excellent impact resistance [8] and composites made with them generally have good toughness [6].

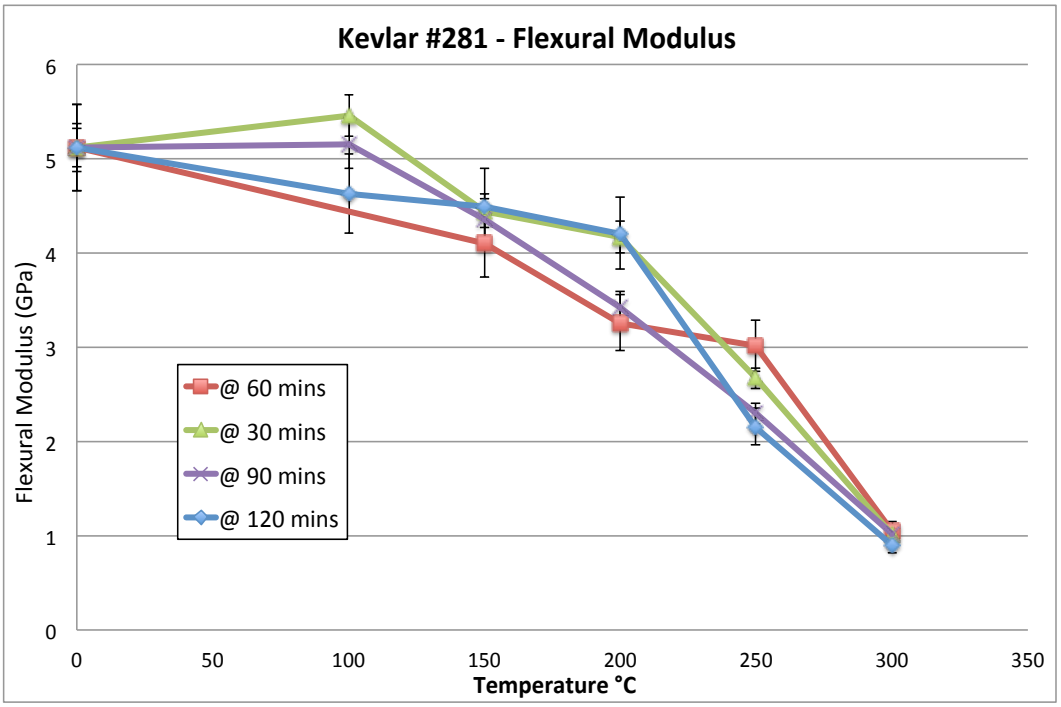

A.

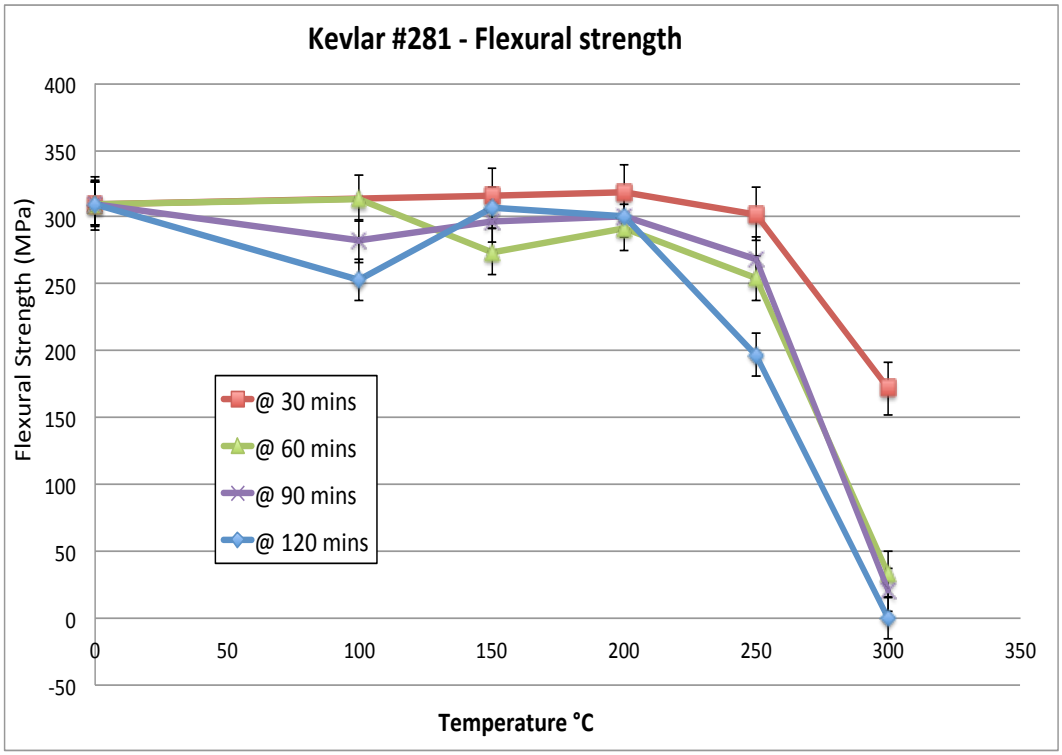

B.

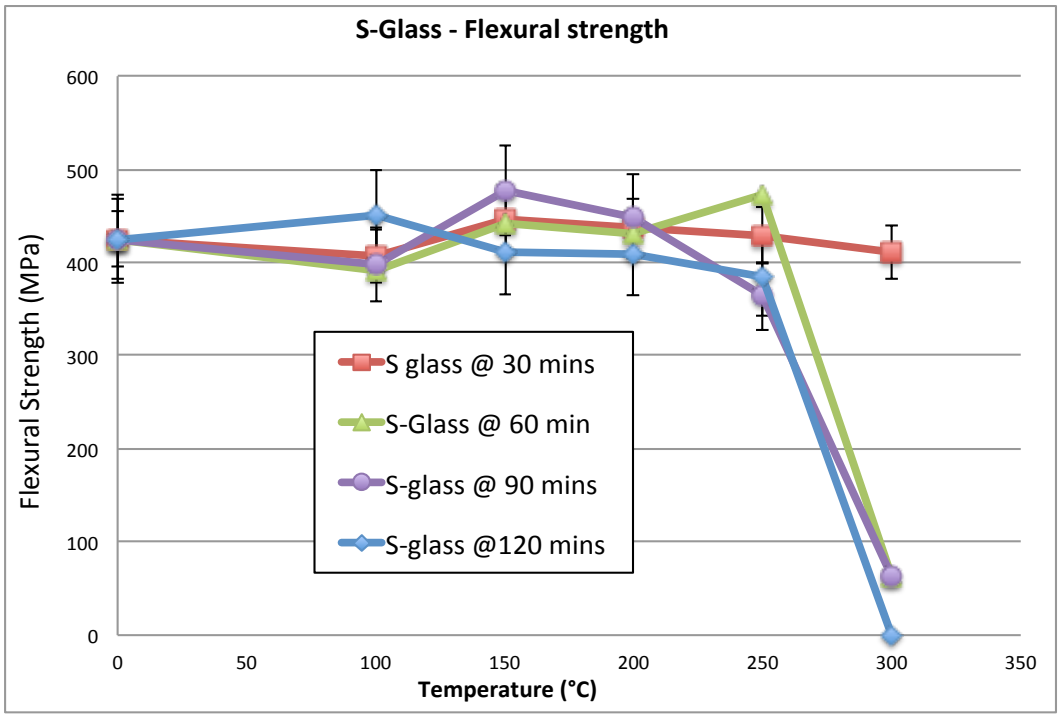
S-Glass - Flexural strength
Flexural Strength (MPa)
600
500
400
300
200
100
0
0
50
100
150
200
250
300
350
Temperature (°C)
S glass @ 30 mins
S-Glass @ 60 min
S-glass @ 90 mins
S-glass @120 mins

C.

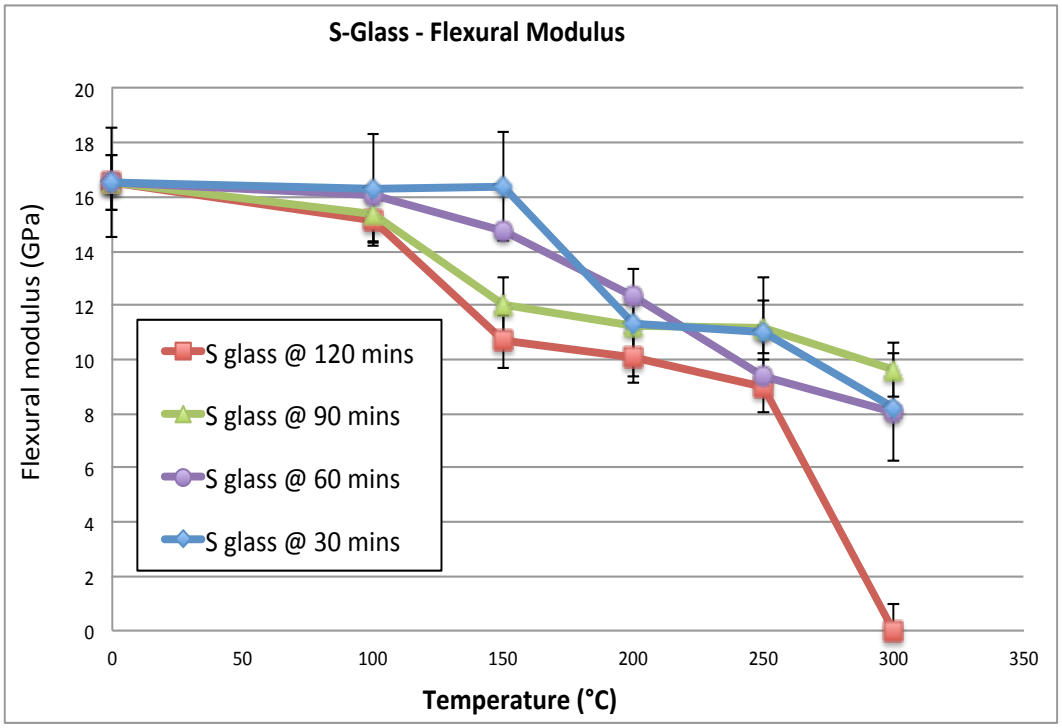
S-Glass - Flexural Modulus
Flexural modulus (GPa)
20
18
16
14
12
10
8
6
4
2
0
0
50
100
150
200
250
300
350
Temperature (°C)
S glass @ 120 mins
S glass @ 90 mins
S glass @ 60 mins
S glass @ 30 mins

D.

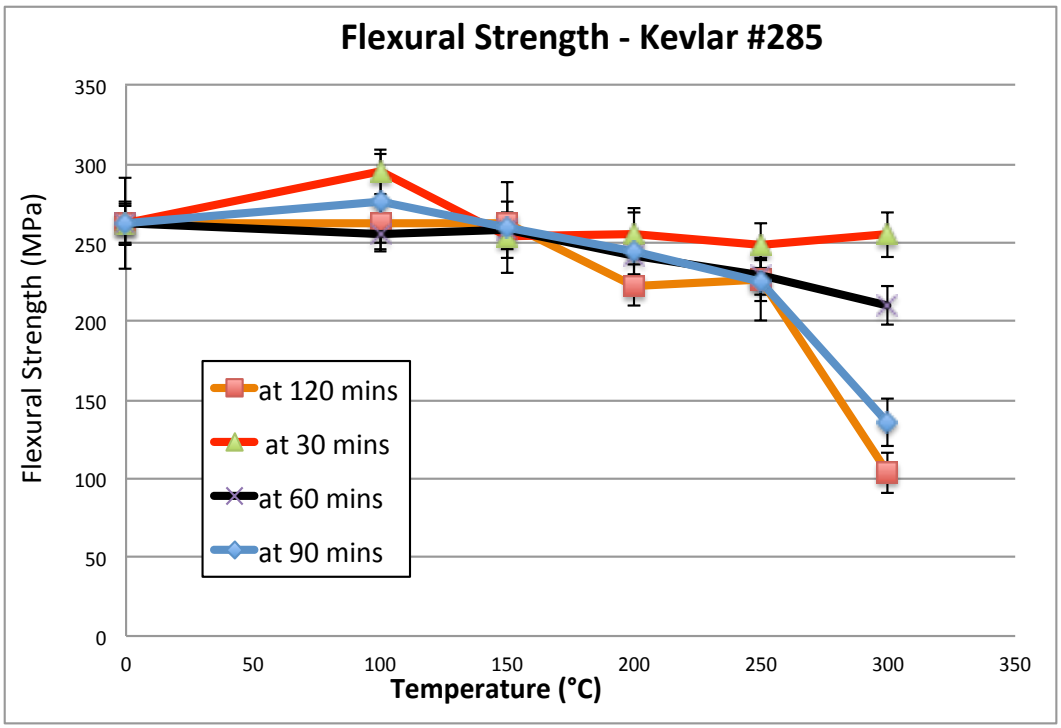

E.

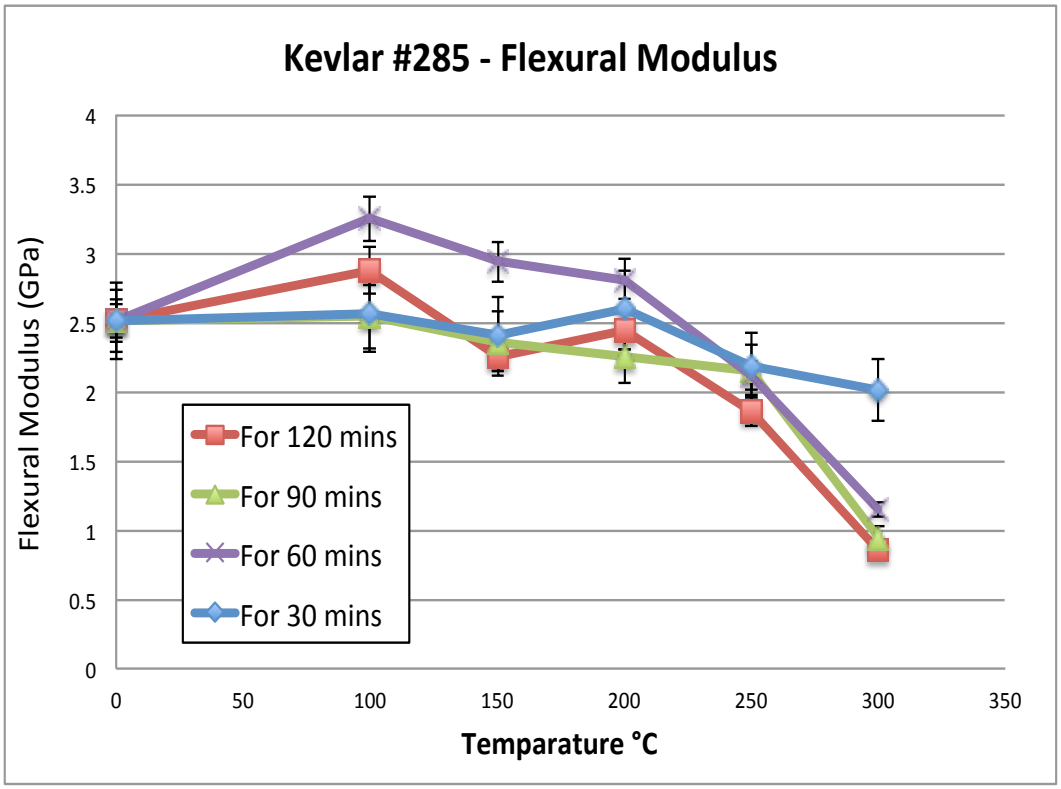

F

Fig 4.30 (A-F) Effect of exposure temperature on the flexural strength and flexural modulus of glass and Kevlar® fibers reinforced epoxy matrix composite.

The flexural strength of the composites made with S glass fibers are about 20 % higher than that of those made with E glass fibers while the flexural modulus of composite made from S glass are about 14 % higher than that of those made with E glass fibers. From the data provided by the supplier of these fibers, the S glass fibers are 30 % stronger and 15 % stiffer than the E glass fibers (Table 3.1). The bundle size of the E glass fibers is about half of that of the S glass fibers while the weave pattern of the E glass fibers and S glass fibers are crowfoot and plain weave, respectively. The fiber volume fraction of the composites produced from the S-glass and E glass fibers are 66.5±7.5 and 60.5±8.5 vol. % respectively. The difference in volume fraction of the composites made from the two fibers is much smaller compared with the difference in the strength and modulus of their resulting composites. Thus, the higher strength of the S glass reinforced epoxy matrix composites compared to that of composite made of E glass fibers can be traced to the higher strength of the S glass fibers.

Kevlar® 49 fibers were used in this study. The difference in the three applied Kevlar® fibers is in their fabric style; bundle size and the weave type as shown in Table 3.1. Kevlar® # 285 and #281 have the same bundle size and the same breaking strength but differ in their weaving pattern; crow weave for Kevlar® # 285 and plain weave for Kevlar® #281. Kevlar® #120 on the other hand has a bundle size than is about 35% that of the other two Kevlar® fibers and its breaking strength is about 40% that of Kevlar® #281 and Kevlar® #285 from the specification data provided by the manufacturer. The fiber volume fraction of the Kevlar® fiber reinforced epoxy matrix composites produced using Kevlar® # 285, #281 and #120 are 61.5 ±3.5, 57.5±4.5 and 55.0±4.0 vol. %, respectively. Despite the difference in the weave pattern and bundle size of the Kevlar® fibers, the differences observed in their flexural strength are negligible and within the limit of experimental error. Although the flexural strength of composites made from S glass fibers are about 40 % higher than those made from Kevlar® fibers, the difference in their flexural modulus is much higher (Fig. 4.32). For example, the flexural modulus of the S-glass fiber reinforced epoxy is about 3 times higher than that of Kevlar® # 281. Glass fiber reinforced epoxy are much more rigid than Kevlar® fiber reinforced epoxy.

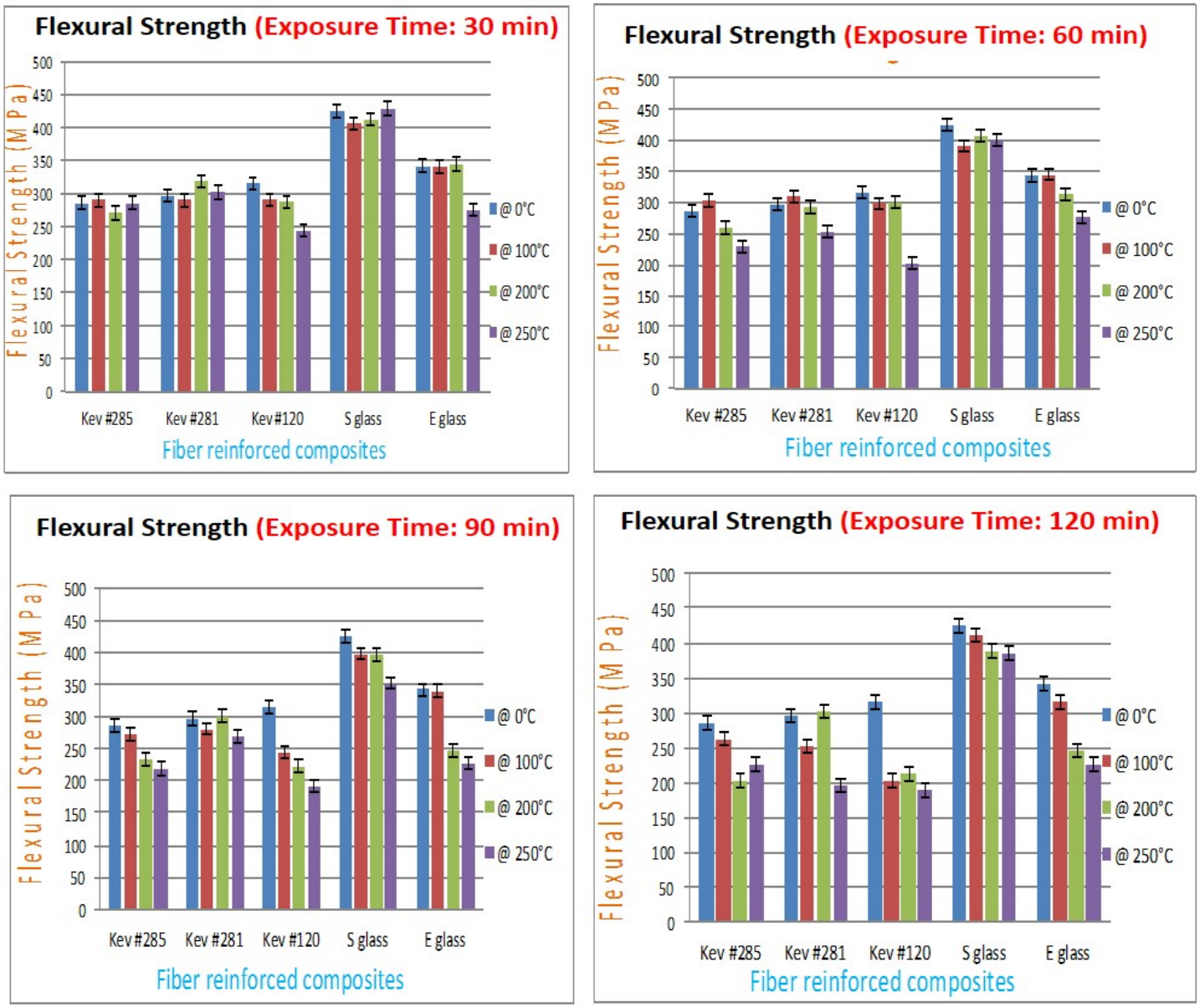

Fig 4.31. Flexural strength of fiber reinforced epoxy composites as a function of the type of reinforcing fiber, post cured thermal exposure temperature and time.

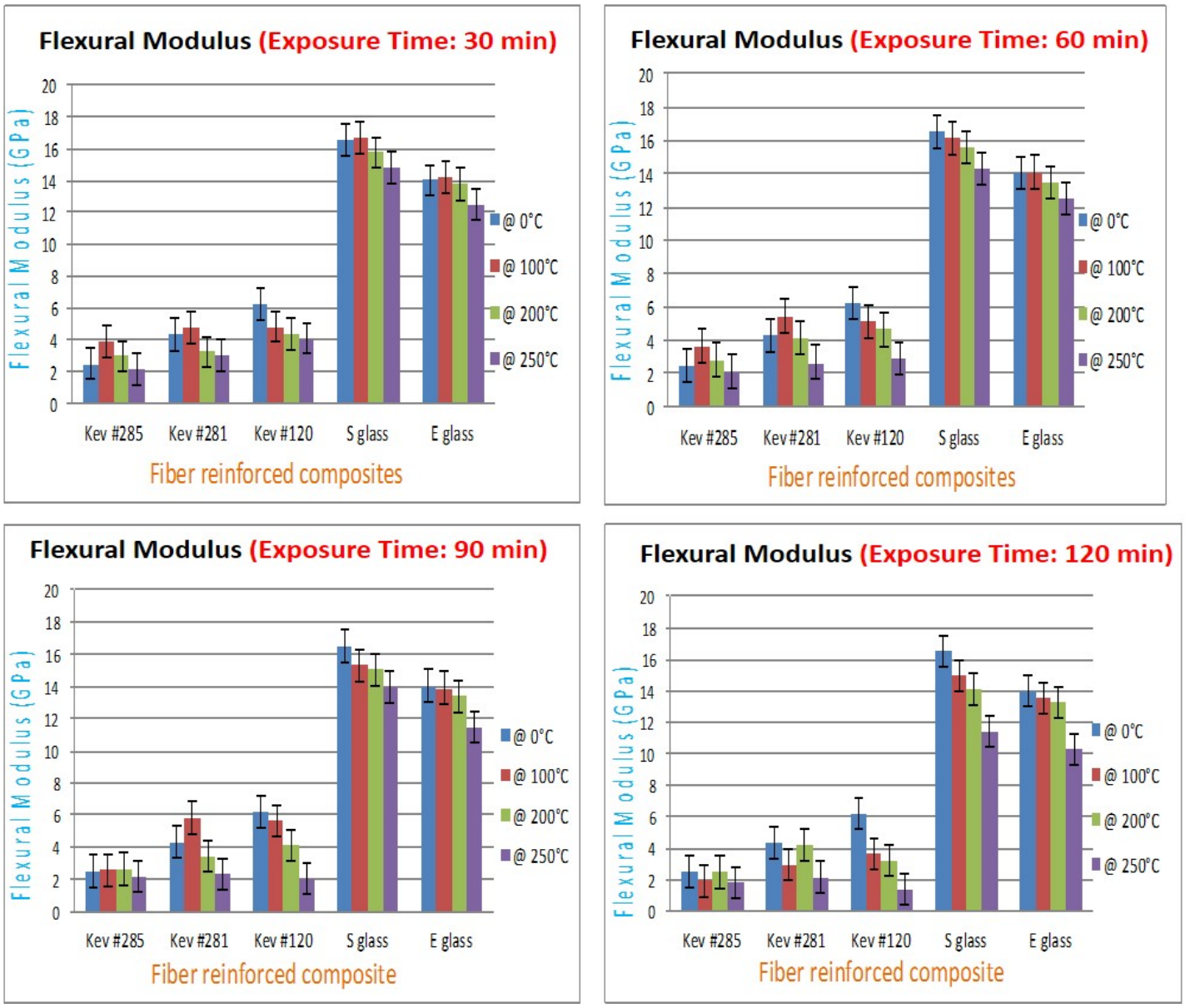

Fig 4.32. Flexural modulus of fiber reinforced epoxy composites as a function of the type of reinforcing fiber post cured thermal exposure temperature and time

4.5.2 The effects of radiative thermal exposure in cone calorimeter on the flexural strength and modulus

The result of flexural test showing the effects of radiative heat fluxes, in cone calorimeter on the flexural strength and flexural modulus of the Kevlar® and glass reinforced epoxy are presented in tables 4.5 - 4.7. The radiative thermal exposure simulates operational service condition in the cowling chamber; the cowling material is consistently exposed to thermal radiation from the engine whenever the aircraft is in operation. Cessna aircraft field operation was studied during the course of this research work and the heat transfer analysis was done. The

heat transfer values recorded are similar to the simulated values in the laboratory when samples were exposed to radiative thermal conditions.

Table 4.2 shows that Only slight variation occurred in the flexural strength and modulus of Kevlar® fiber reinforced epoxy an exposure time of up to 3 h (maximum flight duration for a typical light engine recreational aircraft) to radiative heat fluxes of 3.7, 5.0 and 7.0 kW/m^2. This suggests the suitability of the composite material for the proposed field application that requires a heat flux of only 4.7 kW/ m^2. Only slight difference was observed in the flexural strength and modulus of the composite fabricated from each of the two selected resin hardeners, which is within the limit of experimental error. Tables 4.3 and 4.4 show how the choice of the applied fiber and exposure to radiative heat flux affects the flexural strength and flexural modulus of the composite. The difference in the flexural strength for the composites made from Kevlar® #285 and #281 fibers after exposure to 5 kW/m^2 for 3 h and 7 kW/m^2 for 2 h are less than 2 % for these two conditions of radiative heat flux exposure. The difference is much higher for E and S glass fibers reinforced epoxy, which was found to be about 6 % and 10 % respectively. The results of these investigations suggest that radiative heat exposure may have a more damaging effect on glass fiber reinforced epoxy than exposure to convective heat flux. On the contrary, the convective heat flux appeared to have more damaging effect on Kevlar fiber reinforced epoxy than radiative heat flux. The reason for this is not very clear and may have been due to different responses of the fibers to various types of heat fluxes. This should be a subject of further investigations in the future.

Table 4.2. Effects of the applied resin hardener and radiative heat flux exposure on the flexural strength and flexural modulus of Kevlar® #285 fiber reinforced epoxy.

Composite	Hardener	Heat Flux kW/m^2	Exposure time (min.)	Flexural Strength (MPa)	Standard Dev. (FS)	Flexural Modulus (GPa)	Standard Dev. (FM)
Kevlar® #285	PH3665	0	0	288	10	12.28	1.5
Kevlar® #285	PH3660	0	0	275	11.05	11.15	1.5
Kevlar® #285	PH3665	3.7	60	284	43.04	14.76	1.59
Kevlar® #285	PH3660	3.7	60	280	41.94	14.31	1.63
Kevlar® #285	PH3665	5.0	360	246	24.83	12.31	1.87
Kevlar® #285	PH3660	5.0	360	284	12.62	14.25	2.10
Kevlar® #285	PH3665	7.0	120	234	54.80	14.40	3.38
Kevlar® #285	PH3660	7.0	120	281	3.04	15.30	2.89

Table 4.3. Flexural strength and flexural modulus fiber reinforced epoxy after exposure to 7 kW/m^2 heat flux for 2 h.

Composite	Hardener	Heat Flux Kw/m^2	Exposure time (min.)	Flexural Strength (average)	Standard Dev. (FS)	Flexural Modulus (average)	Standard Dev. (FM)
Kevlar® #285	PH3660	7.0	120	281	3.04	15.30	2.89
Kevlar® #281	PH3660	7.0	120	294	7.61	16.80	2.11
E glass	PH3660	7.0	120	382	22.32	14.72	0.23
S Glass	PH3660	7.0	120	466	32.82	16.09	1.62

Table 4.4. Flexural strength and flexural modulus of fiber reinforced epoxy after exposure to 5 kW/m^2 heat flux for 3 h

Composite	Hardener	Heat Flux Kw/m^2	Exposure time (min.)	Flexural Strength (average)	Standard Dev. (FS)	Flexural Modulus (average)	Standard Dev. (FM)
Kevlar® #285	PH3660	5.0	360	284	12.62	14.25	2.10
Kevlar® #281	PH3660	5.0	360	293	7.32	17.52	0.87
E glass	PH3660	5.0	360	345	22.84	14.92	0.82
S Glass	PH3660	5.0	360	499	17.23	18.93	0.31

4.5.3 Dynamic Impact test

The dynamic impact test was carried out on composite specimens in their original as-cured states (i.e. no thermal exposure) and also on specimens samples thermally exposed to convective heat flux in the furnace at temperatures ranging between 100°C and 300°C for up to 2 hr. Typical stress strain curves obtained from Kevlar® and glass fibers reinforced epoxy matrix composites are shown in Fig. 4.33 to 4.36. A linear relation can be observed between stress and strain up to the yield point of between 25 and 50 MPa. The value of the yield point is dependent on the strain rate and the degree of thermal exposure before impact test. Beyond the yield point, the relationship becomes nonlinear. Eventually a peak stress is reached, beyond which the stress begin to drop with further increase in strain. This will correspond to point of unloading or loss loading carrying capability due to matrix cracking, delamination or fiber rupture.

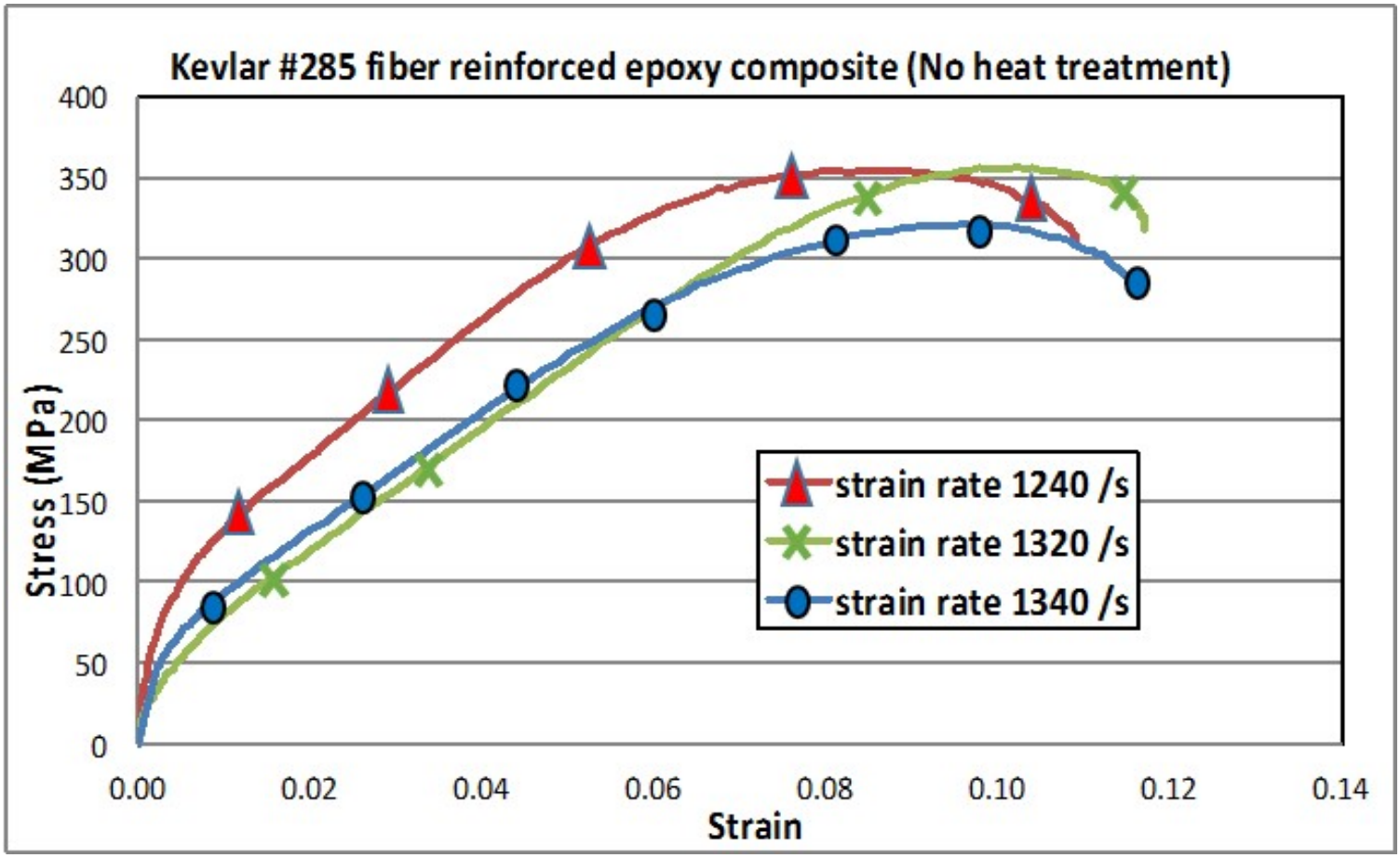

Fig. 4.33 Dynamic stress strain curves for Kevlar® fiber reinforced epoxy showing the effects of strain rates.

The impact tests results generally indicate that the dynamic stress strain response of the composites is very sensitive to strain-rate and the degree of thermal exposure. As the strain rates increased the peak flow stress attained by the impacted composite specimens increased and then dropped as the strain rates become very intense to cause early matrix fracture or fiber rupture. Figure 4.33 showed a typical effect of strain rates on the impact stress-strain curves of as-cured Kevlar® fiber reinforced epoxy (no thermal exposure). Generally for glass fibers reinforced epoxy exposed to a given thermal condition, no significant reduction in impact strength was noticed until exposure temperature exceeded 200ºC (Fig. 4.34). Samples exposed at 300ºC do not possess any capacity to absorb impact load as delamination readily occurred at this temperature. The Kevlar® fiber reinforced epoxy, on the other hand, showed a marked decrease in peak stress for exposure temperature as low as 100 °C (Fig. 4.35).

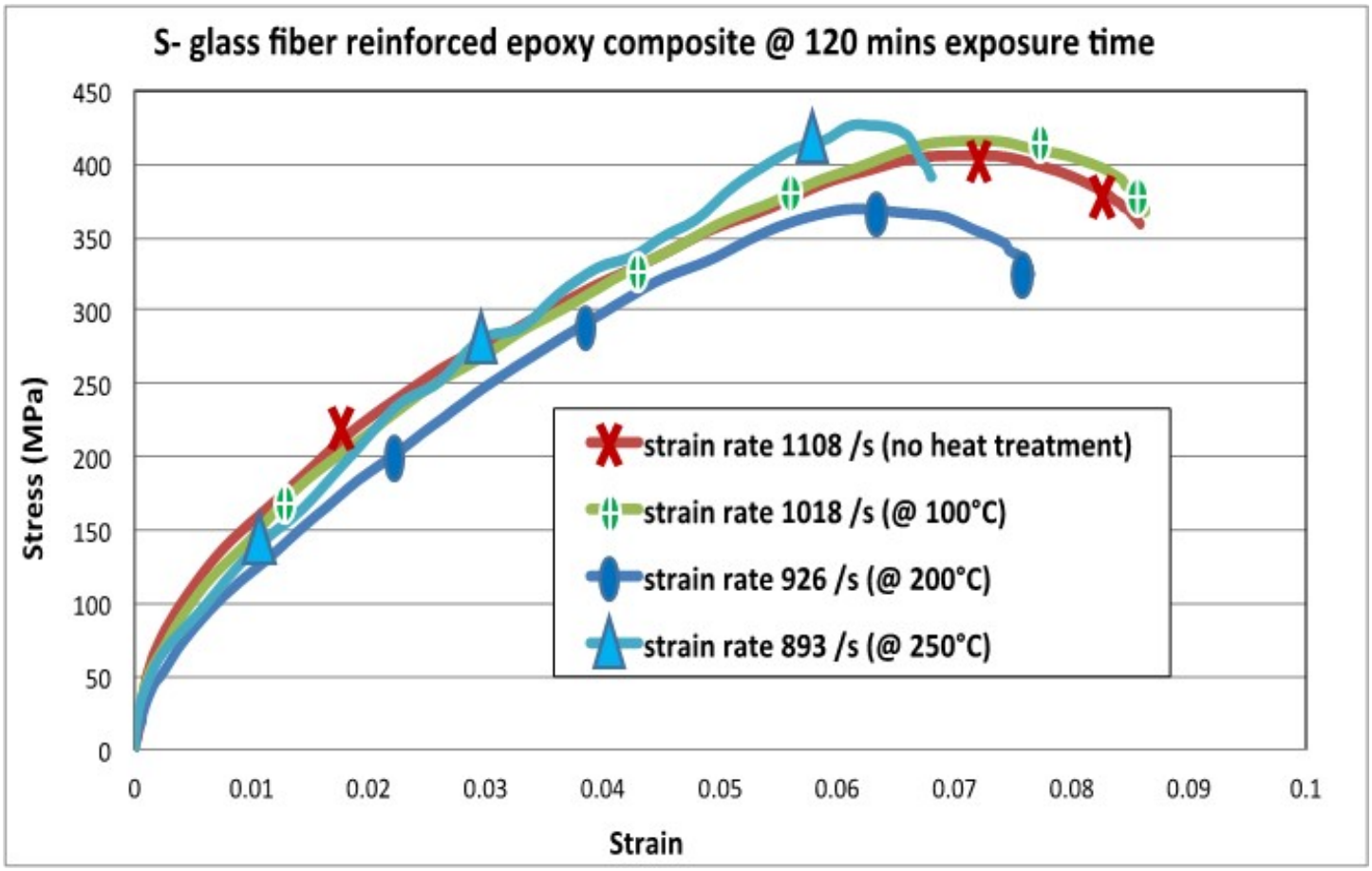

Fig. 4.34 Effect of exposure temperature on the dynamic stress-strain curves of S glass fiber reinforced epoxy. These specimens were subjected to the same impact load

The specimens shown in Fig. 4.34 and 4.35 were subjected to the same impact load as the projectile was fired at a pressure of 140 kPa for each test. It was observed that as the firing pressure was increased from 140 kPa to 160 kPa the test sample failed more rapidly under the impact loading, especially samples exposed to elevated temperature beyond 150ºC. This was more common for glass fiber reinforced composite test samples, which may be due to increase in the brittleness of both the reinforcing glass fibers at elevated temperatures. Fig 4.36 shows comparative stress-strain curves for both Kevlar® and glass fiber reinforced epoxy composite after thermal exposure.

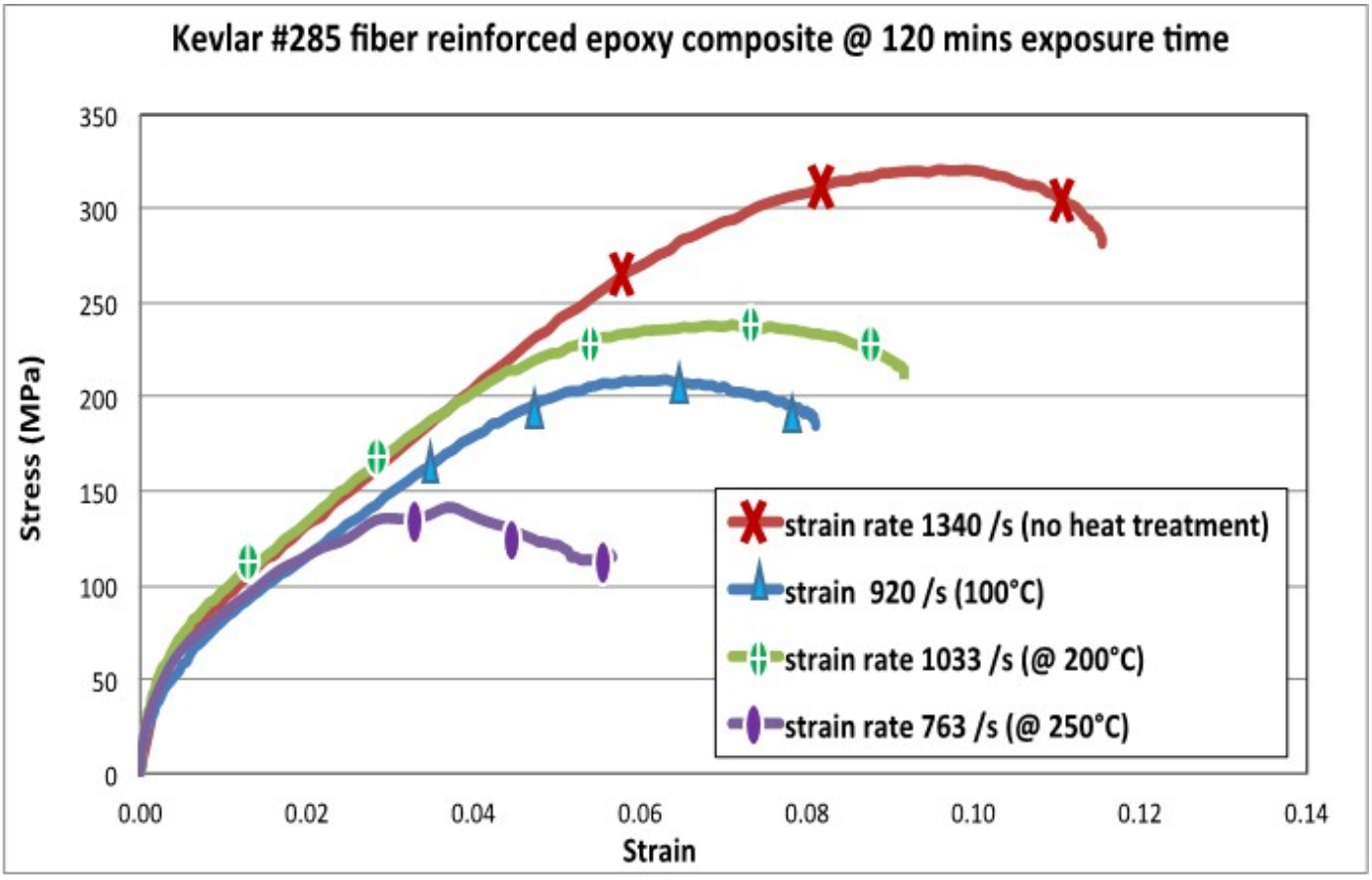

Fig. 4.35 Effect of exposure temperature on the dynamic stress-strain curves of Kevlar® fiber reinforced epoxy. These specimens were subjected to the same impact load.

As observed in the composites specimen impacted in the as-cured state, with no thermal exposure, peak stress attained in the glass fiber reinforced epoxy before failure was higher than that for the Kevlar® fiber reinforced epoxy. Epoxy reinforced with Kevlar® and glass fibers at 250ºC for 1 h attained higher peak stress before rupture compared to samples exposed at 100ºC for 2 hr. Prolonged exposure thus appears to have more damaging effect on the impact resistance of the composite than the damage resistance under flexural loading. The glass fiber reinforced epoxy showed a higher tendency for catastrophic failure under impact loading than the epoxy reinforced with Kevlar® fibers. This makes epoxy reinforced with Kevlar® a better choice than glass fiber reinforced epoxy in application where exposure to impact loading is inevitable. The average impact load the composite can withstand before failure decreased with increasing exposure temperature.

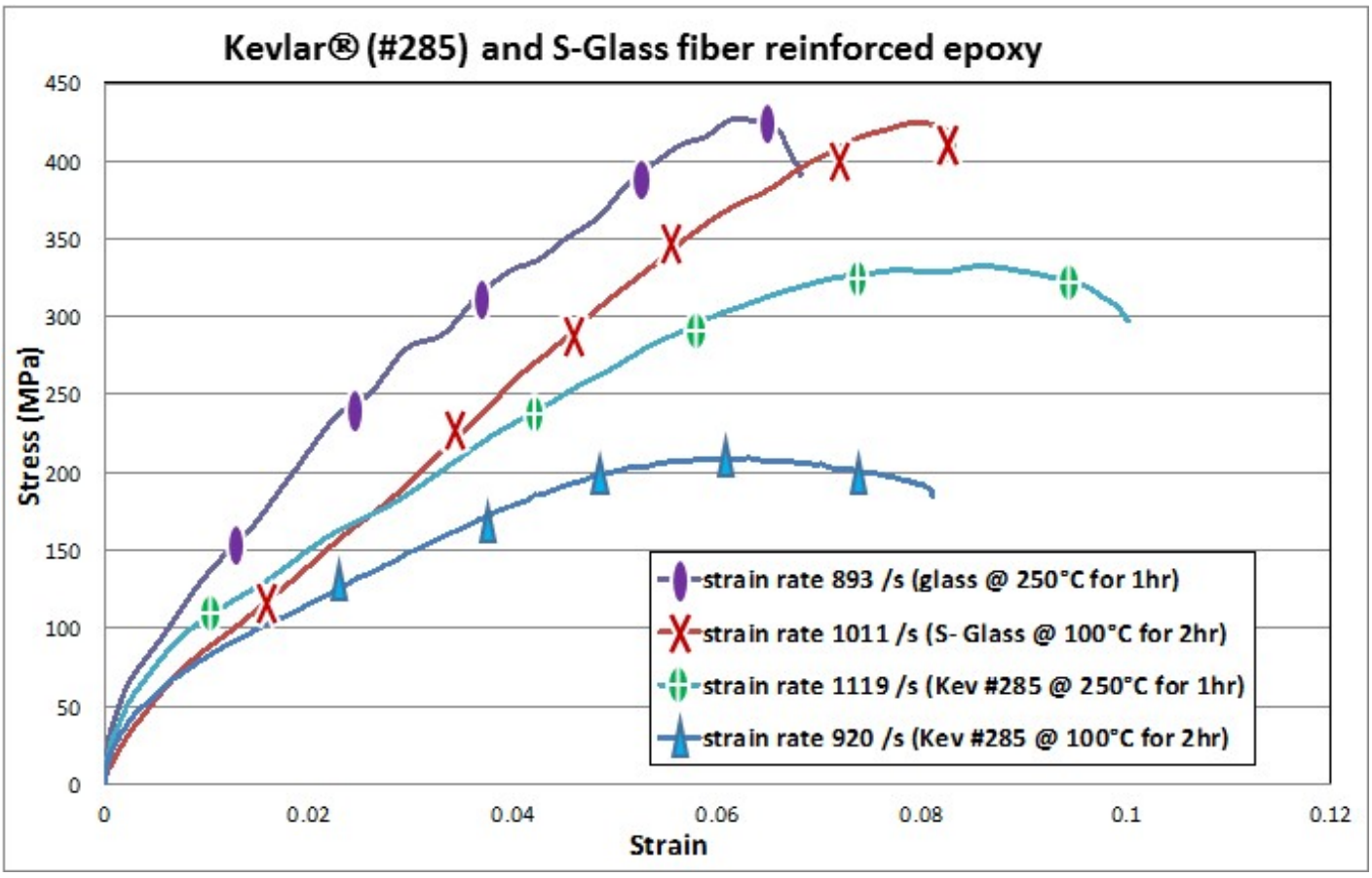

Fig 4.36. Stress-strain curves comparing the behavior of Kevlar® fiber (#285) and S-glass fiber reinforced epoxy under impact loading.

4.5.3.1 Composite fracture under impact loading

Typical photographs showing fractured surfaces of Kevlar® and glass fibers reinforced epoxy composites specimens after failure under impact loading are presented in Fig. 4.37 and 4.38 respectively. Whereas the Kevlar® fiber reinforced epoxy failed by delamination between two adjacent fiber bundles, the glass fiber reinforced epoxy sheared along an uneven surfaces along the diagonal axis of the cuboidal test specimen as schematically presented in Fig. 4.39. The slant deformation geometry mode observed in the glass composite under impact loading is similar to previous result obtained by Liren et al [28] who attributed this deformation mode to complex architectural design of the material itself, which has to do with the impedance and geometric mismatch at various length scales of the composite.

The results of the scanning electron microscopic investigation of the delaminated surface of the Kevlar® fiber reinforced epoxy (Fig. 4.40) showed no evidence of fiber rupture during failure under impact loading. Instead of

fiber rupture fiber splitting along the axis of some filaments were observed. Damage control mechanisms such as fiber pullout or crack bridging were not observed to occur during failure of the Kevlar® fiber reinforced epoxy under dynamic impact loading. It was observed the fracture tendency and the number of delaminated laminates increased as the post cured thermal exposure temperature was increased from 100 to 250°C. There was no need to conduct impact test on specimens exposed to 300°C because of the excessive delamination already observed in these samples after thermal exposure. As the temperature increased, the amount of degradation that occurs at the fiber matrix interface increased resulting in lower resistance to delamination under impact loading.

Fig 4.37. Photograph of delaminated Kevlar® fiber reinforced epoxy after impact loading.

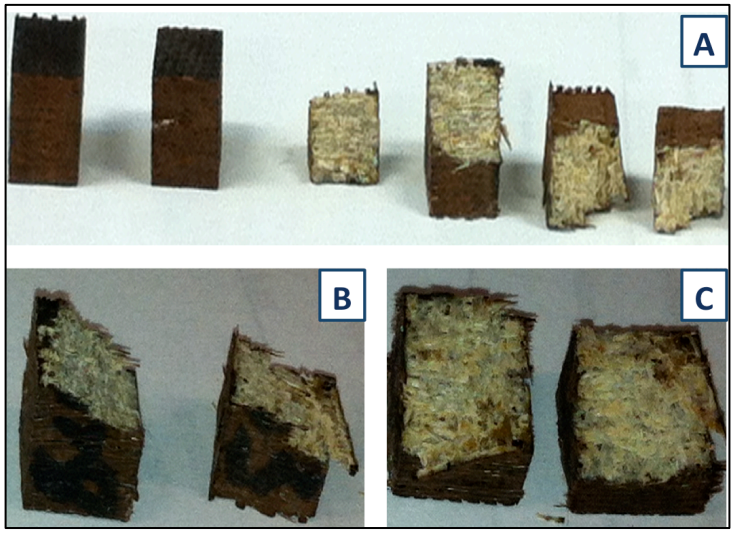

Fig 4.38. Photograph of glass reinforced epoxy after rupture under impact loading

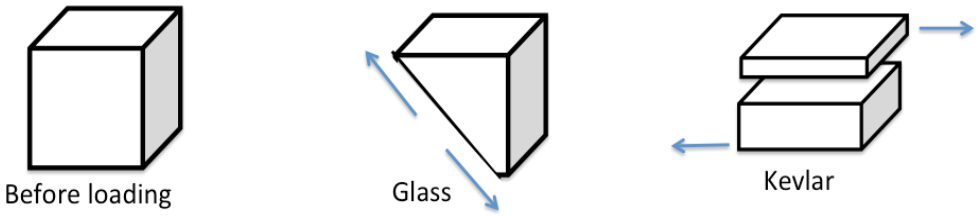

Fig. 4.39. Schematic representation of the fracture pattern of fiber reinforced epoxy composite under impact loading.

As can be observed in Figs. 4.38 and 4.41, extensive fiber rupture occurs in the glass fiber reinforced epoxy matrix composite leading to fragmentation along the specimens' diagonal with no evidence of delamination. Unlike the Kevlar® fiber reinforced composites, which failed mostly by delamination (Fig.4.40), glass fiber reinforced epoxy failed predominantly by fiber rupture.

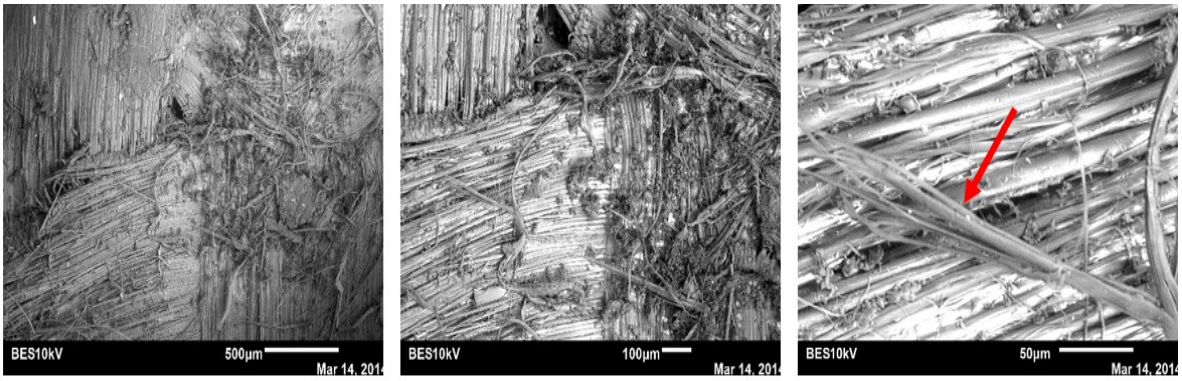

Composite exposed to 100 °C for 1 h before impact loading

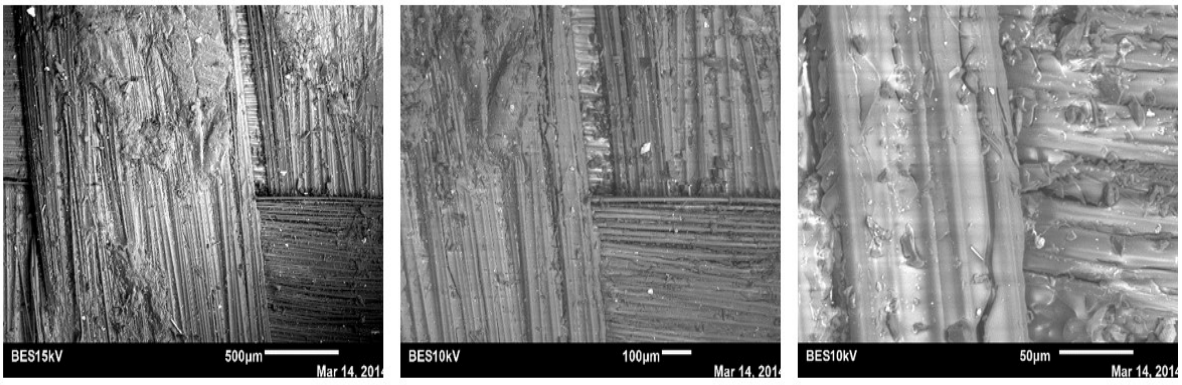

Composite exposed to 250 °C for 1 h before impact loading

Fig. 4.40. Delaminated surface of Kevlar® fiber reinforced epoxy after failure under impact loading. Arrow indicates a split filament.

The results of scanning electron microscopic investigation of the fracture surface of glass fiber reinforced epoxy showed extensive fiber pullout and fiber-matrix debonding, and very little delamination compared with the Kevlar® reinforced epoxy (Fig. 4.41). The brittle nature of the glass fibers impairs the resistance of the glass fiber reinforced to fracture under impact loading. Thus the Kevlar® fibers shows a higher capability to withstand fragmentation under impact loading. Extensive brittle fracture of glass fibers into small fragments were observed to occur in the composites during impact loading as shown in Fig. 4.42.

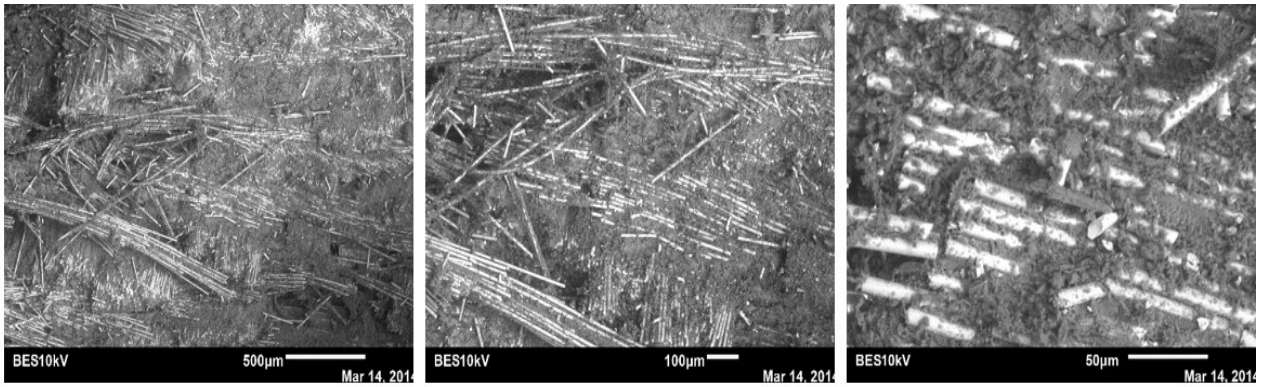

Composite exposed to 100 °C for 1 h before impact loading

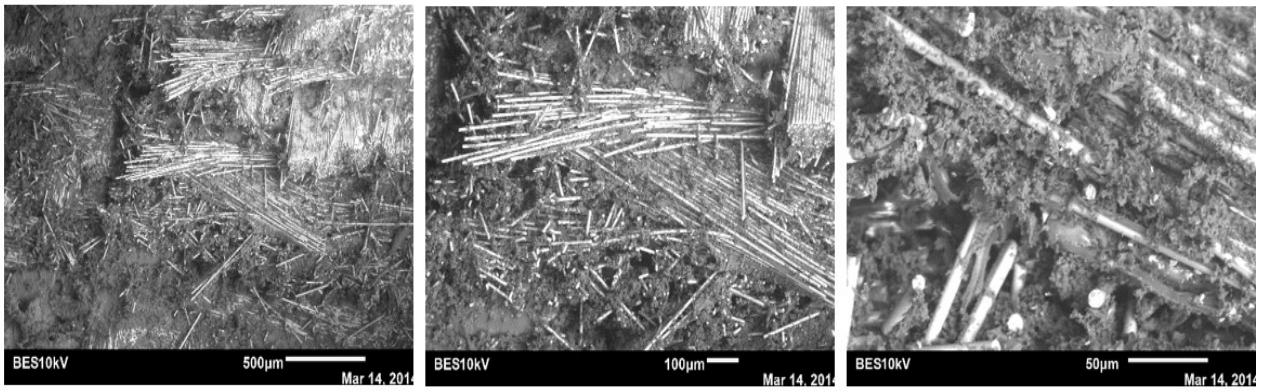

Composite exposed 250 °C for 1 h before impact loading

Fig. 4.41. Fracture surface of Glass fiber reinforced epoxy after failure under impact loading showing fiber pullout, debonding and delamination.

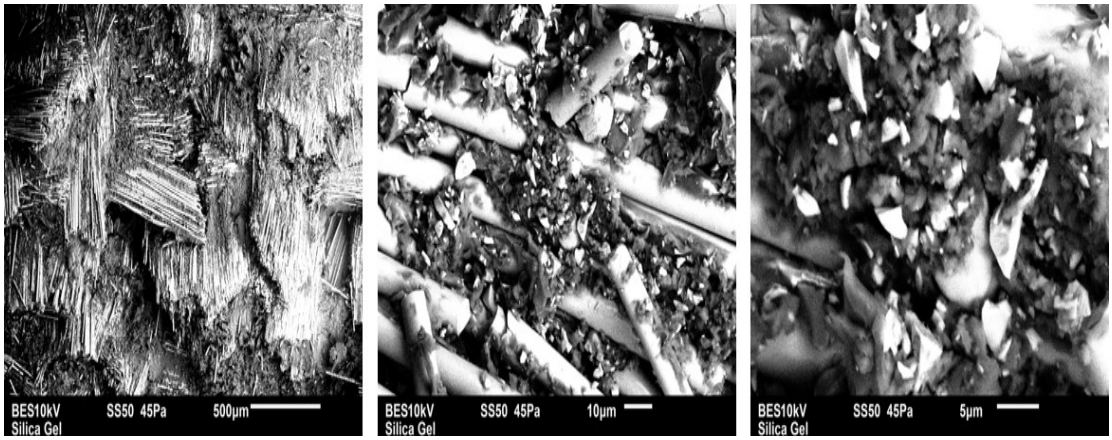

Fig. 4.42. Fracture surface of a glass fiber reinforced epoxy composite that failed under dynamic impact loading showing (a) fiber bundle rupture and (b, c) brittle fracture (shattering) of the reinforcing glass fibers.

Analysis of the fracture surface of the glass fiber reinforced epoxy subjected to various degree of thermal exposure shows catastrophic failure characterized by glass fiber breakage and subsequent fiber pullout. Matrix cracking was also observed on the fracture surface of the fragmented specimen as shown in Fig. 4.43. More damage was experienced as the fiber reinforced composite was exposed to higher temperature before impact testing. The thermal mismatch between the Kevlar fiber and the epoxy resin most likely affect the fiber matrix bonding make the composite more prone to delamination under impact loading or prolonged exposure at high temperatures. Fiber dominated properties such as strength and E modulus experience deterioration leading to the observed brittle failure in the glass fiber reinforced epoxy under both impact and flexural loading. According to Bhavesh [10], excessive brittleness can occur within fiber reinforced epoxy composite that is exposed to ultraviolet radiation leading to chain scission and micro cracking.

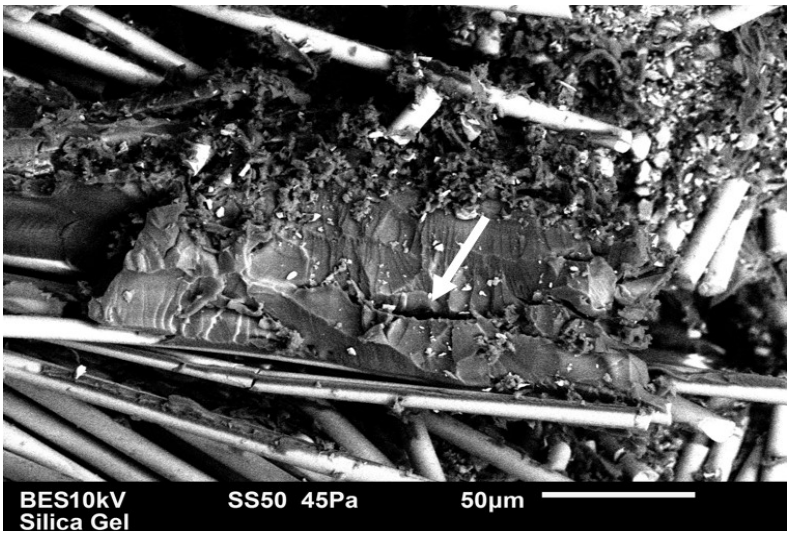

Fig. 4.43. Fracture surface of a fragmented glass fiber reinforced epoxy, showing matrix cracking (arrow) after fragmentation under impact loading.

In summary, Kevlar® fiber reinforced epoxy composite exhibits a different mode of failure under impact loading when compared with glass fiber reinforced epoxy composite. Rapid lost in strength and module was observed by the increasing thermal exposure in excess of 300°C for both Kevlar® and glass fibers reinforced epoxy. The strong resistance of Kevlar® fiber to impact failure is reflected in the more damage tolerance of the Kevlar® reinforced epoxy when compared to the glass fiber reinforce epoxy. With the exception of a few filaments splitting under high impact loads the Kevlar® fiber effectively resisted fracture under impact loading. Thus the damage to the Kevlar® reinforced composite could only occur within the epoxy matrix and at the fiber matrix delamination leading to failure by delamination.

5.0 SUMMARY, CONCLUSIONS AND RECOMMENDATIONS

5.1 Summary.

As a result of their high specific strength and stiffness, fiber reinforced plastics (FRP) composites are gaining acceptance as replacements for conventional monolithic materials for load-bearing applications in aircrafts, ships, buildings and automobiles. The weight reduction achieved through the application of fiber reinforced polymer laminates in the aircraft industry, in the recent times, offers a significant contribution to fuel efficiency, reduction in greenhouse gas emission as well as increase in speed and payloads. However, when exposed to a heat source, FRP can suffer loss of mechanical strength and stiffness as a result of the resin depolymerisation leading to delamination

In this research work, series of fiber reinforced epoxy matrix composites were manufactured and investigated for potential use as suitable replacements for aluminum alloys used in the fabrication of cowling panels for a small engine recreational aircraft such as Cessna 177. However, such application could expose the material to radiant and convective heat flux from the aircraft engine in flight or impact from extraneous objects such as in the case of bird strike. These operational conditions could pose a threat to the mechanical integrity of FRP when used in cowling panels of light engine aircrafts. Hence, the need for characterization of fiber reinforced epoxy under carefully defined experimental conditions simulating the anticipated service condition. In the course of this study, the thermal conditions of the engine and the cowling of a Cessna 177 aircraft during flight were assessed and it was observed from the real life data that the maximum temperature of the engine, if the cooling system works effectively as expected, is 260°C with the estimated radiative heat flux from the engine heating to the cowling causing a maximum temperature of 65°C on the inner surface of the cowling panel.

Kevlar® and glass fiber reinforced epoxy composites were fabricated using hand laying of impregnated fiber laminates and allowing the resin to cure to a C stage under pressure. Three different types of Kevlar® 49 fibers (#285, #281 and #120) and two different glass fibers (E-glass and S glass fibers) were used as reinforcements for the epoxy matrix, while two different resin hardeners (PH 3665 and PH3660) were used as curing agents for the epoxy resin. The obtained composite were characterized using Thermogravimetry Analysis (TGA), Flexural Test, Dynamic Mechanical Thermal Analysis (DMTA), Impact Test and Optical and Scanning Electron Microscopy to

determine the effects of radiative and convective heat flux, impact loading and vibratory force on the mechanical performance of fiber reinforced epoxy as influenced by the materials and process variables during the manufacture.

5.2 Conclusion.

It was found that:

1. Thermogravimetric analysis of glass and Kevlar® fibers reinforced epoxy confirmed thermal stability of the composites as exposure temperature increased from room temperature to 250°C. Above this temperature, resin decomposition begins and becomes very prominent beyond 300°C.
2. The color change observed in the composites with increasing degree of thermal exposure can provide an indication of the extent resin degradation during thermal exposure if properly calibrated.
3. Both glass and Kevlar® fibers are properly wetted by epoxy resin leading to production of FRP with strong fiber matrix bonding by simple hand lay-up manufacturing technique. This translates to composite strength that is comparable to those of many aluminum alloys.
4. Dynamic thermal analysis shows that the glass transition temperature of the fiber reinforced composites range between 80 and 100°C while the maximum exposure temperature for the proposed application is 65°C.
5. Epoxy matrix composite made using glass fibers are more stable and less prone to thermal induced damage at elevated temperature than those made with Kevlar® fibers.
6. Glass fiber reinforced epoxy show better stiffness and a higher deformation resistance while Kevlar® fiber reinforced epoxy composites are more damage tolerant.
7. No significant loss in flexural strength occurs in glass or Kevlar® fibers reinforced epoxy composite materials for thermal exposure temperature that is less than 200ºC.
8. While Kevlar® fiber reinforced epoxy fails by delamination under impact loading and is more resistant to impact failure, fiber rupture is the predominant cause of failure in epoxy reinforced with glass fibers.
9. Since the glass transition temperature of fiber reinforced epoxy is very close to the anticipated temperature of the inner surface of a cowling panel, lining the inner surface of cowling made of fiber reinforced epoxy composite with a thermal insulator is recommended to preserve its mechanical integrity during prolonged flight duration

5.3 Recommendations for future work

The following are recommended for future work:

1. The research majorly focused on elevated temperature as it affects the thermo-mechanical behavior of both glass and Kevlar® fiber reinforced epoxy composite. Since the aircraft also operates at subzero temperature during winter season, extensive study of low temperature effect on the glass and Kevlar® fibers reinforced epoxy is recommended. This will help the design engineers when selecting engineering materials for structural applications in extremely cold region.
2. It is recommended that the mechanical performance of the composites be investigated in-situ while still under thermal exposure to adequately determine the exact strength of the composite materials under the simultaneous actions of the thermal fluxes and mechanical loading.

REFERENCE

1. W. Lee, W. Sue and S. Chiou, "Effect of Reinforcement Orientation on the Impact Fracture of Carbon Fiber Reinforced 7075-T6 Aluminum Matrix Composites", Japan Institute of Metals, Materials Transactions, 8 (2000) 1055-1063.
2. A. Brent, "Strong Plastics: Materials and Processing- 3rd edition", 2006 Pearson Education, Inc., New Jersey (2006) 321-325, 690-691.
3. E. Kandare, B.K. Kandola, P. Myler and G. Edwards, "Thermo Mechanical Responses of Fiber-reinforced Epoxy Composites Exposed to High Temperature Environments: Part I. Experimental Data Acquisition". Journal of Composite Materials, 44 (2010) 309-322.
4. S. L. Bazhenov, "Bending Failure of Aramid Fiber-Reinforced Composites", Journal of Composites. 26 (1995) 757 – 765.
5. M. Patmore, J. Cruthers, R. Patmore, S. Rushmer, "1968 Cessna 177 Aircraft Engine Cowling Redesign and Manufacture." 2010 BSc Thesis, Mechanical Engineering Department, University of Saskatchewan, Canada.
6. P.K. Mallick, "Fiber-Reinforced Composites – Materials, Manufacturing and Design," CRC Press, Taylor & Francis Group, LLC. Marcel Dekker Inc, 3rd edition, 1993 (pp. 6- 44).
7. A. Sommers, Q. Wang, X. Han, C. T'Joen, Y. Park, and A. Jacobi, "Ceramics and Ceramic Matrix Composites for Heat Exchangers in Advanced Thermal Systems- A review", Applied Thermal Engineering (2010) 02.
8. W. D. Callister, Jr., "Material Science and Engineering, An Introduction", John Wiley and Sons, 7th edition, 2007 (pp. 6, 10, 535-541, 578-607).
9. M. Rosso, "Ceramic and Metal Matrix Composites: Route and Properties. Journal of Materials Processing Technology, 175 (2006) 364-375.
10. G. K. Bhavesh, P. S. Raman and T. Nakamura, "Degradation of Carbon Fiber-Reinforced Epoxy Composites by Ultraviolet Radiation and Condensation", Journal of Composite Materials 36 (2002) 2713 – 2721.
11. Y. Ozawa, M. Watanabe, T Kikuchi and H. Ishiwatari, "Mechanical and Thermal Properties of Composite Material System Reinforced with Micro Glass Balloons", IOP Conf. Series: Materials Science and Engineering 10 (2010) 1088 – 1757.
12. S. Kumar, K.V.V.S. M. Reddy, A. Kumar, and G. R. Devi, "Development and Characterization of Polymer-Ceramic Continuous Fiber Reinforced functionally Graded Composites for Aerospace Application", Journal

of Aerospace Science and Technology, 26 (2013) 185 - 191.

13. D.L McDanels, T.T. Serafini and J.A. DiCarlo, "Polymer, Metal, and Ceramic Matrix Composites for Advanced Aircraft Engine Applications", Advanced Composite Conference paper. American Society for Metals and the Engineering Society of Detroit 26 (1985) 3- 14.
14. R. Warren, "Ceramic Matrix Composites". Blackie and Son Ltd, USA: Chapman and Hall, 1997 (pp. 7- 22).
15. B. Tang, "Fiber Reinforced Polymer Composites Applications in USA", Fiber Reinforced Composite Bridge Technology, USA. Korea/USA Road workshop Proceedings, Jan 1997. (pp. 1 – 7).
16. R.W. Cahn, P. Haasen, E.J. Kramer, "Materials Science and Technology. A comprehensive treatment", John Wiley and Sons-VCH Publisher, 1st Edition, 2008 (pp. 469 – 507).
17. S. Wang, S. Adanur and B. Z. Jang, "Mechanical and Thermo-mechanical Failure Mechanism Analysis of Fiber/Filler Reinforced Phenolic Matrix Composites", Composites Part B 28B (1997) 215 – 231.
18. S. S. Samal, S. Bal, "Carbon Nanotube Reinforced Ceramic Matrix Composite – A Review". Journal of Minerals and Materials characterization and Engineering, 7 (2008) 355 – 370.
19. S. Wang, Z. Liang, T. Liu, B. Wang and C. Zhang, "Effective Amino – Functionalization of Carbon Nanotubes for Reinforcing Epoxy Polymer Composites". Nanotechnology 17 (2006) 1551-1557.
20. D. Cohen, K. A. Lowe, "The Influence of Epoxy Matrix Properties on Delivered Fiber Strength in Filament Wound Composite Pressure Vessel", Journal of Reinforced Plastics and Composites, 10 (1991) 112.
21. I. Pesneau, A. AitKadi, and M. Bousmina, "From Polymer Blends to in Situ Polymer/ Polymer Composites: Morphology Control and Mechanical Properties", Polymer Engineering and Science, 42, (2002) 1990 – 2004.
22. G. Sarkhel, and A. Choudhury, "Dynamic Mechanical and Thermal Properties of PE-EPDM Based Jute Fiber Composite", Journal of Applied Polymer Science, 108 (2008) 3442 – 3453.
23. M. Barcikowski, "Glass Fiber / Polyester Composites under Ballistic Impact", Journal of Kompozyty (Composites), Polish Society for Composite Materials, 8 (2008) 70-76.
24. S. Rudzinski, L. Haussler, Ch. Harnisch, E. Mader, and G. Heinrich, "Glass Fiber Reinforced Polyamide Composites; Thermal Behavior of Sizings", Journal of Composites; Part A 42 (2011) 157 – 164.
25. T. Johnson, "The Evolution of Lightweight Composite Materials", Composites / Plastics Guide. 12 (2011).
26. Y. Hirai, H. Hamada, and J. Kim, "Impact Response of Woven Glass-Fabric Composites – II. Effect of Temperature", Composite Science and Technology 58 (1998) 119 – 128.

27. L. M. Manocha, “High performance Carbon-Carbon composites, Parts 1 & 2”, 28 (2003) 348 – 358.

28. L. Tsai, F. Yuan, V. Prakash, and D. P. Dandekar, “Shock Compression Behavior of a S2 – Glass Fiber Reinforced Polymer Composite”, Journal of applied Physics, 105 (2009) 93526.

29. S.T. Peters, “Hand book of Composites, Second edition”, Chapman and Hall, 1998. pp 48.

30. S. Ma, W. Liu, C. Hu and Z. Wang, “Modification of Epoxy Resins with Polyether-g-Polysiloxanes”, Iranian Polymer Journal, 19 (2010) 185 - 196.

31. B. M. Icten, C. Atas, M. Aktas, R. Karakuzu, “Low Temperature Effect on Impact Response of Quasi-Isotropic Glass/Epoxy Laminated Plates”, Composite Structure 91 (2009) 318 – 323.

32. M. Shinohara, J. J. Miyashiro, “Epoxy Resinous Moulding Composition Having Low Coefficient of Thermal Expansion and High Thermal Conductivity”, 19 (1982) 11-45.

33. A.P. Mouritz, Z. Mathys, and A.G. Gibson, “Heat Release of Polymer Composites in Fire”, Journal of Composites: Part A 37 (2006) 1040-1054.

34. M.A Caminero, S. Pavlopoulou, M. Lopez-Pedrosa, B.G. Nicolaisson, C. Pinna, and C. Soutis, “Analysis of adhesively bonded repairs in Composites: Damage Detection and Prognosis. Composite Structures,” 95 (2013) 500-517.

35. A.E. Elmughrabi, M. Robinson, A.G. Gibson, “Effect of Stress on The Fire Reaction Properties of Polymer Composite Laminates”, Centre for Composite Materials Engineering, University of Newcastle upon Tyne, NE1 7RU, United Kingdom - Polymer Degradation and Stability 93 (2008) 1877–1883.

36. H. Lee and K. Neville, “Handbook of Epoxy Resins” McGraw-Hill, New York, 1982. 142.

37. I. Chatys, R. Chartys, “The Influence of Technology and Atmosphere on the Properties of Fiber-Reinforced Polymer-matrix Composite Materials”, 2006 UTRAGARSAS, Ultrasounds Institute, Kaunas, Lithuania. 1245 – 1344.

38. V. M. Karbhari, J. W. Chin; D. Hunston, B. Benmokrane, T. Juska, R. Morgan, J. J. Lesko, U. Sorathia, and D. Reynaud, “Durability Gap Analysis for Fiber-Reinforced Polymer Composites in Civil Infrastructure”, Journal of composites for construction. 11(2003) 238 – 247.

39. A. P. Mouritz, “Post-Fire Flexural Properties of Fiber-Reinforced Polyester, Epoxy and Phenolic Composites”, Journal of Material Science, vol. 37 (2002) 1377 – 1386.

40. J. R. Brown and B.C Ennis, “Thermal Analysis of Nonmex and Kevlar® fibers”, Texile Research Journal. 1977; (47) pp. 62-66.

41. J. R. Brown and N. NcM. Browne, “Materials Research Laboratory Report MRL-R-674”, Melbourne, Australia, 1976.

42. F. Le Lay, J. Gutierrez, “Improvement of The Fire Behavior of Composite Materials for Naval Application”, Journal of Polymer Degradation and Stability 64 (1999) 397- 401

43. N.A. St John, P. D. Fawell and J. R. Brown, “Defense Science and Technology Organization Report DSTO-1P1C-0012”, Melbourne, Australia (1995).

44. Y. Bai and T. Keller, “Time Dependence of Material Properties of FRP Composites in Fire” – Journal of Composite Materials, 43 (2009) 2469 - 2484.

45. G. A. Bibo, D. Leicy, P. J. Hogg and M. Kemp, “High Temperature Damage Tolerance of Carbon of Carbon Fiber Reinforced Plastics: Part I. Impact Characteristics”, Composites in Press, 25 (1994) 414 – 424.

46. B. Y. Lattimer, J. Ouellette, J. Trelles, “Thermal Response of Composite Materials to Elevated Temperature”, Fire Technology Journal, 47 (2011) 823 – 850.

47. R. E. Evans and J. E. Masters, “A new Generation of Epoxy Composites for Primary Structural Applications: Materials and Mechanics.” Toughened Composites, ASTM STP 937, N.J. Johnston.” Ed., American Society for Testing and Materials, Philadelphia, Pennsylvania, 1987, (pp. 413 – 436).

48. W. L. Bradley, “The Effect of Resin Toughness on Delamination Toughness and Post-Impact Compression Strength. In Proceedings of ‘Benbana’ Int. Symp. On how to Improve the Toughness of Polymers and Composites Toughness, Fracture and fatigue of Polymers and Composite”, Yamagata, Japan, (1990) 221 – 230.

49. G. A. Bibo, P. J. Hogg and M. Kemp, “High Temperature Damage Tolerance of Carbon Fiber Reinforced Plastics, Part I. Impact Characteristics”. Composites, 25 (1994) 414-424.

50. Kim, J.K. Mackay, D.B. and Mai, Y.W., “Drop-Weight Impact Damage Tolerance of CFRP with Rubber Modified Epoxy Matrix Composite”, 24 (1993) 458-494.

51. H. K. Jain, A. Upadhyay, “Laminated Composite Stiffened Panels: Applications and Behavior.” Civil Engineering Conference Innovation without Limit (CEC-09), NIT Hamirpur (2009) 89 – 96.

52. A.P. Mouritz, Z. Mathys, and C.P. Gardiner, “Thermomechanical Modeling the Fire Properties of Fiber–Polymer Composites”, Composites: Part B 35 (2004) 467–474.

53. R. Strumpler, J. Glatz-reichenbach, “Conducting Polymer Composites”, Journal of Electro ceramics 3:4 (1999) 329-346.

54. Y. Sun and R. N. Singh, “The Generation of Multiple Matrix Cracking and Fiber–Matrix Interfacial Debonding in a Glass Composite”, Acta Metallurgical Inc, 46 (1998) 1657-1667.

55. C.Y. Yue and H. C. Looi, “Influence of Thermal and Microwave Processing on the Mechanical and Interfacial Properties of a Glass/epoxy Composite”, 26 (1995) 767-773.

56. A.R Boccaccini, D.H Pearce, J. Janczak, W. Beier, and C.B. Ponton, “Investigation of Cyclic thermal shock behavior of fiber reinforced glass composites using non-destructive forced resonance technique”, Material Science and Technology, 13 (1997) 852-858.

57. I. Ozdemir and M. Toparli, “An Investigation of Al-SiCp Composites Under Thermal Cycling”, Journal of Composite Materials. 37 (2003) 1839-1850.

58. Z. X. Zhang, J. Zhang, B. Lu, Z. X. Xin, C. K. Kang, and J. K. Kim, “Effect of Flame Retardants on Mechanical Properties, Flammability and Foamability of PP / wood–fiber Composites”, Composites: Part B. 43 (2012) 150-158.

59. S.W Tsai (Ed.), “Composite Materials: Testing and Design (Fifth Conference)”, American Society for testing and Materials, STP 674. 5th edition, 1979 (pp. 14 – 40).

60. Abdul-Hamid Zureick, Richard M. Bennett, and Bruce R. Ellingwood, “Statistical Characterization of Fiber-Reinforced Polymer Composite Material Properties for Structural Design”, – Journal of Structural Engineering – ASCE, 132 (2006) 1320 – 1327.

61. Y. Ohama, “Recent Progress in Concrete – Polymer Composites”, Journal of Advanced Cement Based Materials, 5 (1997) 31 – 40.

62. ASTM D 7264 / D7264M -07 – Standard Test Method for Flexural Properties of Polymer Matrix Composite Materials. 2007 ASTM International, U.S.A

63. Perkin Elmer, “Introduction to Dynamic Mechanical Analysis”, PerkinElmer, Inc. 1st edition, 2008 (pp. 3 – 23).

64. Cessna sales and Service 1968– Model 177 and Cardinal under FAA Certification No. A13CE.

65. W. Chen, B. Song, “Split Hopkinson (Kolsky) Bar: Design, Testing and Applications”, Springer Science +Business media, 2011 edition, 2011 (pp. 1-35).

66. E. Kandare, B. K. Kandola, E. D. McCarthy, P. Myler, G. Edwards, Y. Jifeng and Y. C. Wang, “Fiber Reinforced Epoxy Composites Exposed to High Temperature Environments. Part II: Modeling Mechanical Property Degradation” Journal of composite materials, 45 (2011) 1511 – 1521.

67. A. G. Odeshi, H. Mucha and B. Wielage, “Manufacture and Characterization of Low Cost Fiber Reinforced Carbon Fiber Reinforced C/SiC Dual Matrix Composite”. Carbon 44 (2006) 1994-2010.

68. M. Idicula, S.K. Malhotra, K. Joseph, S. Thomas, “Dynamic Mechanical Analysis of Randomly Oriented Intimately Mixed Short Banana/Sisal Hybrid Fiber Reinforced Polyester Composites”, Compos Sci Techno, 65 (2005) 1077–1087.

69. S. Keusch, R. Haessler, “Influence of Surface Treatment of Glass Fibers on The Dynamic Mechanical Properties of Epoxy Resin Composites”, Composites A, 30 (1999) 997–1002.

70. A. Mouritz and A. Gibson, “Fire Properties of Polymer Composite Materials, Solid Mechanics and its Applications”, Springer, 1st edition, 2006 (pp. 215-236).

APPENDICES

APPENDIX 1: Thermal flux studies of Cessna aircraft engine cowling chamber– Data from field application.

The total heat flux to the cowling can be estimated using the sum of the convection and radiation heat fluxes to the cowling.

(Total $_{\text{heat flux}}$) = (Rad $_{\text{heat flux}}$) + (Conv $_{\text{heat flux}}$))..... (A1.1)

Convective can be written as:

$q''_{conv} = h\,(T - T_{cowl})$ ..... (A1.2)

And Radiative heat fluxes written as:

$$q''_{rad} = \frac{q}{A} = \varepsilon E_b(TS) - \alpha G = \varepsilon\sigma(T_{eng}^4 - T_{cowl}^4) \quad \text{.....(A1.3)}$$

Total heat flux absorbed = Radiant $_{\text{heat flux}}$ + Convective $_{\text{heat flux}}$ ..... (A1.4)

The following assumptions were made in respect to the thermal flux within the cowling chamber when flight is in service:

Steady state condition,

a. Negligible heat loss from cowling back surface,
b. Negligible convective heat flux within the cowling chamber,
c. Area of field application (inside the cowling chamber) is considered a blackbody; therefore, reflective heat transfer is negligible; hence, total rate of heat flux absorbed at the sample surface (cowling) is given as:
d. The engine block and the cowling large chamber is assumed a *gray surface* for which emissivity is equal to absorptivity ($\varepsilon=\alpha$)

Therefore, radiative heat flux: $q'' = h(T_{cowl} - T_\infty) + \varepsilon\sigma(T_{eng}^4 - T_{cowl}^4)$ ..... (A1.5)

where: q is the rate of heat transfer to the material,

q'' is the rate of heat flux transfer,

A is the area of the surface,

TS is the temperature of the surface

ε is the emissivity of the exposed surface,

σ is the Stefan-Boltzmann constant,

G is the irradiation (W/m^2),

E is the emissive power, W/m^2 while

α is the absorptivity, which indicates rate of absorption of radiation.

q''_{conv} = Convective heat flux

q''_{rad} = Radiative heat flux

T_{eng} = exposed surface temperature, K (Engine block temperature).

T_{cowl} = cowling chamber gas temperature, K.

T_{∞} = Surrounding fluid (ambient temperature, 20°C), K

h (W/m^2) is the convection heat transfer coefficient (W/m^{2}K) (The value of h ranged between 2 and 25 for free convective gases and 25 to 250 for forced convective gases).

Heat Transfer analysis inside a cowling

Total heat flux

$$q''_{total} = q''_{conv} + q''_{rad} \quad \text{.....(A1.6)}$$

Assuming that the radiation between the engine and the cowling can be treated as a two surface enclosure (i.e., there is no radiation heat transfer between the cowling and any other surfaces or gases):

$$q''_{rad} = \frac{\sigma(T_{eng}^4 - T_{cowl}^4)}{\frac{1}{\varepsilon_{eng}} + \frac{1}{\varepsilon_{cowl}} - 1} \quad \text{.....(A1.7)}$$

Using 20°C for cowling as the initial temperature (maximum radiation heat transfer),
the convection heat transfer between the cowling and its surroundings can be calculated using

$$q''_{conv} = h(T_{\infty} - T_{cowl}) \quad \text{.....(A1.8)}$$

The convection heat transfer coefficient was assumed to be 25 W/m^{2}C, which is consistent with forced convection in air. Using the temperature measured inside the compartment during the tests in Saskatoon for the ambient temperature, the convection heat transfer is calculated using ambient = 65°C and cowling = 20°C.

If ε = 0.91 (for plastic / polymer) and 0.96 (steel rough surface – engine block),

σ = 5.67 x 10^{-8} w/m^2 .K^4

T_{eng} = 260ºC (533K), T_{cowl} = 65ºC (338K), T_{∞} = 20°C (293K)

The radiative heat flux in the cowling chamber can be calculated as follows:

Using equation A1.7:

$$q''_{rad} = \frac{\sigma(T_{eng}^4 - T_{cowl}^4)}{\frac{1}{\varepsilon_{eng}} + \frac{1}{\varepsilon_{cowl}} - 1}$$

$$\Rightarrow q''_{rad} = \frac{5.67X10^{-8}(533^4 - 338^4)}{\frac{1}{0.96} + \frac{1}{0.91} - 1} = 3363\text{W/m}^2$$

The convective heat flux will be

$q''_{conv} = h(T_\infty - T_{cowl}) = 25(338 - 293) = 1125\text{W}/m^2$

The total heat flux is given by

$$q''_{total} = q''_{conv} + q''_{rad}$$

Therefore total heat flux is $q''_{total} = 3363 + 1125 = 4488$ W/m^2 *or* 4.49 kW/m^2

From the above heat transfer analyses; it can be assumed that the maximum heat flux transferred from the engine to the cowling material within the cowling chamber is about 5kW/m^2. This explains why the fabricated fiber reinforced epoxy composite was exposed to heat flux of 5 kW/m^2. A lower heat flux of 3.7 kW/m^2 and a higher heat flux of 7 kW/m^2 were also used in the study to provide a range of exposure.